TRISAFE
SINGLE AXIS FLIGHT CONTROL SYSTEM

H. L. EHLERS
R. D. BLOSSER
H. O. WILLIAMS

AUTONETICS DIVISION OF NORTH AMERICAN AVIATION

FOREWORD

The demonstration model of the TRISAFE Single Axis Flight Control System has been developed by the Autonetics Division of North American Aviation for the Research and Technology Division of the Air Force under Contract AF33(615)-1479. The effort was first proposed in November of 1963 with the contract being let in May of 1964. Mr. Charles Harmon was Project Engineer for RTD and Mr. Harold Ehlers was Project Engineer for the Data Systems Division of Autonetics. The simulator was designed and fabricated under the supervision of Mr. R. D. Blosser of Autonetics. The controller design and fabrication was accomplished under the supervision of Mr. H. O. Williams of Autonetics. Those contributing to the success of this program at Autonetics included: Mr. B. N. Gaon, Mr. R. J. Knight, Mr. D. V. Yoxthimer, and Mr. D. S. Simpson.

Manuscript of this report released by the authors May 1965 for publication as an RTD technical report.

This technical report has been reviewed and is approved.

W. A. Sloan, Jr.
Colonel, USAF
Chief, Flight Control Division
AF Flight Dynamics Laboratory

ABSTRACT

The TRISAFE Single Axis Flight Control System developed for the Research and Technology Division of the Air Force Systems Command consists of a deliverable controller and simulator with associated recorder. This equipment is to be used primarily as a laboratory demonstration model of a triple redundant, self-adaptive flight control system.

The controller incorporates the Autonetics developed triple redundant, analog circuit method called TRISAFE which is a highly efficient redundancy technique for achieving an ultra reliable system. The use of a square wave 400 cps carrier decreases the number of circuit components and reduces the size of compensation capacitors. Integrated circuits and a multilayer circuit board for system interconnection further reduces the weight and volume of the controller. The controller measures 3 x 9.7 x 12 inches and weighs approximately 9 pounds. Plug-in modular packaging is used for maintainability.

The controller design is based on the dynamics of a high performance tactical aircraft and provides stability augmentation for the pitch axis. To provide for optimum gain throughout the performance range of the aircraft, a self-adaptive system is used. Known as the dither-adaptive technique, it employs a low level test signal to measure the response of the airframe and adjust the gain accordingly.

The controller is used in conjunction with a desk top simulator to demonstrate the TRISAFE fail operational concept and the self-adaptive system. The simulator is a d-c analog computer which is used to simulate the aircraft servo dynamics, and the airframe dynamics for flight conditions representing extremes in the flight envelope. It also provides pilot command signals as well as servo position and pitch rate feedback signals to the controller. Used in conjunction with the controller and the recorder, the response of the flight control system under different flight conditions can be demonstrated.

By means of a selector switch, any one of six known flight cases can be selected to test the response of the system to a step input. Five of these flight cases are stable while the sixth is unstable. Two manual positions allow the use of potentiometers for setting the airframe transfer function to other than the six conditions as noted above. System inputs may be internal or external, and readout meters offer

visual monitoring of command and response signals. Recorder channel select switches provide the capability for external monitoring and recording of several system parameters.

Known failures can be introduced into the controller by means of switches on the simulator so that the effects of these failures on the system transient response can be demonstrated.

TABLE OF CONTENTS

ILLUSTRATIONS

TABLES

I. INTRODUCTION

A requirement exists for fail operational flight control systems for specific modern aircraft in particular flight regimes. A fail operational system is defined as a system which provides non-degraded system performance after one or more component failures have occurred. The need for a fail operational system exists wherever continuous flight control system operation is required for flight safety. This requirement for fail operational systems has been identified with

1. Low level automatic terrain following flight,

2. Automatic landing to touchdown under zero visibility conditions,

3. Yaw damper on particular high performance vehicles, and

4. VTOL vehicles during hover and transition.

Although added system reliability is obtained through improved component reliability and quality control procedures, achievement of fail operational performance can only be achieved by the use of redundancy techniques.

A high level of redundancy effeciency is provided by TRISAFE (Triple Redundancy Incorporating Self-Adaptive Failure Exclusion), a triple redundancy concept developed by Autonetics which results in fail operational system performance.

The resultant component additions to provide redundancy would normally cause an unacceptable increase in system size and weight.

A countering influence to the additional size and weight has been provided by recent progress in the art of molecular electronics. Microelectronic integrated circuits (MICs), complete solid-state molecular circuits contained in an element the size of a single transistor, have been used in digital mechanizations and are now being applied to analog circuits.

Self-adaptation in stability augmentation has been a prime study concern at Autonetics, and concentrated effort has resulted in a spectrum of techniques for various vehicle and mission applications. Included are model-reference techniques for rotary-wing vehicles,

dither-adaptive concepts for fixed-wing vehicles and some VTOLs, spectral-identification methods for flexible launch-vehicle application, and gust alleviation techniques.

As a result of the above background, Autonetics proposed to the Research and Technology Division of the Air Force in 1963 to design and build a TRISAFE Single Axis Flight Control System. This system consists of a controller and a simulator that when used together provide a laboratory demonstration model. (See Figure 1.) The effort was started in May of 1964 and was completed in May of 1965.

The TRISAFE Single Axis Flight Control System takes maximum advantage of recent developments in the areas of self-adaptation, redundancy, and microelectronics at Autonetics.

Figure 1. TRISAFE Single Axis Flight Control System

II. SYSTEM DESCRIPTION

A. FUNCTIONAL ANALYSIS

1. System Configuration

The block diagram of the closed loop controller/simulator is shown in Figure 2. The airframe dynamics, approximated by the lift and pitching moment equations for a high performance tactical aircraft, are presented by an effectiveness coefficient, a zero, and a dominant pole pair. All these parameters are expected to vary over a wide range. The series servo-surface actuator combination is characterized by two lags in series. The time constants associated with the dynamics are representative of present-day servo responses. A switch to allow checks of open loop airframe response is indicated in the block diagram. Due to the poorer damping present, with regard to that of the closed-loop system, it is recommended that the input command be limited to a maximum of two deg/sec. to prevent saturation. Two interdependent paths are apparent: (1) the stability loop, and (2) the self-adaptive loop. Their basic functions are to:

1. Improve airframe stability characteristics

2. Provide closed-loop response characteristics and pilot handling qualities in compliance with MIL-F-8785.

The simulator output signal depicting pitch rate ($\dot{\theta}$) is fed back through an inverse model linear network. The inverse model contains a set of complex zeros to capture the short period roots and to provide more invariant damping and frequency. Two real poles, one of which has a long time constant, are also included in the inverse model. Mechanization of the model in three parallel paths allows use of the long time constant lag to minimize steady state errors.

An analog computer study was conducted to optimize transient response and provide verification of analytical results. Improvement in leading edge shaping and further minimization of steady state error was obtained through incorporation of an externally shaped command, summed into the series servo. This signal by-passes the long time constant lag inserted for purposes of steady-state error and stability considerations. Faster rise times are attainable and the added benefit of reduced steady-state error is also realized. A listing of pertinent performance results is given in Table 1. Rise times are based on peak overshoot.

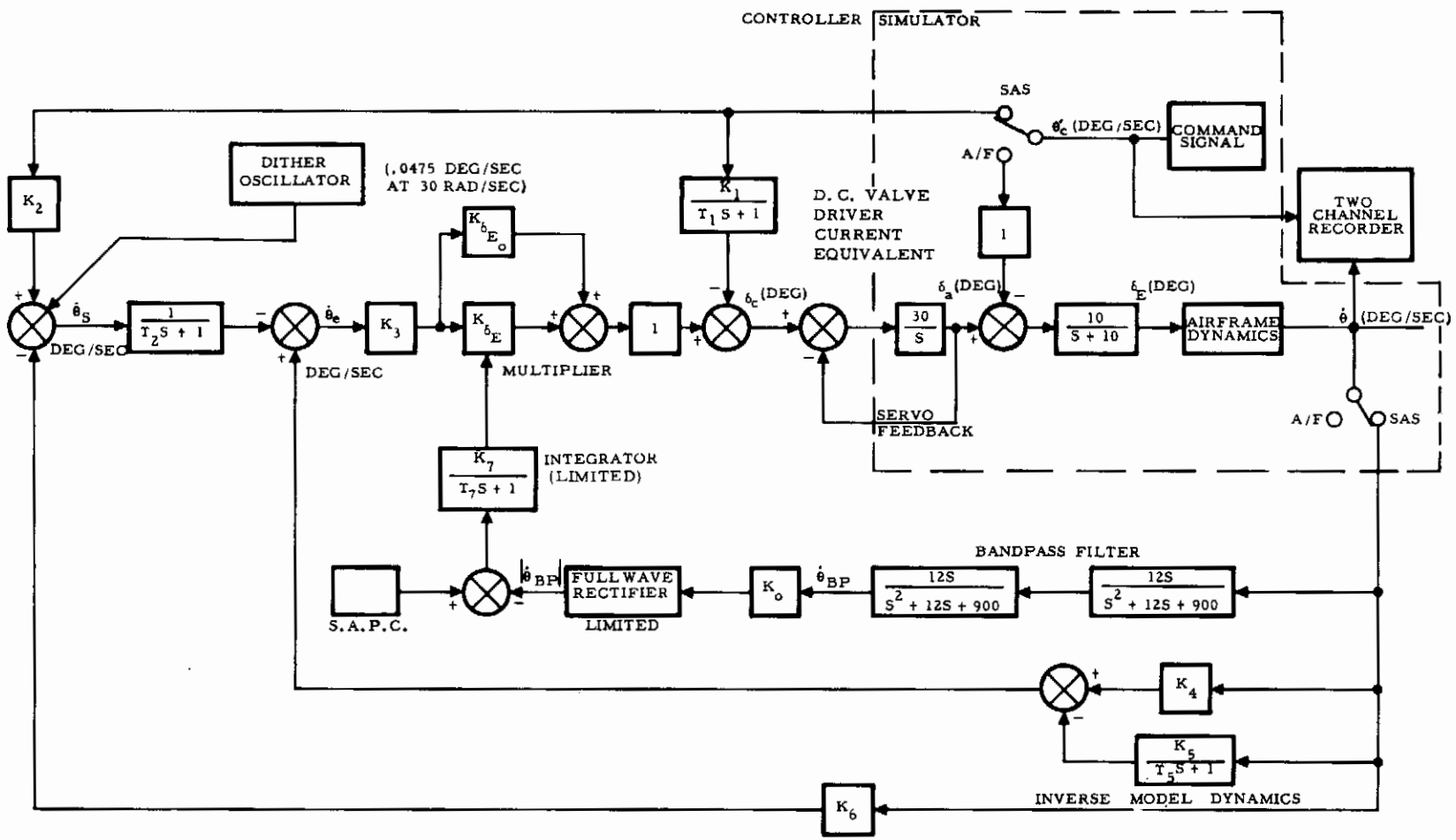

Figure 2. TRISAFE Single Axis Flight Control System Controller and Simulator Block Diagram

Table 1. Performance Results

Flight Case	Rise Time (sec)	Overshoot (%)	Damping Ratio	Steady-State Error (%)	K_{δ_E}
1	1.0	13	0.6	4.0	5.0_{limited}
2	0.7	10	0.7	3.1	2.6
3	0.6	6	0.7	3.1	2.6
4	0.8	5	0.7	5.1	.7
5	0.8	7	0.7	3.3	.06
6	0.5	10	0.7	0.3	0

2. Stability Loop

From the stability loop, the control equation for an elevator command is:

$$-\delta_c = \dot{\theta}_c \left[\frac{K_1}{\tau_1 s + 1} + \frac{K_2 K_3 \left(K_{\delta_E} + K_{\delta_{E_o}}\right)}{\tau_2 s + 1}\right] - \dot{\theta}\left[\left(K_4 + \frac{K_6}{\tau_2 s + 1} - \frac{K_5}{\tau_5 s + 1}\right) K_3 \left(K_{\delta_E} + K_{\delta_{E_o}}\right)\right] \quad (1)$$

where:

$K_1 = 0.90$

$K_2 = 0.97$

$K_3 = 10$

$K_4 = 0.25$

$K_5 = 0.17944$

$K_6 = 0.929$

$K_{\delta_{E_o}} = 0.1$

K_{δ_E} = f (flt. Environment, 0.15 to 0.5)

$\tau_1 = 0.625$

$\tau_2 = 5$

$\tau_5 = 0.04$

3. Self-Adaptive Loop

The dither adaptive system employs the simplest of tests to determine airframe characteristics, by the application of a low-level test signal and measurement of airframe gain at a discrete, fixed frequency. The dither concept is to insert a dither signal of frequency ω_o at a point ahead of the gain changer, and measure the output amplitude at the rate gyro. The rate gyro output at ω_o is separated from other signals by a bandpass filter, rectified, limited and summed with the Self-Adaptive Performance Criterion (SAPC) reference. This error signal formed by comparing the rectified output of the band-pass to the self-adaptive performance criterion (SAPC) will adjust the variable gain ($^{K}\delta_E$) through action of a passive integrator. This adjustment will occur until the error signal converges and the value of $|\dot{\theta}|_{BP}$ equals the SAPC (assuming a perfect integrator). The comparison phase relationship is such that $\int$(SAPC)dt increases $K\delta_E$, while $\int|\dot{\theta}|_{BP}dt$ decreases $K\delta_E$. Satisfying the performance criterion is equivalent to keeping the gain product $(K\delta_E + K\delta_{E_o})M\delta_E$ constant regardless of flight environment. The closed loop gain at the dither frequency (ω_o) will vary somewhat due to the finite gain of the passive error integrator.

The SAPC in system operation is a d-c voltage whose selected value is based upon the desired speed of response of the adaptive loop and the desired range of gain variation ($^{K}\delta_E$) between low and high dynamic pressure flight cases. The interrogation signal is set to a frequency of 30 radians/sec at an amplitude commensurate with MIL specifications for residual oscillations. This value is associated with the most critical flight condition (highest dynamic pressure) and its magnitude based upon two considerations: (1) sufficiently large to attenuate the effects of low signal level nonlinearities and (2) low enough so as not to exceed the pilot's feel threshold. Converted to deg/sec of pitch rate the maximum allowable amplitude due to the dither input signal is 0.061. The adaptive equation for the variable gain adjust is:

$$K_{\delta_E} = \left[\text{SAPC} - K_o (.637) (\dot{\theta})_{\omega_o} \right] \frac{K_7}{(\tau_7 s + 1)} \qquad (2)$$

where:

SAPC = 0.8 = adaptive reference

K_o = 19.8 = adaptive loop fixed gain

K_7 = 10 = steady state gain of the passive integrator

τ_7 = 20 = passive integrator time constant

.637 = gain of the rectifier

ω_o = 30 = dither signal frequency

Two limits are contained in the adaptive path as indicated in Figure 2. The output of the rectifier is limited to attenuate the 30 rad/sec content of an input command signal and to prevent an undesireable gain variation. This value should be set to approximately 1.5 times the value of the SAPC, i.e. to approximately 1.2.

An additional limit is imposed on the K_{δ_E} signal. A low limit, set at zero, prevents a change in sign in the stability loop during transient conditions and an upper limit due to hardware considerations to allow more favorable scaling. The upper boundary should limit K_{δ_E} to not less than 5.15.

Figure 3 shows a typical adaptive gain, K_{δ_E}, as a function of time along an extreme trajectory. On the same illustration, dynamic pressure in pounds per square foot is plotted. Note that an inverse relationship between these curves exists, as would be expected.

Figure 4 illustrates the response of the adaptive controller to a gain offset at some particular point along the extreme trajectory. The response when the adaptive gain K_{δ_E} is much too high is illustrated. Speed of adaption is quite rapid, attaining nearly the optimum value within 3 sec.

Figure 4 also illustrates the adaptive response to a gain that is initially too low. The speed of adaption is somewhat slower than when the initial K_{δ_E} is too high. This occurs because the adaptive response relation for small changes in K_{δ_E} is:

$$\left| \frac{\partial \dot{\theta}(\omega_o)}{\partial K_{\delta_e}} \right| \approx \left| \frac{\omega_o - \omega_s}{\omega_o - (\omega_s \pm \Delta\omega_s)} \right| \qquad (3)$$

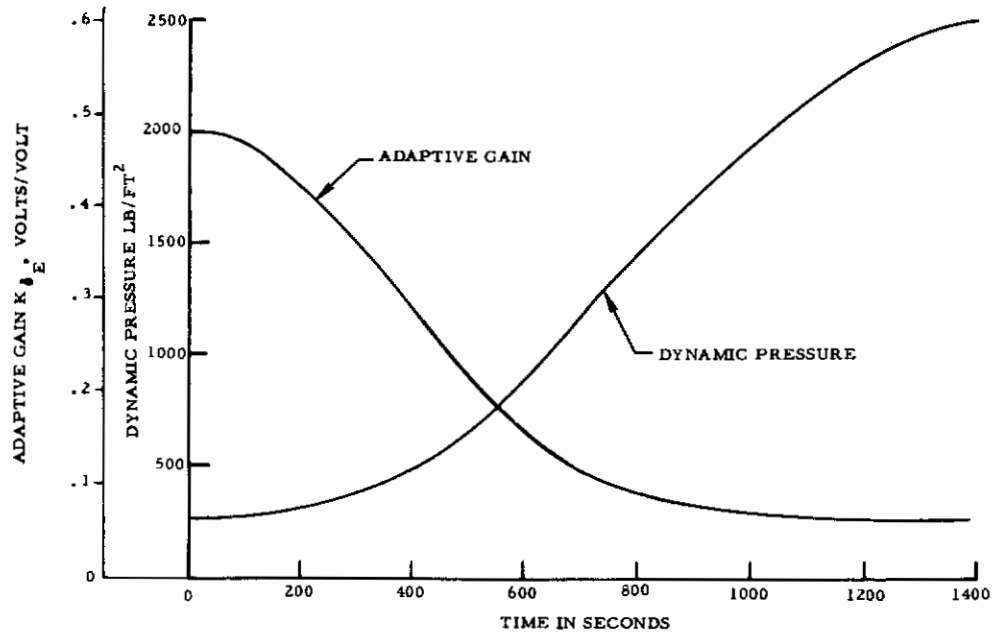

Figure 3. Adaptive Gain Along Extreme Trajectory

where ω_s is steady state servo mode frequency. Note that if $\Delta\omega_s$ is zero, the expression is normalized to unity, satisfying the SAPC. If $\Delta\omega_s$ is increased by nearly $|\omega_o - \omega_s|$ the expression $\partial\ddot{\theta}(\omega_o)/\partial K_{\delta_e}$ approaches infinity and the fastest adaptive loop time constant is achieved; T_A = 1/2 times real part of bandpass filter poles. On the other hand, if $\Delta\omega_s$ is decreased by the same amount, $|\omega_o - \omega_s|$, then $\partial\ddot{\theta}(\omega_o)/\partial K_{\delta_e}$ changes by a factor of two. Consequently, the performance error is small and the gain change is somewhat slower. It can be seen that the adaptive loop is very effective for controlling high frequency instability. The adaptive loop response time can be made more uniform by inserting a squaring circuit between the integrator and the gain change multiplier, but it is not necessary since the minimum gain is limited. The squaring circuit does, however, minimize the gain excursion due to gusts in high dynamic pressure flight environments.

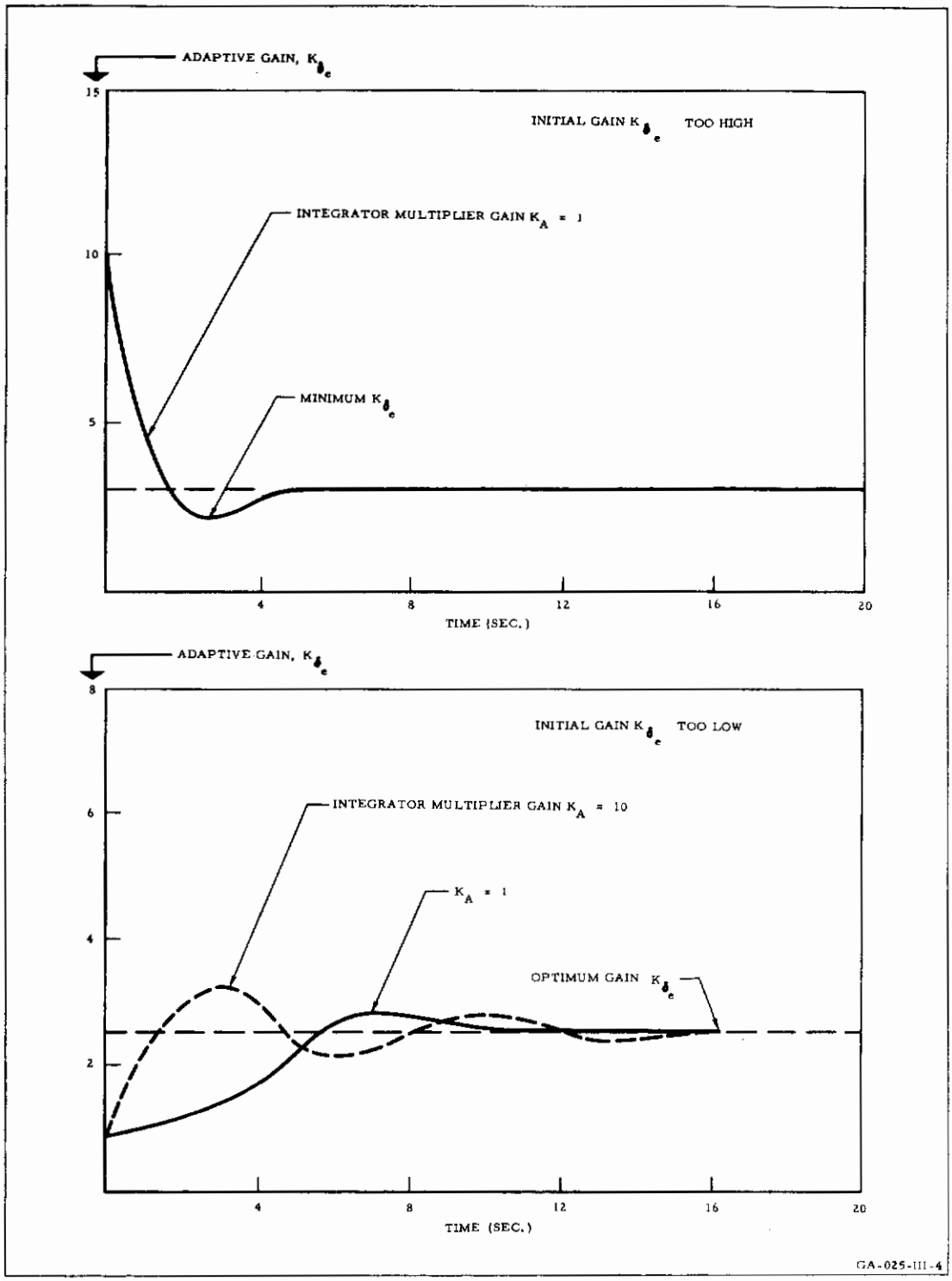

Figure 4. Adaptive Response to Gain Offset

The advantages and disadvantages of the dither concept are summarized below:

1. Advantages

   a. Positive gain control is maintained at all times. There is no gain limit cycle due to servo nonlinearities, no gain error due to lapses of identification inputs, and no significant gain error due to mismatch of oscillator frequency and bandpass filters.

   b. High gain is not inherently required. Closed loop roots may be deliberately well damped; there is no need to allow oscillation of poorly damped roots.

   c. As a result of positive gain control, derived gain information may be used directly to change other parameters such as variable poles or zeros.

   d. Mechanization is relatively simple.

   e. Growth potential exists for the sensing of phase information at the dither frequency and for further parameter adjustment.

2. Disadvantages

   a. In order to maintain control over the gain, a relatively high level test signal is required.

   b. If bending frequencies (structural) closely approach control frequencies, it may be difficult to select a dither frequency high enough to exclude control energy, yet low enough to exclude bending energy.

4. Acceleration Command SAS

Although the controller is not mechanized to incorporate this feature, the system could be extended to an acceleration command SAS. Figure 5 shows the manner in which the system could be changed.

Pilot handling qualities would be improved for high Mach number flight conditions, for the following reasons:

1. Steady state acceleration error is uniform and very small because the integrator/multiplier supports the pitch rate necessary to achieve the desired steady-state acceleration.

2. The gain change, K_{N_V}, assures a nearly uniform rise time in response to commanded "g's" regardless of flight condition.

3. The K_{δ_E} gain change in conjunction with pitch rate inverse model feedback maintains good system stability when closing the acceleration loop.

When the Mach number is low, the system could be automatically switched back to a pitch rate command system to assure that no pilot induced oscillations occur in precise low speed maneuvers such as landing.

B. DYNAMIC ANALYSIS

An analytical investigation involving aircraft pitch stabilization using an inverse model plus dither adaptive control is described here. The airframe dynamics used in the study were those describing a modern high performance fighter aircraft for which airframe data were available. The flight conditions range from a high dynamic pressure environment to that of a landing configuration.

Six flight conditions based on Mach number and altitude were selected for evaluation of system performance. Damping ratios of the open-loop airframe were both positive and negative and natural frequency ranged from approximately .8 to 10 rad/sec. Table 2 contains a tabulation of the six flight cases including altitude and Mach number and the transfer functions which describe the aircraft's short period mode.

In the initial effort to control the pitch rate response of the aircraft, a derived angular acceleration was fed back, through associated gains, to the servo-actuator in an attempt to provide uniform response in the short period mode. Optimum gains and pole positions were first obtained.

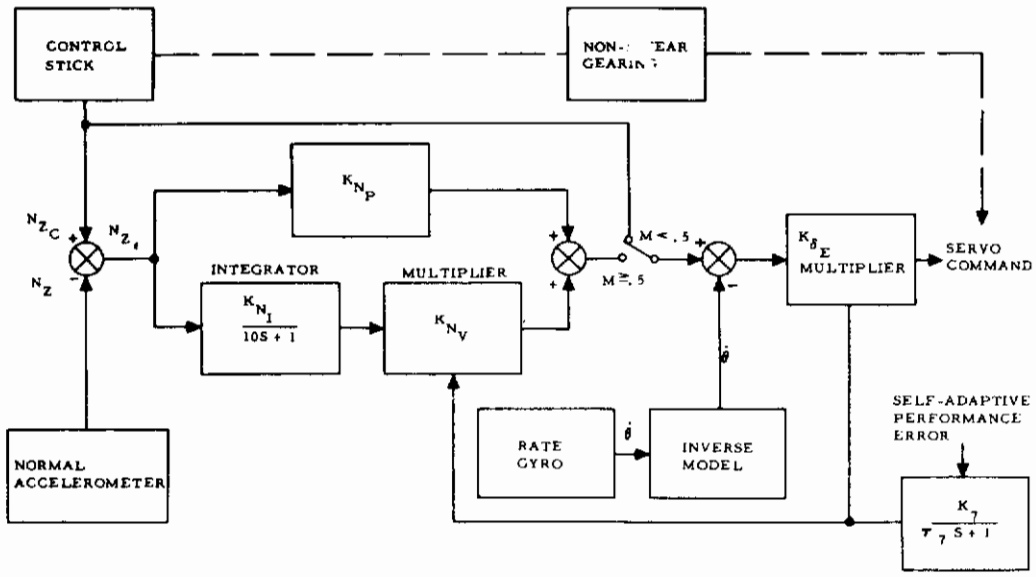

Figure 5. Normal Acceleration Command System

Figures 6, 7 and 8 are root locus plots of the poles and zeros of airframe, servo valve, and inverse model dynamics for three of the flight cases. A simplified block diagram of the system is shown in Figure 9. The open loop transfer for the system is:

$$\frac{K_{\delta_E} \; M_{\delta_E} \; K_{\dot{\theta}} \; 300 \; (s + a) \; (s + 4 \pm j2)}{(s + 30) \; (s + 10) \; (s^2 + 2\zeta\omega_n \; s + \omega_n^{\;2}) \; (s + .2) \; (s + 25)} \tag{10}$$

Closing the loop yields the transfer function:

$$\frac{\dot{\theta}}{\theta_c} = \frac{K_{\delta_E} M_{\delta_E} 300 (s + a) (s + 25) (s + .2)}{(s + 30) (s + 10) (s^2 + 2\zeta\omega_n s + \omega_n^2) (s + 25) (s + .2)}$$

$$+ M_{\delta_E} K_{\delta_E} K_{\dot{\theta}} 300 (s + a) (s + 4 \pm j2) \qquad (11)$$

Table 2. Airframe Flight Conditions

Flight Case	Altitude (ft)	Mach	$\dot{\theta}/\delta_E$
1	0	.161	$\frac{-1.14 (s + .415)}{s^2 + .604 s + .7074}$ (4)
2	30,000	.6	$\frac{-5.31 (s + .478)}{s^2 - .692 s + 2.585}$ (5)
3	30,000	.6	$\frac{-5.31 (s + .478)}{s^2 - .692 s + 2.585}$ (6)
4	0	.7	$\frac{-22.97 (s + .761)}{s^2 + 2.088 s + 20.27}$ (7)
5	0	1.2	$\frac{-70.8 (s + 1.27)}{s^2 + 4 s + 85}$ (8)
6	0	1.4	$\frac{-84 (s + 1.408)}{s^2 + 4.32 s + 96.64}$ (9)

It can be seen that the closed-loop positions of the airframe and servo-actuator roots and, hence, vehicle response are determined by $K_{\dot{\theta}}$, the inverse model feedback gain, and K_{δ_e}, the adaptive gain. The latter specifically compensates for poor performance arising from non-optimum airframe gain, M_{δ_e}. The adaptive loop root locus is not considered here.

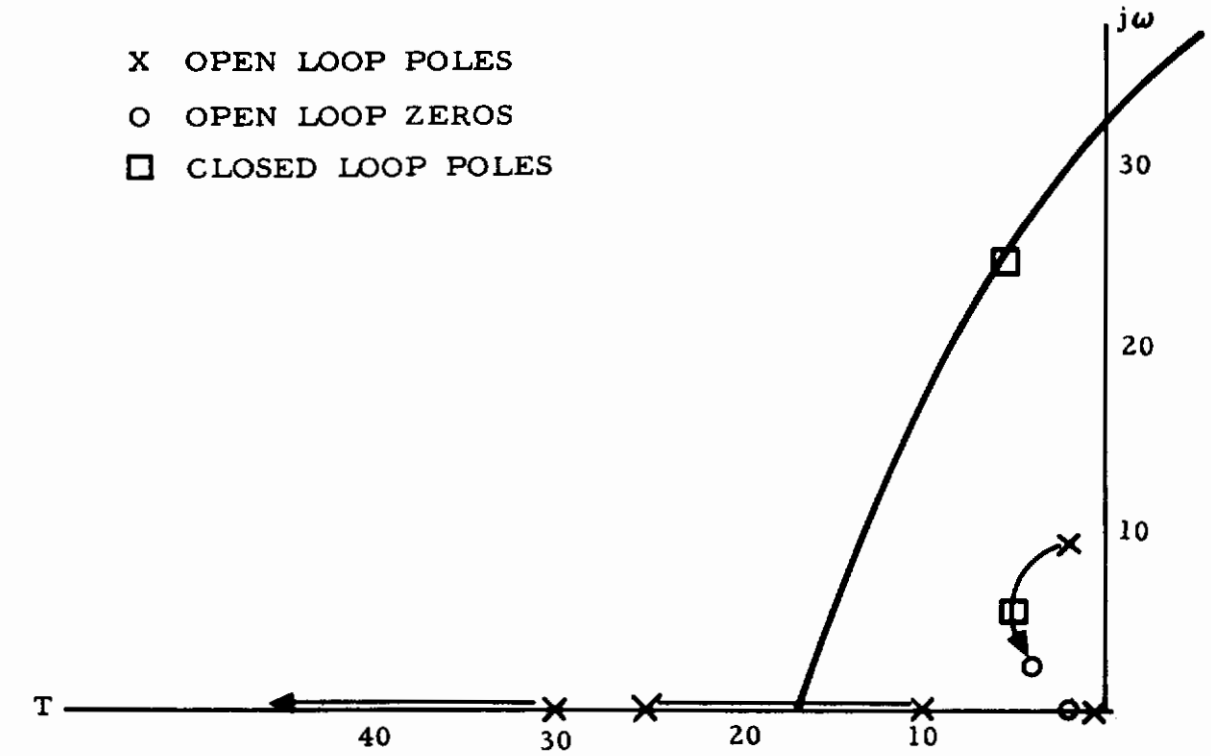

Figure 6. Root Locus, Flight Case 5

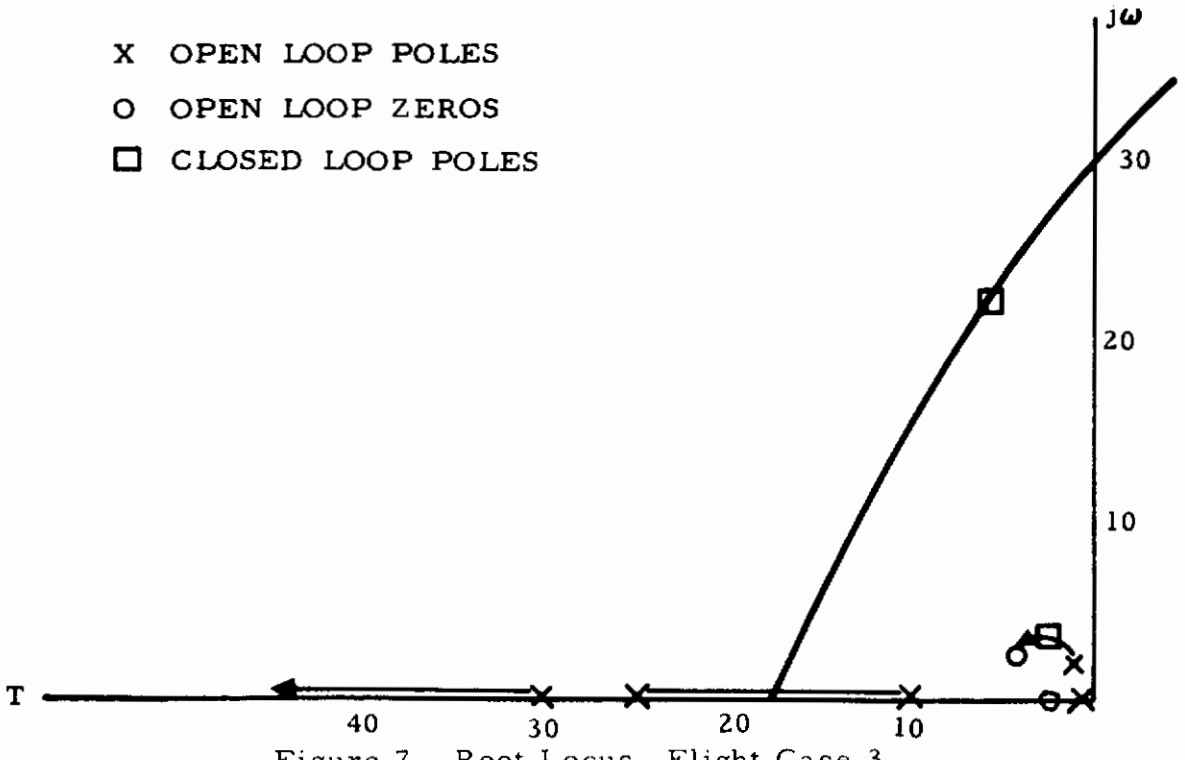

Figure 7. Root Locus, Flight Case 3

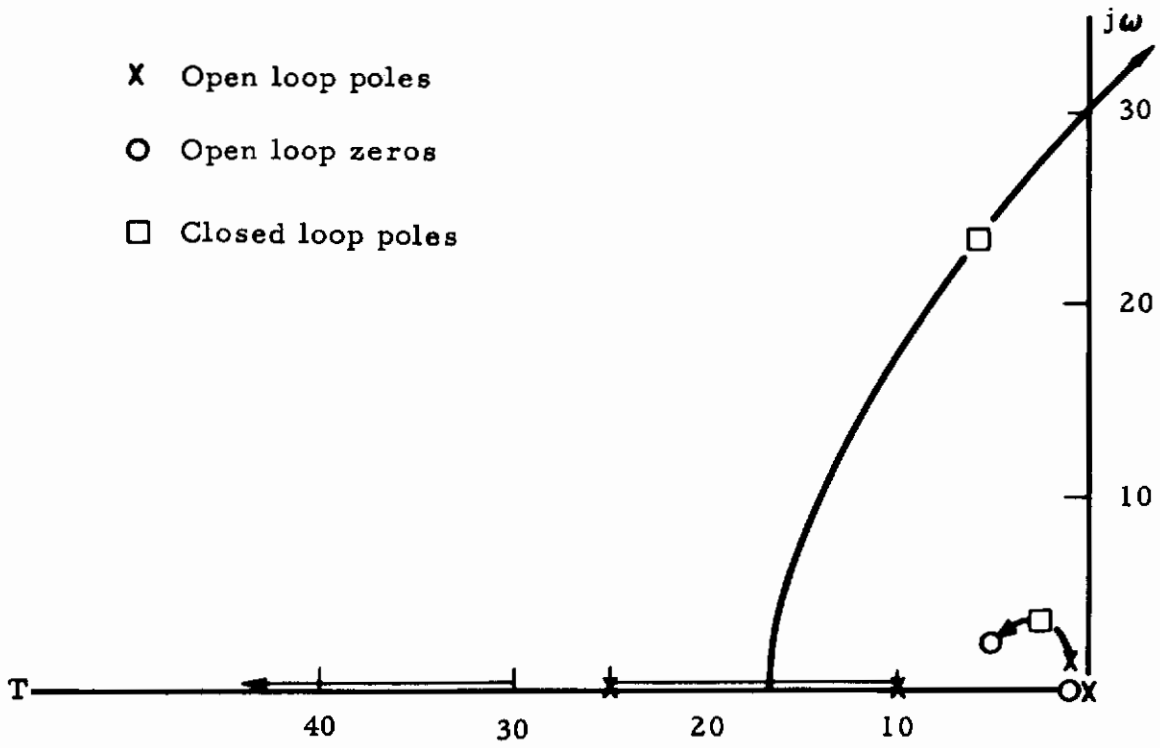

Figure 8. Root Locus, Flight Case 1

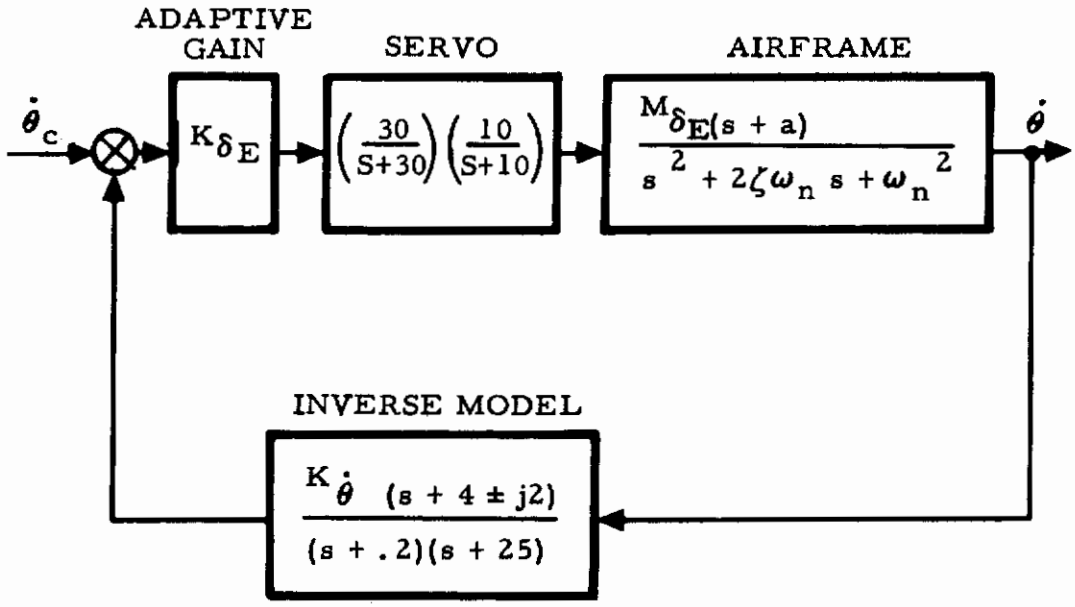

Figure 9. Simplified System Block Diagram

The gain that is chosen by the adaptive gain changer is such that the closed loop servo pole locations are nearly invariant with flight condition and possess a damping ratio between 0.1 and 0.2. This results in very high-loop gain for all flight conditions with tight control on the servo mode stability. Because of the inverse model in the rate feedback path, the closed loop short period pole position is relatively insensitive to gain changes in $K\delta_e$ as long as $K\delta_e$ is high. Consequently, it will be noted that little variation in closed loop short period poles occurs for the three flight cases investigated.

C. TRIPLE REDUNDANCY CONCEPT

An analog triple redundant circuit technique has been developed by Autonetics. The method of automatic failure correction is achieved by making use of analog amplifier voltage-saturation characteristics in high-gain loop with protected common point feedback. The triple redundancy concept is discussed in detail.

There are many routes open for improving the reliability of a system. Some of the more fundamental approaches are:

1. Simplify the system

2. Improve element reliability

3. Provide redundant elements, components, or systems

The first two approaches should be exploited to the extent possible within the limits of system performance requirements and value analysis considerations. It can be shown that the third approach, through proper organization of the redundancy technique, results in orders of magnitude increase in system reliability.

1. Majority Voting

A triple redundant system for the process of control is illustrated in Figure 10. This system has the capability of operating without degraded performance with a failure of any type in any one of the three channels. A system with this characteristic is sometimes referred to as fail operational. This feature is achieved by the majority voting circuit which selects the signal existing in two of the three channels as

the proper control signal and rejects the third signal which is different. It can be shown that the probability of failure for such a system is approximately

$$P_R = 3P^2 + P_M$$

where P is the probability of failure of a single channel and P_M is the probability of failure of the majority voting circuitry. Neglecting for the moment the effects of P_M, it is clear that this technique achieves a remarkable improvement in system reliability. For example, if $P = 0.001$, then $P_R = 0.000003$. If the probability of failure of a single channel is one in a thousand, then the system probability of failure is three in a million. This is because at least two channels of the three must fail in order to have a system failure. In order for P_M not to substantially degrade the system reliability, it must not be greater than approximately P^2. If the majority voting is performed with digital logic, the circuitry is relatively simple. Despite this simplicity, it may have a probability of failure significantly higher than P^2. Consequently, triple redundancy may be required in the logic circuitry so as not to impair the system reliability.

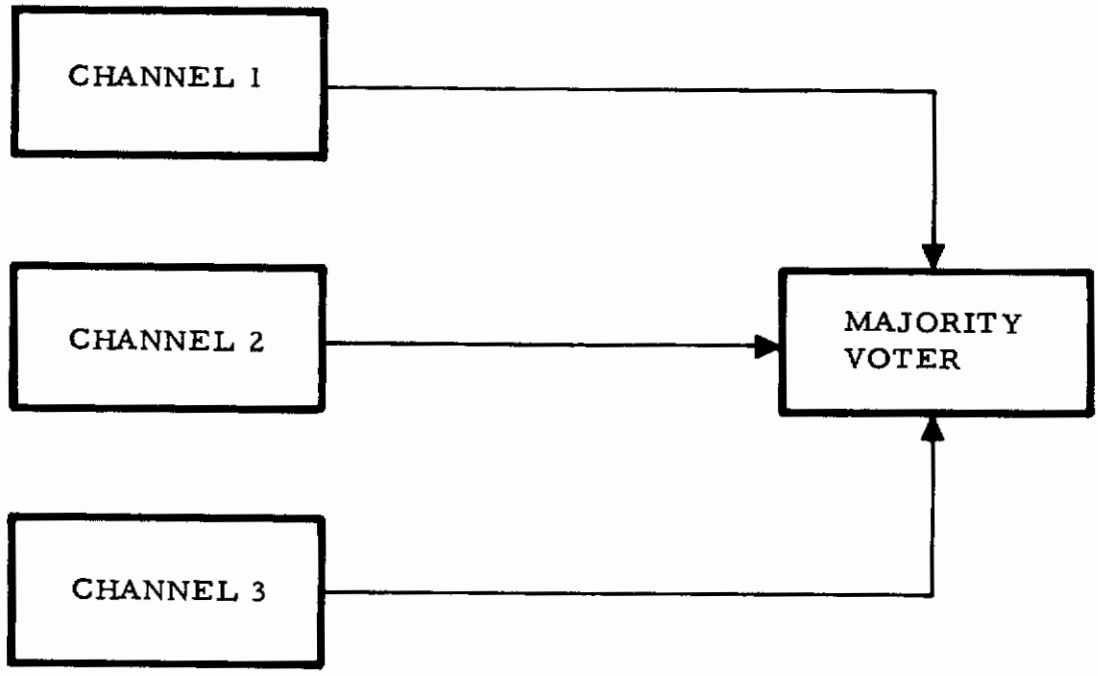

Figure 10. Triple Redundant Majority Voting System Mechanization

If the majority voting is taken several times in the system, this is referred to as majority voting at the unit level. For a system mechanized with N levels of majority voting, the system probability of failure is reduced approximately by the factor N.

2. TRISAFE

Autonetics has developed an analog triple redundant circuit technique that is simple and practically foolproof, called Triple Redundancy Incorporating Self-Adaptive Failure Exclusion (TRISAFE). This type of redundancy is applied on a unit or component level to such items as signal amplifiers, inertial sensors, valve drivers, and shaping units. A TRISAFE mechanization for a signal amplifier is shown in Figure 11. This method of automatic failure correction has been termed self-adaptive failure exclusion because no measuring device outside of the triple unit, such as a majority voter, is required. In addition, failure mode analysis of the proposed redundancy method shows that many types of double failures, two subunits out of three, do not degrade the triple unit operation. The method of automatic failure correction in each unit is achieved by making use of the analog amplifier voltage-saturation characteristics in a high-gain loop with protected common point feedback.

The relationship for the probability of failure of the TRISAFE unit is improved over that of the external majority voter, since

$$P_{Ru} = 3P^n \quad \text{where } 2<n<3 \tag{13}$$

P_{Ru} = probability of failure of a triple unit

P = probability of failure of a subunit

n = number of subunit failures constituting a unit failure

Detailed failure mode analyses result in values of n greater than 2.5. In the case of the external majority voting scheme, n cannot be greater than 2 since any two failures pass a triple unit failure into the next unit, i.e., result in system failure. The TRISAFE method is superior to an external majority voting method, since it provides an equivalent MTBF many times higher, is simple to implement with analog circuits, requires less circuitry through elimination of the external voter, and provides a greater expected life. The overall result represents a nearly optimum approach in redundancy efficiency for triple redundancy.

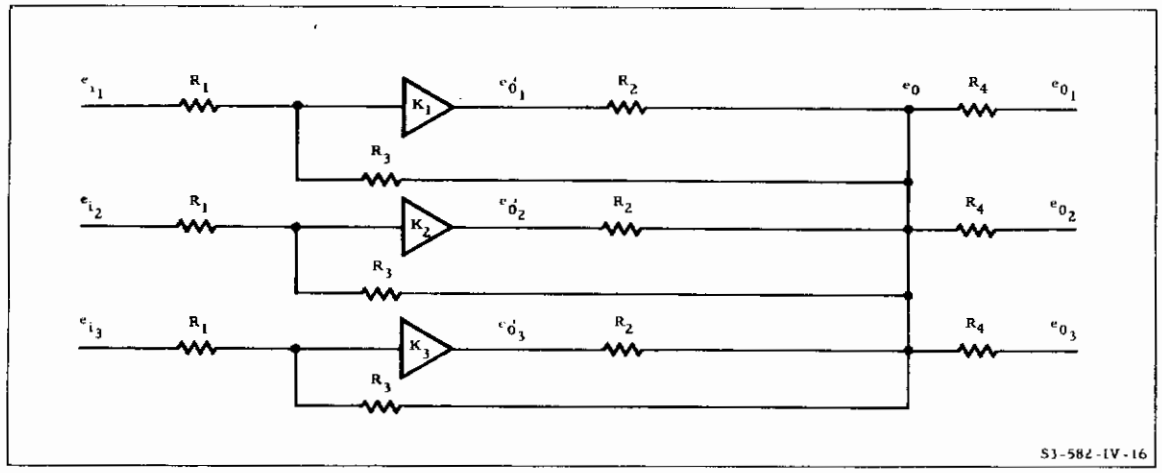

Figure 11. TRISAFE Amplifier Mechanization

Both static and dynamic tests of TRISAFE breadboard units have been performed. For the signal amplifier unit, loop gain requirements and the desired values for R_1, R_2, and R_3 are well within practical ranges. In order to provide a full operating range for the redundant unit with a saturated amplifier, it is necessary to scale the unit so that a maximum signal uses only one-third of the linear range when all amplifiers are operative.

The resistors, R_4, serve to illustrate how the common point is isolated and protected in system packaging.

The extension of triple system redundancy to TRISAFE at the unit level results in the mechanization of several portions of the system with various common points. A mechanization diagram is shown in Figure 12. In this figure, each block has a detail that resembles that of the TRISAFE amplifier previously described. Consideration of the detail reveals that the system operates with nondegraded performance with one or more failures in each triple redundant unit. For example, a rate gyro failure, a signal amplifier failure, a compensation sub-unit failure, and a failure in a valve driver amplifier may occur simultaneously without any apparent degradation in overall system performance from vehicle rate input through valve driver output. Thus, the triple redundancy is utilized to adapt in such a way that the

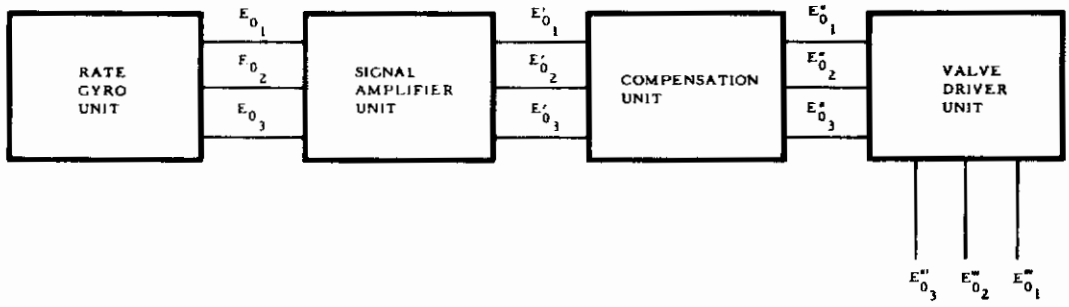

Figure 12. TRISAFE System Mechanization

result of several failures is excluded from having any effect at the system level. Carrying the redundancy to the unit level results in considerable improvement in redundancy efficiency.

If each of the subunits within each redundant unit has a probability of failure of 0.001 then on a single system nonredundant basis, the probability of failure of the simple system shown is 4 x 0.001 = 0.004. If the redundancy is implemented at the system level, then the probability of failure of the system is:

$$3P^2 = 3(0.004)^2 = 0.000048 \qquad (14)$$

With TRISAFE redundancy at the unit level as indicated, and with the conservative assumption that any two failures in a triple unit result in triple unit failure, the probability of failure for the system is:

$$3(0.001)^2 \times 4 = 0.000012 \qquad (15)$$

Thus, in the case cited, where all subunits have the same probability of failure, the system failure probability is reduced directly. The TRISAFE controller is mechanized using the TRISAFE concept.

D. SYSTEM MECHANIZATION

1. Controller

The controller mechanization for the TRISAFE Single Axis Flight Control System is shown in Figure 13. The mechanization utilizes Autonetics developed integrated circuits. A 400 cps square wave suppressed carrier is used to process the information frequencies.

The following is a description of the signal flow from the simulated rate gyro pickoff to the output of the valve drivers. All circuits that are to be described are triple unit redundant.

The simulator included in this system supplies a d-c simulated rate signal to the controller. This signal is modulated by a 400 cps square wave by passing it through a synchronous switch. The resultant modulated signal is then shaped by the inverse model. The inverse model is a second order network consisting of complex zeros and two real poles. The transfer function of this network has the form:

$$Fn(s) = \frac{s^2 + 2\zeta\omega_n s + \omega_n^2}{(s + \alpha)(s + \zeta)} \qquad (16)$$

This network can be realized by the proper summation of two lag networks and one direct path. One lag network is realized by the synchronous switching of a capacitor in the feedback of a high gain, wide-bandwidth amplifier, and the other is realized by an RC network with the capacitor placed between a synchronous switch . The outputs of these networks are added along with a direct output from the simulated rate signal to form the previously noted transfer function.

The dither generator is added to the system through one of the lag networks of the inverse model. The dither generator is an astable 30 radians/sec multivibrator with a synchronous switch modulating its output. Although the dither generator has a square wave output, the output valve current that results will be triangluar due to the shaping networks that are in the direct transmission path. The output of the inverse model is then multiplied by the proper gain that is determined by the adaptive loop. The multiplier is a unique pulse width type, using the same synchronous switches and amplifier modules that are used throughout the rest of the system. The multiplier is a natural outgrowth of the analog type square wave carrier system described in Section IIIA.

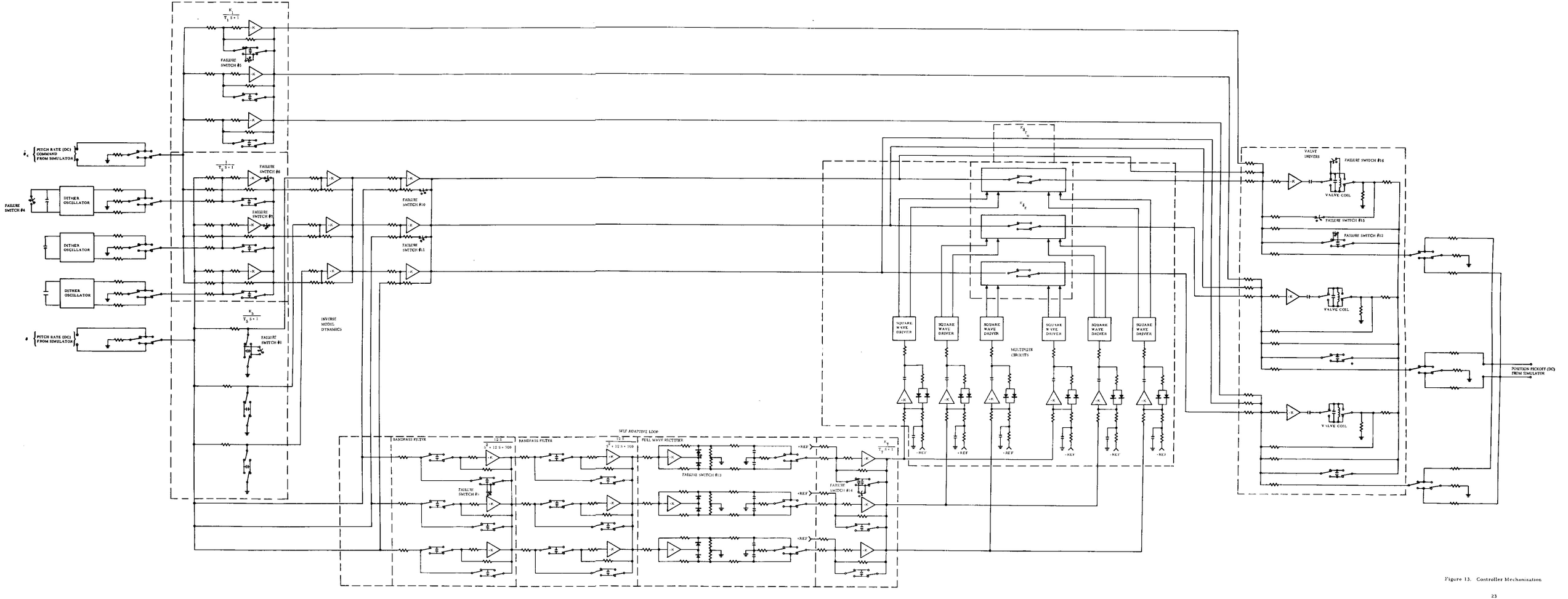

Figure 13. Controller Mechanisation

Capitalization of the square wave forms of the reference voltages and carrier signals has resulted in the relatively simple four-quandrant or two-quandrant multiplier schematically described by Figure 14. The operation of the multiplier can best be understood by means of a graphical analysis. This will require that the wave forms of the e_1 and e_2 voltages be time referenced with the push-pull reference voltages.

It can be reasoned that an increase in magnitude of e_1 will shift the zero cross over points of the sum of the currents leading into the amplifier. The shift in the top and bottom amplifiers will be in opposite directions about the center points of each half cycle of the reference voltages, the actual directions dependent on the polarity at e_1. Thus, if e_1 is zero, but no so e_2, the input currents to the

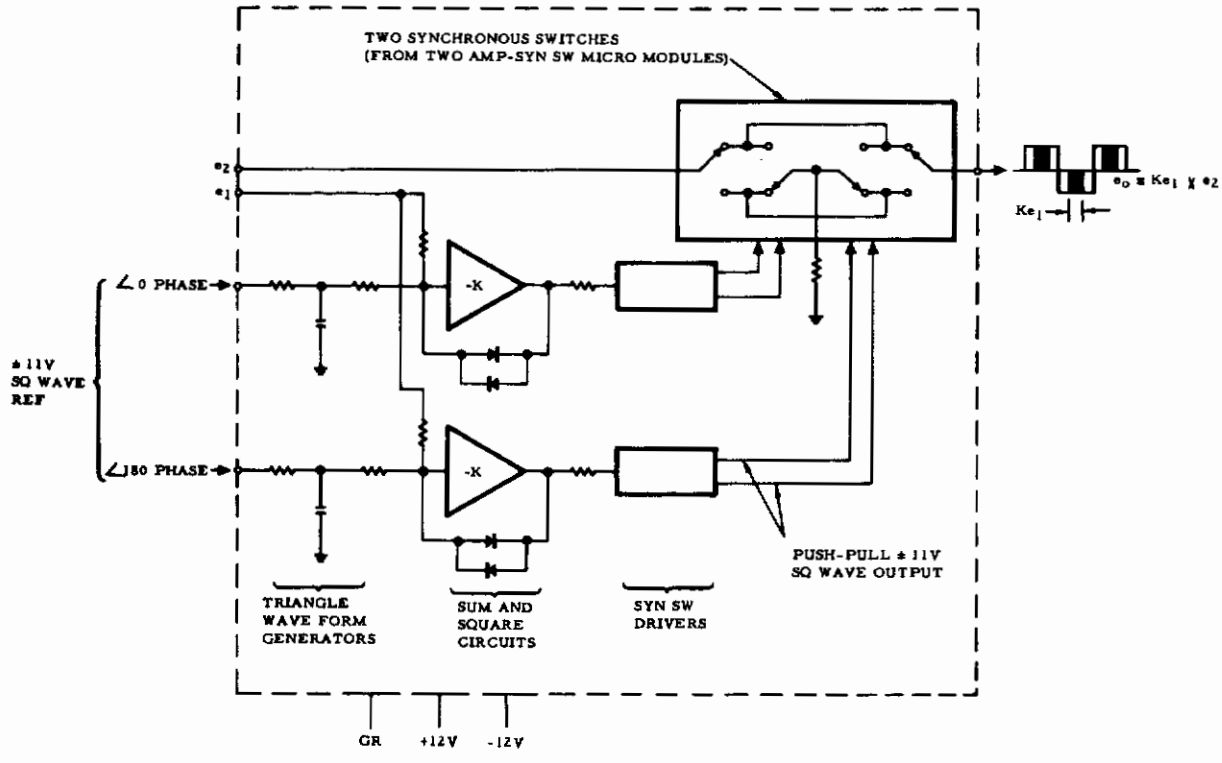

Figure 14. Multiplier Mechanization

amplifier will be 180 degrees out of phase. The two synchronous switches will likewise be 180 degrees out of phase and none of e_2 will be transmitted to the output.

A significant feature is the cancellation of "error" introduced in one channel by the "error" introduced by the other. The error inferred is the shift in the "on-to-off" and "off-to-on" switching points of the synchronous switches by the sources:

1. Imperfect integration of the square wave reference voltages which yields a slight advance in the zero crossing points of the triangular signals

2. Transmission delay across the amplifiers

3. Switching delay in the switching logic switches.

Note that the pulse width, Ke_1, will not be affected, since the shifts in the two channels should be very nearly equal. In particular, this means that the product accuracy as e_1 approaches zero will be exceptionally high. In turn, the usable product range will be high; possibly as high as 1 to 10,000 for a 400 cps carrier. After the proper gain has been established by the multiplier, the signal is sent to the valve driver unit along with the shaped rate command signal. The shaping on the rate command is a lag network comprised of a synchronous switched capacitor in the feedback of an amplifier. The valve driver loop is composed of an amplifier driving a valve coil through a set of solid-state synchronous switches. In this manner, signal frequencies are furnished to the valve coil and carrier frequencies are restored and used for current feedback. The position loop is closed by feedback from the pickoff of the series servo, or from the output of the simulator representing surface position. The information that is used to adjust the gain for different flight cases is processed through the adaptive loop. The adaptive loop is composed of bandpass, full wave detector, and integrator units. Its operation is as follows: The dither frequency that has passed to the hydraulic actuator is sensed by the rate gyros through the dynamics of the aircraft. This frequency is singled out from the composite signal at the output of the rate gyros by passing it into the bandpass unit. The bandpass unit is synthesized by placing synchronous switched capacitors in the feedback

as well as the forward path of an amplifier. The resulting transfer function for the bandpass unit is:

$$F(s) = \frac{Ks}{s^2 + 2\zeta\omega_m s + \omega_n^2} \qquad (17)$$

To obtain the desired selectivity and gain, two of these units are cascaded. After the dither frequency has been recovered, the amplitude is detected by rectifying the signal and filtering out the carrier frequency. To eliminate the dead band in the detector unit, a diode is placed in the forward loop of a feedback amplifier. Once the amplitude of the dither frequency has been detected, the carrier frequency is restored by sampling with a synchronous switch. The amplitude of the dither frequency is then compared with a fixed reference and passed to the integrator unit. The integrator unit is mechanized by placing a synchronous switched capacitor in the feedback of an amplifier. The output of the integrator is used as the gain changing signal for the system.

2. Simulator

The simulator assembly contains the power supply for the controller, the aircraft and servo simulator, and associated controls for these functions. The simulator mechanization is shown in Figure 15.

The open loop dynamics are represented by $\frac{30}{s}$ for the series servo and $\frac{10}{s + 10}$ for the power servo. These transfer functions approximate typical dynamics of hydraulic actuators used in high performance tactical aircraft, and are mechanized with four operational amplifiers. When the loop around the series actuator is closed through the controller, the series servo transfer function becomes $\frac{30}{s + 30}$.

The airframe pitch axis transfer function is mechanized with four operational amplifiers. A flight case switch is provided to give five fixed stable flight cases plus one unstable flight case or the flight cases may be manually set by means of the following potentiometers:

$$\frac{M_{\delta_E}}{100}, \quad \frac{M_{\delta_E}{}^a}{200}, \quad \frac{\zeta\omega}{5}, \quad \frac{\omega^2}{100}.$$

Figure 15. Simulator Mechanization

The airframe transfer function is:

$$\frac{\dot{\theta}}{\delta_E} = \frac{M_{\delta_E}(s + a)}{s^2 + 2\zeta\omega s + \omega^2} \qquad (18)$$

Thus, the airframe poles and zeroes may be made to locate over a large domain of the s plane by merely selecting switch positions and adjusting gain pots.

Monitoring meters are provided on the face of the simulator to display $\dot{\theta}$ and $\dot{\theta}_c$. In addition, two recorder select switches display $\dot{\theta}_c$, δ_a, δ_E, $\dot{\theta}$ and calibrate. An internal source is provided to give pitch rate step command. A three position switch is provided to allow selection of either phase pitch step command, or an external input.

E. RELIABILITY ANALYSIS

1. General

The following analysis shows the reliability that can be attained through a TRISAFE stability augmentation system mechanization. A Mean Time Before Functional Loss (MTBFL) figure, based on two hours of operation, is used since a MTBF figure is not directly applicable in a triple unit-redundant system. This analysis is made using the assumptions:

1. An exponential distribution of time exists between failures for the useful life of the component parts.

2. The failure rate figures apply to operation during the useful life period only. They do not apply to debugging or wearout regions.

3. All electronic parts are operating at 50 percent or less of their maximum ratings.

2. Methodology of Analysis

For ease of analysis, each component of a subunit within the TRISAFE or triple redundant unit is classified according to the effect of its failure on the unit output. Input and feedback components can be considered as compensation components, and failure in one of these components results in a large, erratic amplifier output. Any component

yielding this result is classified as a compensation, subscript C, component. On the other hand, since a failure of an amplifier component nearly always results in a zero or near-zero amplifier output, any component yielding this result is classified as an amplifier, subscript A, component. This classification of components is the basis for the reliability model shown in Figure 16.

A truth table approach is used to derive the approximate equations used in the analysis of the SAS reliability model. For each TRISAFE unit the notation used is:

Amplifier component failure mode = 1

Compensation component failure mode = 2

Normal operation = 0

A failure of any TRISAFE item can occur in two ways: one large output failure coupled with any other failure mode, or two zero output failures when coupled with any other failure mode. Table 3 is the TRISAFE truth table.

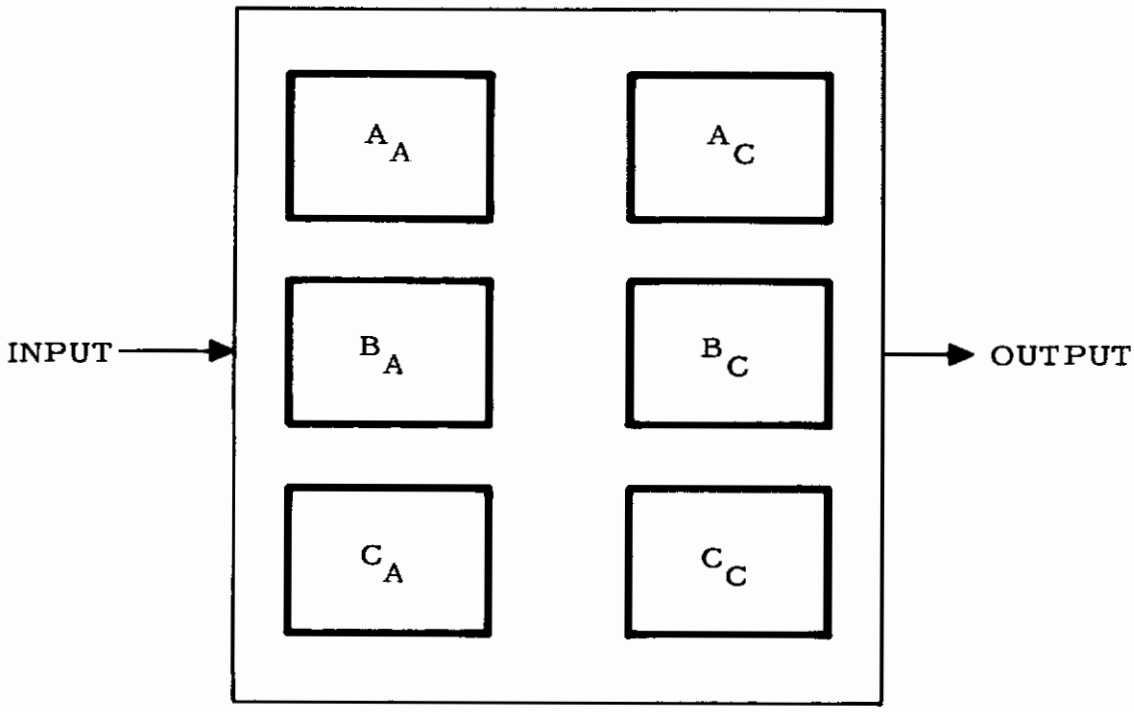

Figure 16. Unit Reliability Model

Table 3. TRISAFE Truth Table

No. of Permutations	Subunit A	Subunit B	Subunit C	Final Condition	Basic Probability		
1	0	0	0	Operates	P	P	P
3	1	0	0	Operates	Q_A	P	P
3	1	1	0	Operates	Q_A	Q_A	P
1	1	1	1	Failure	Q_A	Q_A	Q_A
3	2	0	0	Operates	Q_C	P	P
3	2	2	0	Failure	Q_C	Q_C	P
1	2	2	2	Failure	Q_C	Q_C	Q_C
3	2	1	1	Failure	Q_C	Q_A	Q_A
3	2	2	1	Failure	Q_C	Q_C	Q_A
6	0	1	2	Failure	P	Q_A	Q_C

P = Probability that the total subunit is operating normally.

Q_A = Probability of an amplifier component failure.

Q_C = Probability of a compensating component failure.

The number of permutations in the truth table indicates the number of different ways that combinations can occur, e.g., 100 also could be 010 or 001. It should be noted that failure modes are considered to be independent. Since the approximate equation is of interest and because those probability terms added by considering the dependent model are at least an order of magnitude less than the predominate probabilities, the dependent terms are dropped.

Since the probability of amplifier and compensation component failure, Q_A and Q_C, is small with respect to P, only those probabilitie containing Q_A's or Q_C's are at least one order of magnitude less than those containing one P. Consequently, the probability of failure of the TRISAFE unit as a whole is:

$$Q \approx (3Q_C^2 + 6\,Q_A Q_C) \text{ or } Q = (3/M_C^2 + 6/M_C M_A)\,t^2 \qquad (19)$$

where the equations

$$Q_C = 1 - e^{-t/M_C} \approx t/M_C \qquad (20)$$

$$Q_A = 1 - e^{-t/M_A} \approx t/M_A \qquad (21)$$

are used as good approximations of small Q_A and Q_C. Here, M_A and M_C are MTBF's of the item's amplifier and compensation components, respectively. In terms of failure rates $M_A = 1/Q_A$ and $M_C = 1/Q_C$.

3. Reliability Prediction

To illustrate the reliability improvement afforded by TRISAFE, results of failure probability computations made in accordance with the previous relationships and based upon the failure rates indicated, are presented in Table 4. The failure rates listed for electronic circuits are based upon 1960 figures of MINUTEMAN discrete parts and predicted MINUTEMAN integrated circuit complexity. Derating factors were added to account for a low volume (prototype) system. Failure rates are specified in terms of the zero amplifier output or a large amplifier output within a redundant electronic unit.

This analysis for a previously designed system of the type provided includes only the electronics in the controller package. The mean time before functional loss (based on a two hour mission and corrective maintenance actions as required for first failures) is 1.1×10^9 hour.

Table 4. Reliability Prediction

Units	Q_C	Q_A	Q (first failure)	MTBFF Hrs.	Q* (Functional) 2-Hr Mission	MTBFL* 2-Hr Mission
Differentiator (part of inverse model and adaptive loop)	2.6×10^{-6}	2×10^{-6}	13.8×10^{-6}	72,000	0.000206×10^{-6}	9.7×10^{9}
Lag-Lead (part of inverse model)	0.20×10^{-6}	2×10^{-6}	6.6×10^{-6}	150,000	0.0001×10^{-6}	20×10^{9}
Band Pass filter	2.6×10^{-6}	2×10^{-6}	13.8×10^{-6}	72,000	0.000206×10^{-6}	9.7×10^{9}
Rectifier-Integrator Multiplier	6.8×10^{-6}	2×10^{-6}	26.4×10^{-6}	38,000	0.00088×10^{-6}	2.3×10^{9}
Dither Generator	0.20×10^{-6}	2×10^{-6}	6.6×10^{-6}	150,000	0.0001×10^{-6}	20×10^{9}
Summing Amplifier	0.20×10^{-6}	2×10^{-6}	6.6×10^{-6}	150,000	0.0001×10^{-6}	20×10^{9}
Lead-Lag Servo feedback	2.6×10^{-6}	2×10^{-6}	13.8×10^{-6}	72,000	0.000206×10^{-6}	9.7×10^{9}

Table 4. (Cont)

Units	Q_C	Q_A	Q (first failure)	MTBFF Hrs.	Q* (Functional) 2-Hr Mission	MTBFL* 2-Hr Mission
Valve Driver (includes valve coil	0.1×10^{-6}	20×10^{-6}	60.3×10^{-6}	16,600	0.000048×10^{-6}	42×10^{9}
Total System			268×10^{-6}	3720	0.0018×10^{-6}	1.1×10^{9}

MTBFF = Mean Time Before First Failure in Hours
MTBFL = Mean Time Before Functional Loss in Hours
*Triple Redundant System

It should be pointed out that if redundancy were applied on a channel level, the probability of failure would be 0.096×10^{-6} if an infinitely reliable monitor is assumed compared with 0.0018×10^{-6} for unit redundancy. This is roughly fifty times higher than probability of failure would be with unit redundancy. Actually, the difference between channel level and unit level redundancy would be somewhat higher if monitor failure were considered.

III. EQUIPMENT DESCRIPTION

A. CONTROLLER

1. Circuit Design

Signal processing in control systems can be accomplished in various ways. The most basic is the direct processing of the control frequencies from the sensors to the actuators. Although this method is the least complex, it is not used because of the inherent drift of the d-c amplifiers required. A somewhat more complex system that yields high accuracy can be used to overcome the shortcomings of the d-c system. A-c carrier systems in which the information frequencies are used to modulate a higher carrier frequency are of common use throughout the flight control industry. The conventional carrier system employs a high frequency sine wave for the carrier. When it is required to operate on the information frequencies, the carrier signal must first be removed and then replaced after the actual operation has been performed. The removal of the carrier is accomplished by the use of a demodulator and the replacement of the carrier by a modulator. With the use of a high frequency square wave as the carrier signal, the demodulation-remodulation process becomes much less complex and is accomplished more efficiently. Transfer functions can be realized by operational amplifier techniques, and the number of amplifiers needed to perform the desired operation can be reduced as well as the size and volume of the passive components. Figure 17 shows a typical differentiation network mechanized using both the conventional sinusoidal carrier and the square wave carrier. An approximation of the relative size of the two units can be made by totaling the element volume of each component. In the sine wave system an amplifier is required to drive the demodulator and a ripple filter is necessary after the demodulator. As a result, the sine wave system requires extra amplifiers as well as excessive passive components to realize the same transfer function.

Due to the large insertion loss associated with the passive networks of a sine wave system, an additional amplifier in the output stage would be required to realize the same gain as the square wave network. For networks requiring large time constants, the capacitor size is reduced by the use of a square wave carrier and synchronous shaping.

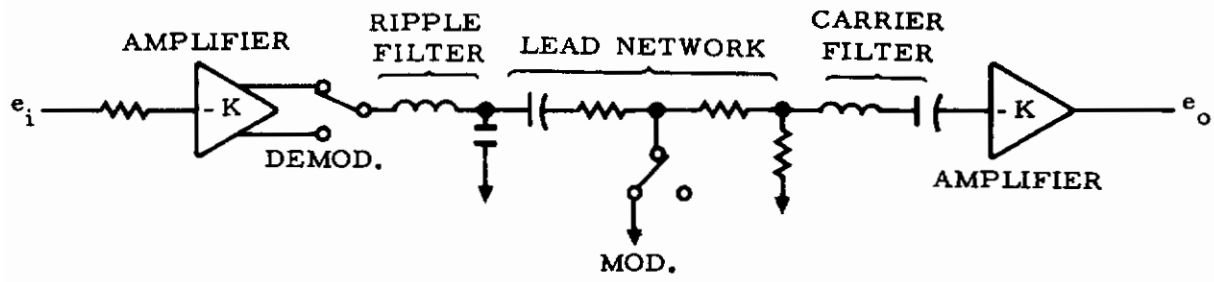

(SINE WAVE CARRIER)

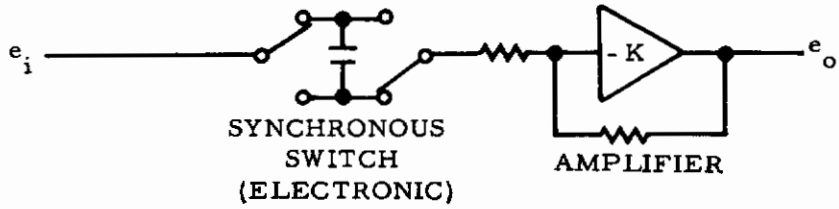

(SQUARE WAVE CARRIER)

Figure 17. Lead Network

Figure 18 shows a typical mechanization of a bandpass filter along with its response to a unit step function. The double envelope of the information frequency caused by the presence of the square wave carrier is shown. As can be seen, good clean signals requiring no additional filtering of the carrier are obtained by this method. Evaluation of this system with respect to theoretical versus actual results has indicated excellent agreement.

It has been shown that the square wave carrier approach is a proven technique and the use of it results in a compact, low cost system exhibiting excellent characteristics.

2. Module Design

a. A-C Amplifier P/N 55150-502

The A-C Amplifier is a three stage d-c coupled amplifier comprising an integrated monolithic circuit and discrete microminiature elements. The amplifier circuit features high a-c gain, low input and output impedance, and output current limiting necessary for TRISAFE operation. Figure 19 is a schematic diagram of the amplifier circuit.

The amplifier which was designed for flight control applications, utilizes d-c feedback to obtain a high degree of d-c stability. The open loop gain (resistor R4 shorted) is 160 volts per microamp minimum to 320 volts per microamp maximum. The value of R4 is such as to make the loop gain KH=20.

The amplifier output with no current limiting is ±5.5V peak into a 10K ohm load. Current limiting is provided by the diode bridge along with R5 and R6. As the amplifier output voltage increases, diode CR1 will become back biased and the current through CR3 will be supplied by the amplifier. The current through CR2 will be supplied by +12V via R5 and the load. Current limiting occurs when the amplifier output supplies approximately 0.8 ma through CR3 and R6 and the load current is supplied via resistor, R5, and diode, CR2. When the amplifier output is negative, the reverse conditon occurs with load current limited by the path through R6 and CR4.

b. Synchronous Switch P/N 55100-504

The Synchronous Switch comprises four junction type field effect

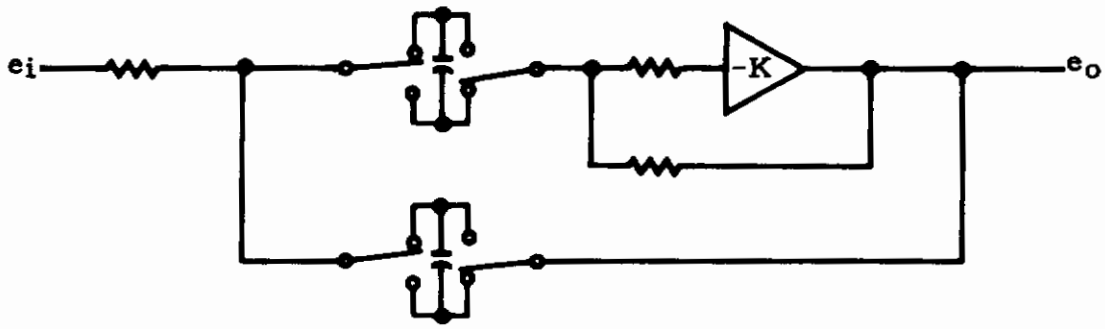

BAND PASS UNIT

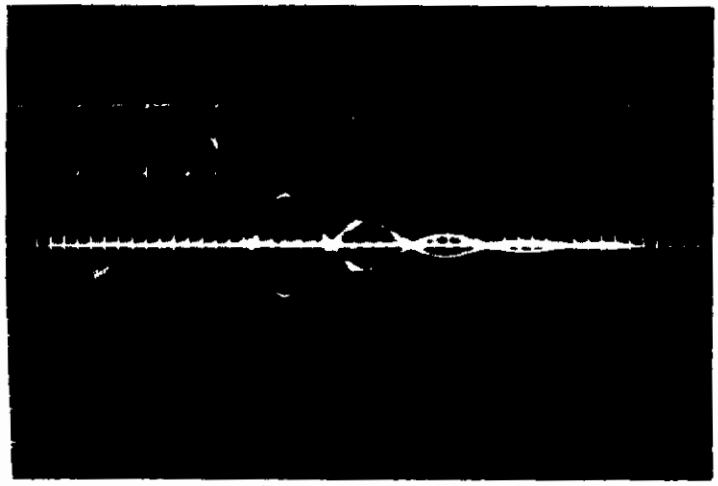

DOUBLE ENVELOPE OF INFORMATION FREQUENCY

Figure 18. Bandpass Filter

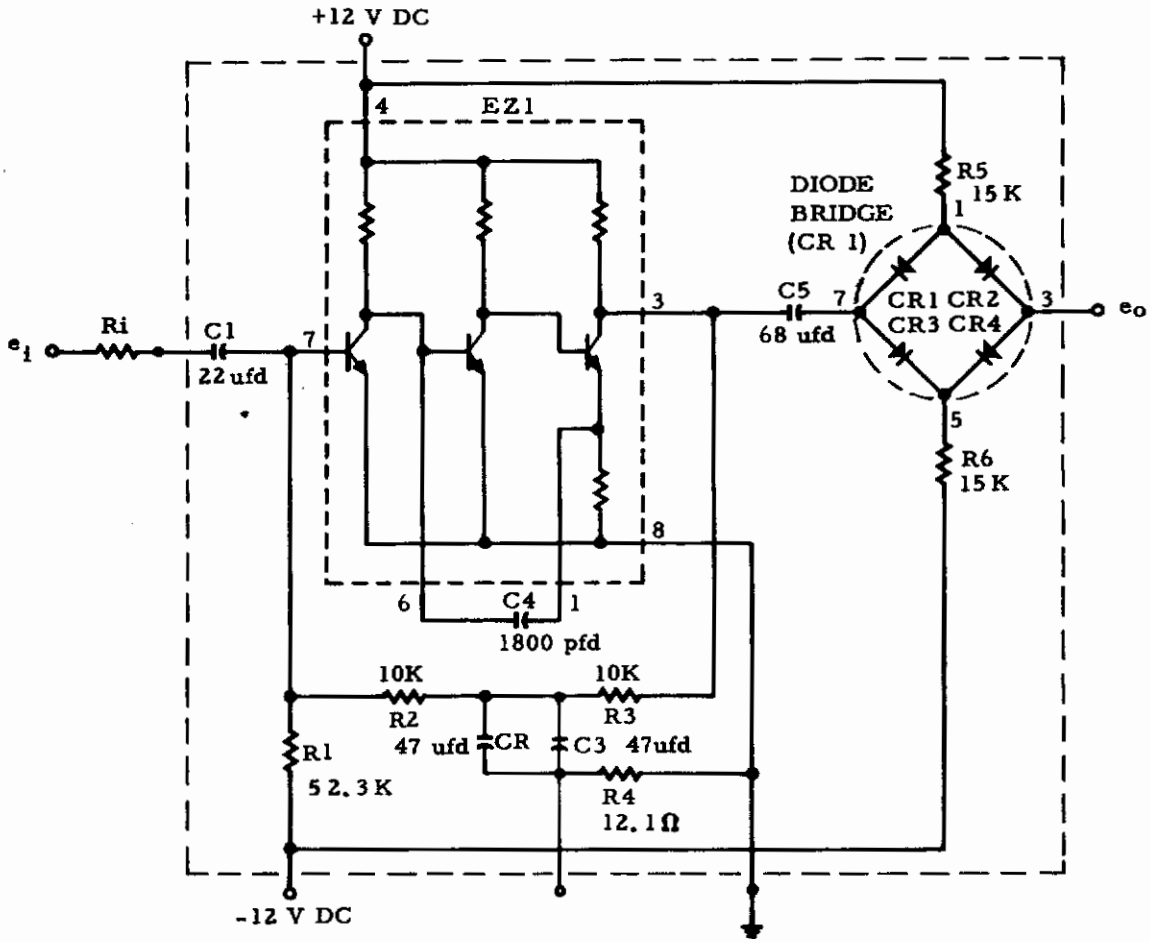

Figure 19. A-C Amplifier

transistors (FET) in a TO-5 can and is shown schematically in Figure 20. The FET's operate as synchronous pairs driven on and off by a two-phase ±11 V square wave reference voltage. When the square wave reference voltage at e_{D1} is positive in respect to e_{D2}, FET's Q7 and Q8 are saturated, and Q3 and Q4 are turned off. An input signal at e_i will then appear across a load impedance connected between terminals, L1 and L2.

The Synchronous Switch is capable of conducting signal currents in either direction with a total on resistance of approximately 150 ohms. The gate power dissipation in the on state is less than 1 mw. In the off state the FET's present an off impedance greater than 10^{10} ohms. The control signal null voltage is dependent upon the rise time characteristics of the square wave reference voltage. With a square wave reference voltage rise and fall time of 20 nanoseconds and a 0.33 mf capacitor connected across the load terminals, the synchronous switch null is less than 0.5 millivolts across a 50 K load resistor.

The diodes are used to prevent the flow of gate current and the capacitors are used to discharge the junction capacitance of each FET.

c. Synchronous Switch Driver P/N 55105-504

The Synchronous Switch Driver circuit is a power flip-flop designed to provide the system with an accurate computational reference voltage and to drive the synchronous switches and excite the sensor pickoffs. Refer to Figure 21.

The input two-phase triggering voltage will be derived from the output of the carrier generator which produces a 400 cps square wave of ±1 V. The output of the switch driver, a ±11 V 400 cps highly symmetrical square wave, has a rise and fall time of less than 20 nanoseconds. The excellent switching characteristics are accomplished by the use of speed-up capacitors and a high amount of regenerative feedback. The two-phase output can deliver switching currents in excess of 100 ma to a 100-ohm load.

d. Voltage Regulator, P/N 56650-401

The d-c Voltage Regulator provides the system electronics with a highly regulated d-c voltage and short circuit load protection.

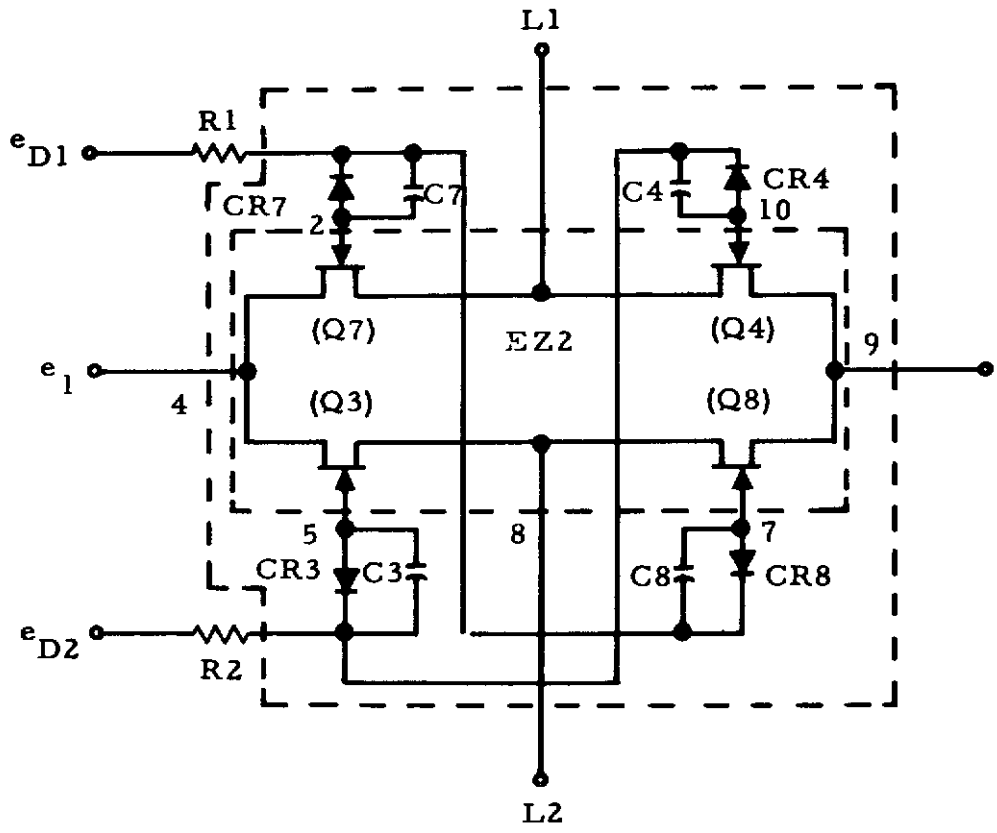

Note: Only half of synchronous switch module is shown, other half is similar. All capacitors are 33pfd. All Diodes are IN457

Figure 20. Synchronous Switch

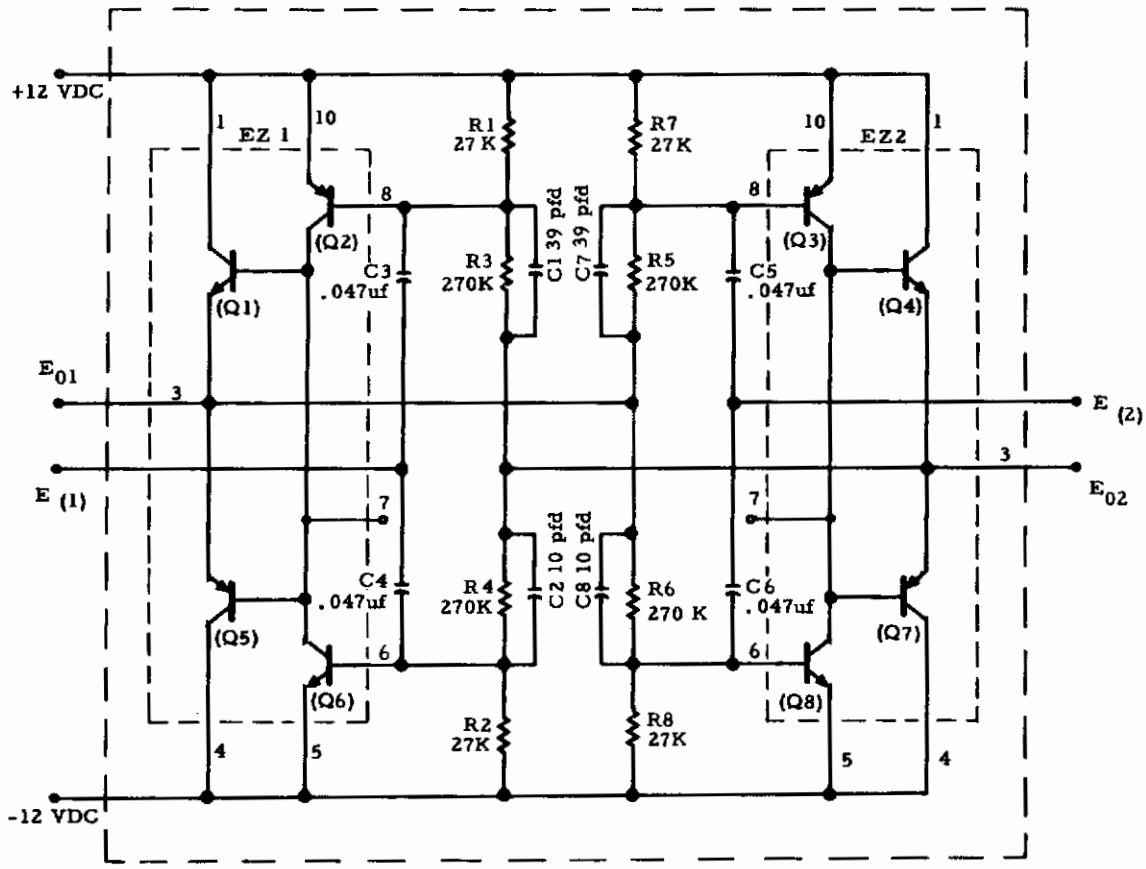

Figure 21. Switch Driver

The circuit is a class A series voltage regulator utilizing high gain, high frequency silicon transistors. Figure 22 is a schematic diagram of the regulator. The effective parallel connected series regulator transistors, Q1 and Q3, share the d-c load current (75 ma) via their emitter current sharing resistors. During normal operation, transistor Q2 is in saturation.

The high gain error amplifier, Q5 derives its collector current from a constant current source comprising Q4, CR1, and CR2. Transistor, Q6, provides the current gain required to drive the series regulator. The E' test voltage is held constant by providing an adquate amount of feedback to the error amplifier via resistor, R3.

Regulation for line and load variations is less than 0.1 percent and the variation due to temperature changes is 0.25 millivolts/degree centigrade. The dynamic output impedance is less than 0.25 ohms at 5 megacycles.

The regulator is inherently short circuit protected from an external load short or a short within the device. An external load short will force transistor Q3 to saturate forcing the collector emitter current of Q6 to cut off transistor Q1 and subsequently Q2. Since the current of transistor Q6 cannot supply the load current, the load current will limit at a very low value.

e. Carrier Generator, P/N 55160-502

The Carrier Generator is a modified emitter coupled multivibrator designed to provide the system electronics with an accurate timing voltage. A schematic of the carrier generator is shown in Figure 23.

The basic emitter coupled multivibrator circuit comprises Q2A, Q2B resistors R2, R3, R4, R7, R8, R10 and a capacitor connected from terminals C1-C2. Transistors Q1A and Q1B, with their associated biasing resistors R1, R5, R6, R9, comprise two constant current generators, one in each emitter leg of the basic multivibrator.

Through the use of a constant current generator, the charge buildup on the timing capacitor is very linear during each half cycle

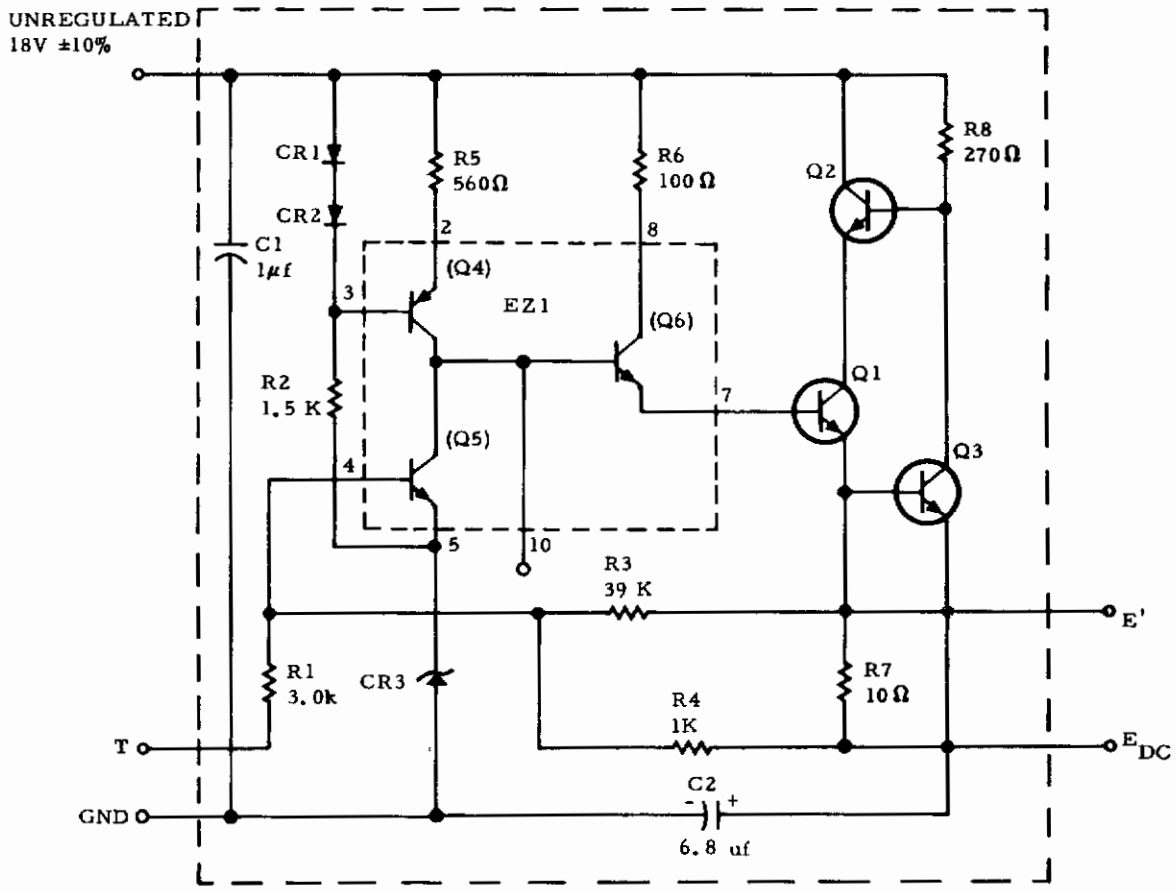

Figure 22. Voltage Regulator

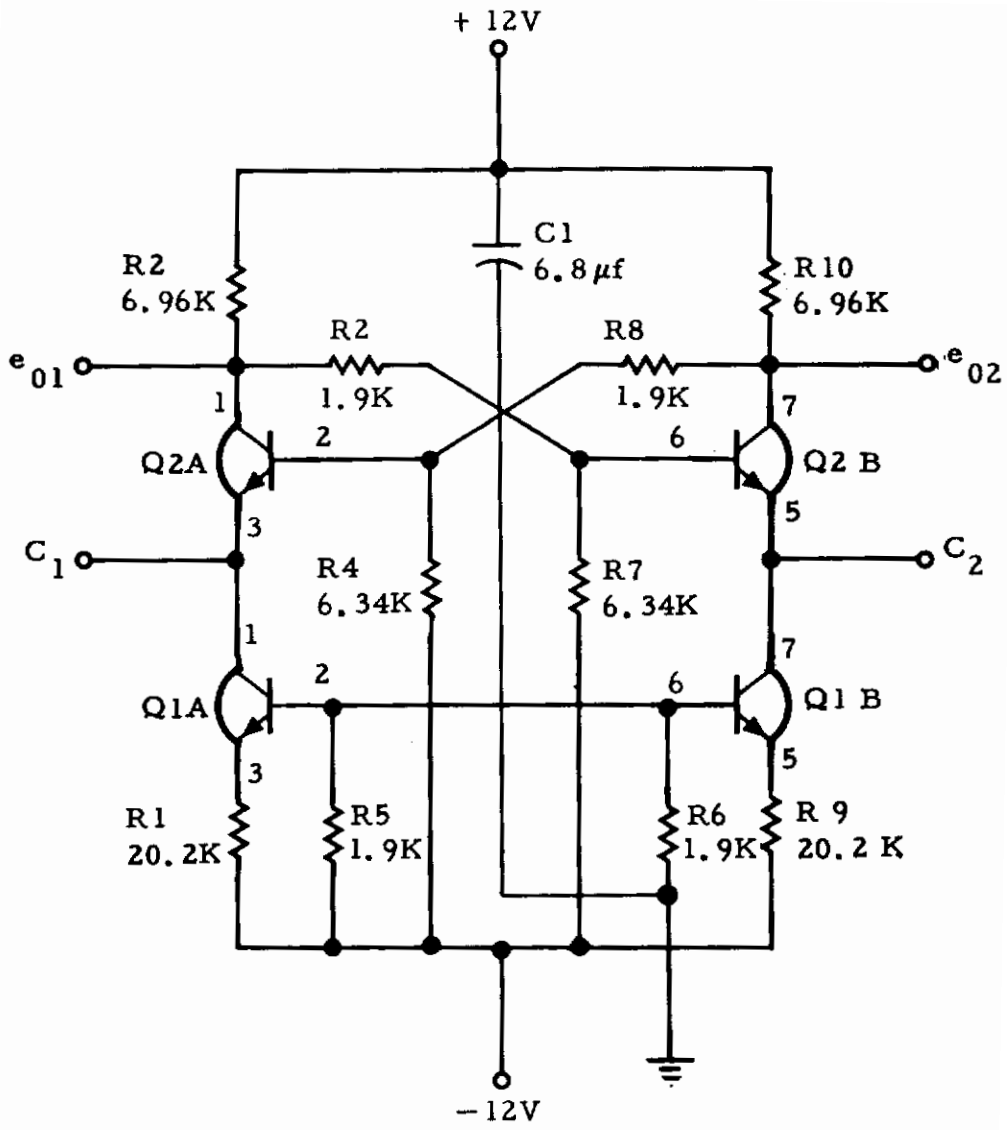

Figure 23. Carrier Generator

of operation. The linear charging of the capacitor results in a highly symmetrical square wave output at e_{01} and e_{02}.

The advantages of this modified multivibrator is the elimination of circuit recovery time to produce a symmetrical square waveform, stable frequency operation with power supply variation, and excellent thermal stability.

3. Packaging

In the interest of maintainability and producibility, a packaging scheme has been adapted wherein each integrated circuit and its associated discrete parts comprising a function are packaged in an encapsulated, plug-in, module (see Figure 24). These modules (76 total) are all of uniform size 0.6 x 0.8 x 1.0 in. The volume of each is approximately 1/2cu. in. Each module has terminal pins protruding from the bottom surface which are plugged into sockets in the master interconnect circuit board, and can be easily removed for replacement as required. All shaping network and gain adjustment components are mounted on the reverse side of the master interconnect board which is of multilayer design. This electronic assembly is then able to slide into the dust cover along positioning rails for insertion into a board edge connector. The side rails are an integral part of the connector, therefore giving ideal positioning of the board into the connector. The back panel is rigidly attached to the electronic assembly. This furnishes a sliding drawer technique for easy insertion and removal of the entire electronic assembly. After insertion of the electronic assembly, four screws hold it in place in the dust cover.

B. SIMULATOR

In order to demonstrate the operation of the system without requiring a large amount of peripheral equipment, a flight simulator has been designed which is shown in Figure 25. The controller is connected by cable to the simulator, and all adjustments, both system gains and of airframe characteristics, are accomplished by means of controls on the face of the simulator.

The simulator is a compact, self-contained analog computer. The circuitry within the computer has been mechanized with solid state chopper-stabilized d-c operational amplifiers. This approach

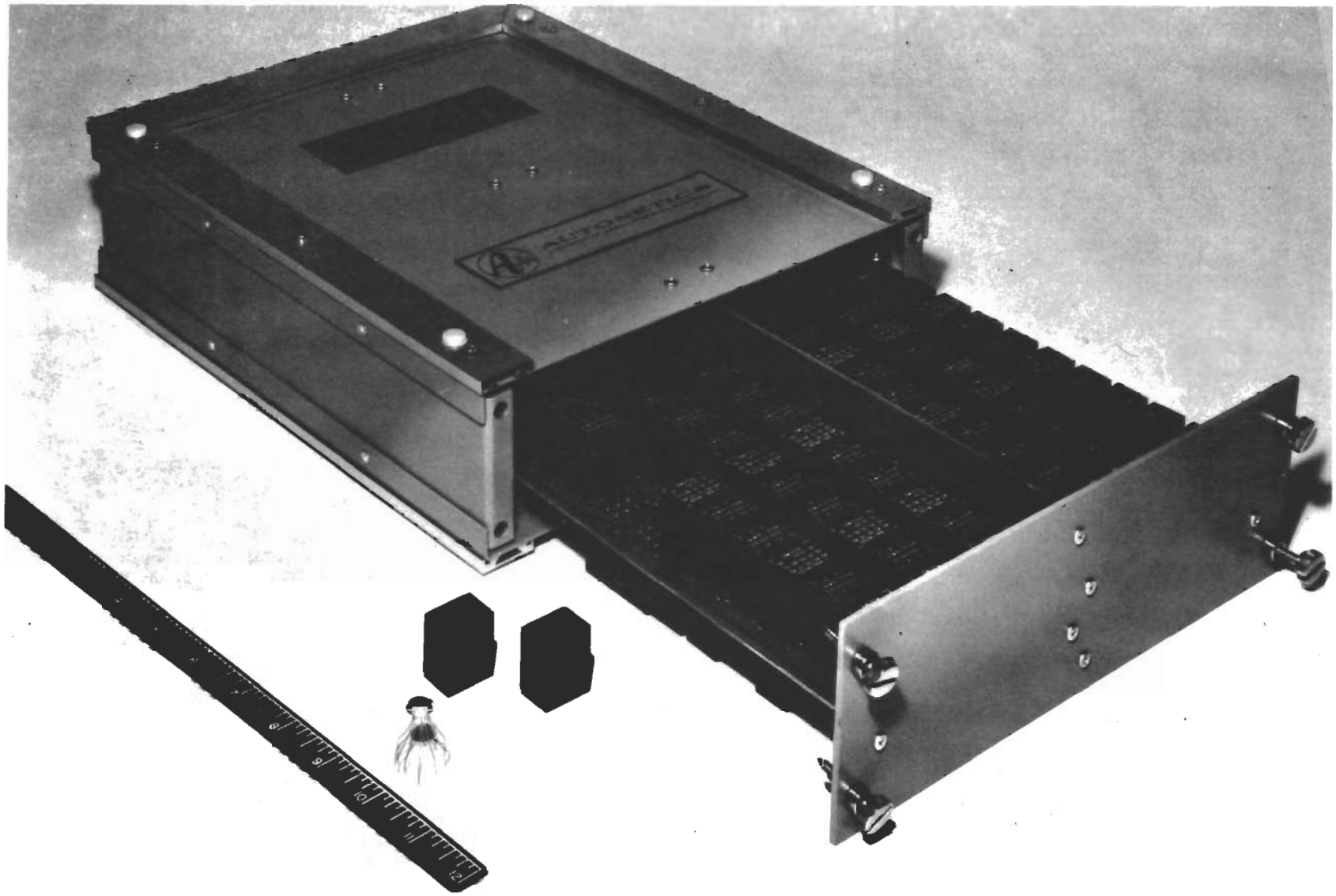

Figure 24. Controller Packaging

Figure 25. Simulator Assembly

was chosen because of the extreme flexibility and precision it provides for the variation of airframe and servo dynamics.

The chopper-stabilization in the operational d-c amplifiers provides for continuous automatic balancing while the amplifier is in operation. This feature in the amplifier reduces any drift voltage at the input by a factor of about 1,000. Without this feature d-c amplifiers have a tendency to drift, giving some output voltage for zero input, and thereby yielding erroneous results in the simulation. These amplifiers are also provided with a manual balance control which supplies a voltage to null any existing drift voltage at the amplifier input. When this adjustment has been made, the automatic balancing circuit keeps the amplifier in balance during the operation of the simulator. When the automatic balancing circuit is in operation, any drift voltage at the input to the d-c amplifier is converted to a-c by a chopper, amplified as a-c, converted to a pulsating d-c signal, filtered to become d-c again and applied to the d-c amplifier input in opposite polarity to null the drift. A separate meter and amplifier selector switch is provided under the top panel cover to select and read the amplifier null. The meter and selector switch are disconnected when the mode switch is not in balance check.

C. POWER SUPPLIES

A power supply is provided within the simulator unit to furnish all required a-c and d-c potentials to the electronic components and amplifiers in the simulator. The power supply for the controller is also located in the simulator and provides all the d-c power to the controller. These supplies are built in a conventional manner, using standard parts and circuits.

In order to provide maximum ease and convenience of use of the system, the power supply will work from either aircraft of laboratory electrical supply sources (115 V, 50 to 400 cps).

D. RECORDER

A dual-channel recorder, complete with high-sensitivity d-c amplifiers and slaving capabilities to the simulator master control, is provided for use with the simulator. This recorder has solid state electronics, heat writing styli, roll or Z fold paper packs and weighs approximately 50 pounds. See Figure 26.

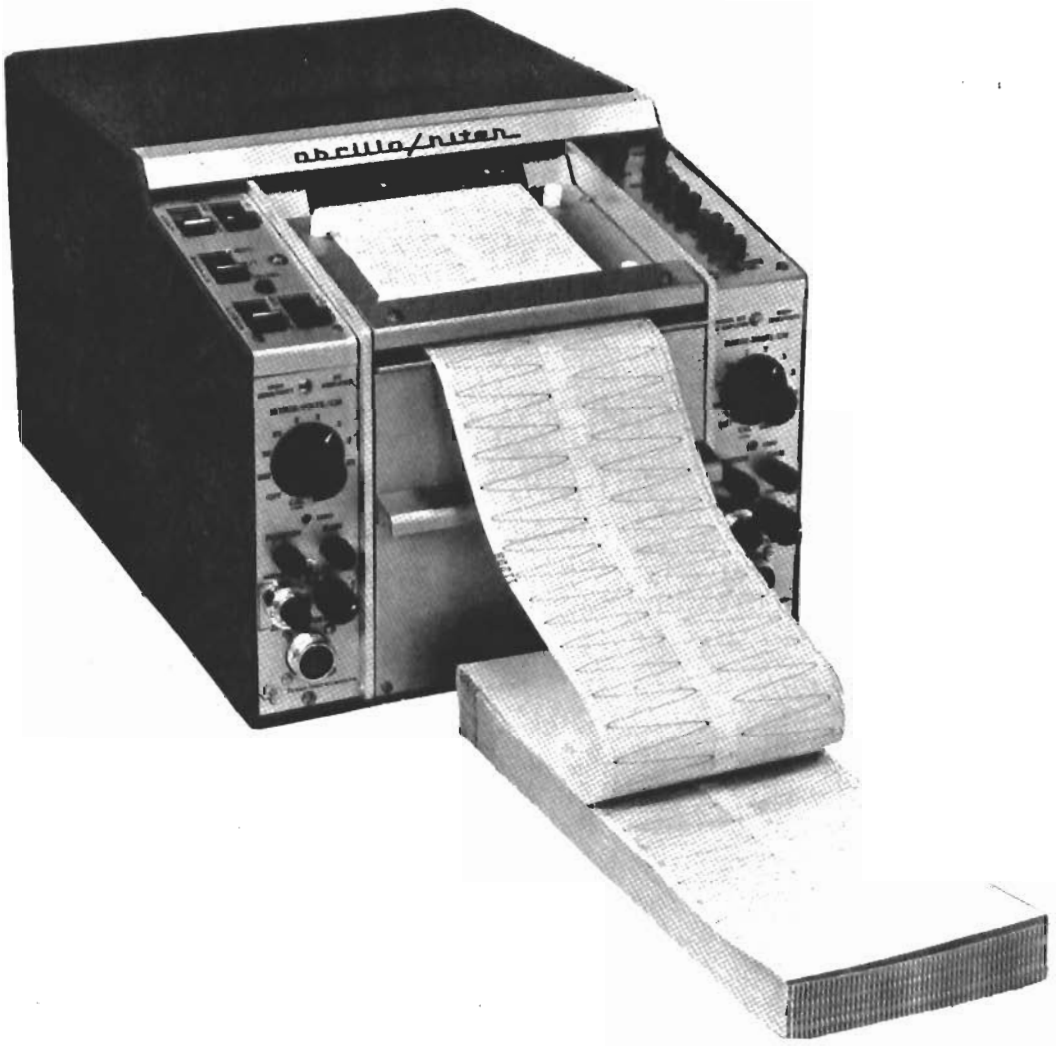

Figure 26. Dual-Channel Recorder

IV. SYSTEM DEMONSTRATION

The system is fabricated to provide flexibility of circuit parameters for demonstration. This flexibility allows variation of the airframe dynamics, servo dynamics, controller dynamics, and provides the capability of failure simulation.

A. AIRFRAME DYNAMICS

Because the simulator contains provision for variation of the short period dynamics to other than those depicted, a criteria must be introduced to prevent unrealistic combinations of pole-zero locations and elevator effectiveness.

The following ranges and relationships should be adhered to when selecting flight conditions at random:

$$1 < M_\delta < 90 \text{ deg/deg } M_\delta = M_{\delta_E} - L_{\delta_E} M\dot{\alpha} \tag{22}$$

$$0.2 < a < 2.0 \text{ rad/sec } a = \frac{\frac{T}{mV} M_{\delta_E} + M_{\delta E} L_\alpha - M_\alpha L_{\delta_E}}{M_{\delta_E} - L_{\delta_E} M_{\dot{\alpha}}} \tag{23}$$

$$-0.4 < \zeta_A < 1.0 \qquad \omega_A \zeta_A = \frac{\frac{T}{mV} + L_\alpha - M_q - M_{\dot{\alpha}}}{2} \tag{24}$$

$$0.5 < \omega_A < 10 \text{ rad/sec} \qquad \omega_A = \left[-Mq \left(L_\delta + \frac{T}{mV} - M_\delta\right]^{\frac{1}{2}}\right. \tag{25}$$

While it is felt that any combination of the above parameters will be stabilized by the system with a large improvement in transient response, it is stressed that his system is tailored to a particular aircraft. Since fixed compensation and shaping networks are specified, it is unrealistic to assume these same values will be appropriate for the dynamics of an aircraft whose geometry may be completely different. This system is not a universal SAS and degradation in system performance may be expected.

The transfer functions and the parametric ranges available include the short period dynamics of most high performance aircraft. The availability of plus and minus signs on two terms of the characteristic equation provides the capability of selecting the dynamics of either a stable or an unstable aircraft, i.e., airframe dynamics with real poles in the left and right half-planes.

B. SERVO DYNAMICS

The simulator assembly, when coupled to the controller, provides the following transfer function to represent the series and power servos:

$$\frac{\delta_E}{\delta_c} = \left(\frac{30}{s + 30}\right)\left(\frac{10}{s + 10}\right) \tag{26}$$

This transfer function is representative of present state-of-the-art servo actuators incorporating feedback shaping.

C. CONTROLLER DYNAMICS

The dynamics of the controller are fixed. The controller is a mechanization of a single-axis stability augmentation system with an adaptive loop gain. The functions designed provide the required inverse model compensation, adaptive loop dynamics, dither oscillator, and gain changing multiplier. This mechanization is designed to provide stability augmentation to the full regime of dynamics in the short period frequency range.

D. FAILURE SIMULATION

In order to evaluate the reliability provided by the TRISAFE mechanization of the controller, a provision is made in the design to simulate typical failures. Failure mode test switches are provided on the simulator which actuate miniature relays in the controller and simulate failures (see Figure 27). The proper use of these switches allows the simulation of all typical failures.

E. CONTROL PANEL

The control panel shown on the front of the simulator in Figure 27 is divided into two parts. The upper part contains the

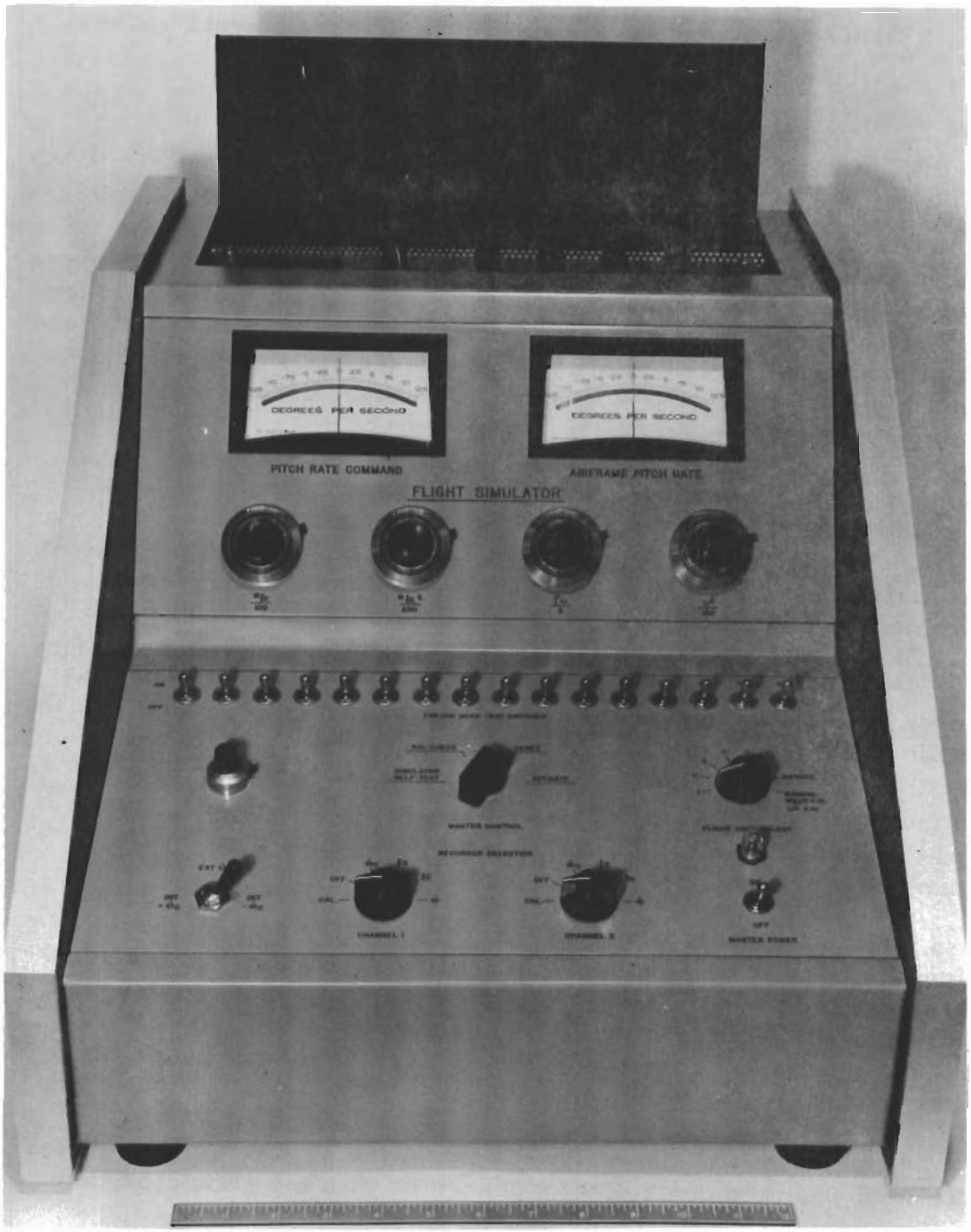

Figure 27. Simulator Showing Control Panel

$\dot{\theta}_c$, $\dot{\theta}$ meters and also the manual set flight case potentiometers:

$$\frac{M_{\delta_E}}{100}, \quad \frac{M_{\delta_E}{}^a}{200}, \quad \frac{\zeta_\omega}{5}, \quad \frac{\omega 2}{100}$$

The lower panel has a Master Power switch, Recorder Selection switches, $\pm\dot{\theta}_c$ switch, $\frac{\theta_c}{10}$ potentiometer, 15 Failure Mode Test switches, Flight Case Select switch and the Master Control switch. The operator may desire to choose any of the six fixed flight cases, thereby eliminating setting of the manual potentiometers. The second flight case is unstable. The other five flight cases are stable. If manual setting of any flight case is desired, the Flight Case Select switch must be set on Manual.

If a low dynamic pressure flight case is to be manually set, then the Flight Case Select switch must be set on Manual $M_{\delta_E}{}^a \times 10$, $\omega^2 \times 10$. This setting provides more amplifier gain in the airframe dynamics. A list of dial and switch settings for various high performance aircraft flight conditions will be provided.

The Master Control switch provides four functions which are: Reset, Operate, Bal-Check, and Simulator Self-Test. To check the offset or balance conditions of amplifiers, the Master Control switch must be placed in Bal-Check position. Located under a hinged door on the top are the Amplifier Balance pots, Amplifier Select switch, and the Balance Meter. The Balance Meter is switched off in the other positions of the Master Control switch.

To self-test the simulator, set the Master Control switch to the Simulator Self-Test position. By actuating the $\dot{\theta}_c$ switch to either plus or minus, the transfer function of any flight case may be observed on the $\dot{\theta}$ meter or recorded on the recorder. Since the controller is not checked in this mode, it need not be connected to the simulator during self-test.

The Reset and Operate positions of the Master Control switch are used when the controller is connected with the simulator, and system response tests are to be performed.

The rear panel has pilot input jacks for plus and minus external $\dot{\theta}_c$, and connectors for the controller, recorder, auxiliary and a-c power.

F. SYSTEM RESPONSE

Figures 28 through 33 are time responses of the open-loop airframe to a step command. Figures 34 through 39 indicate the closed-loop response with adaptive features in operation.

Calculations have indicated a minimum signal level of .02 deg/sec must be sensed for proper adaptive loop operation. Considering system saturation and assuming a maximum elevator deflection of 20 deg., a maximum pitch rate of 10 deg/sec was determined to be realistic for the system configuration and gains used. Linearity should be maintained between these extremes. Other data to be used for scaling are contained in Table 5. These values are the maximum expected for the six designated flight cases utilizing the gain distribution indicated in Figure 2.

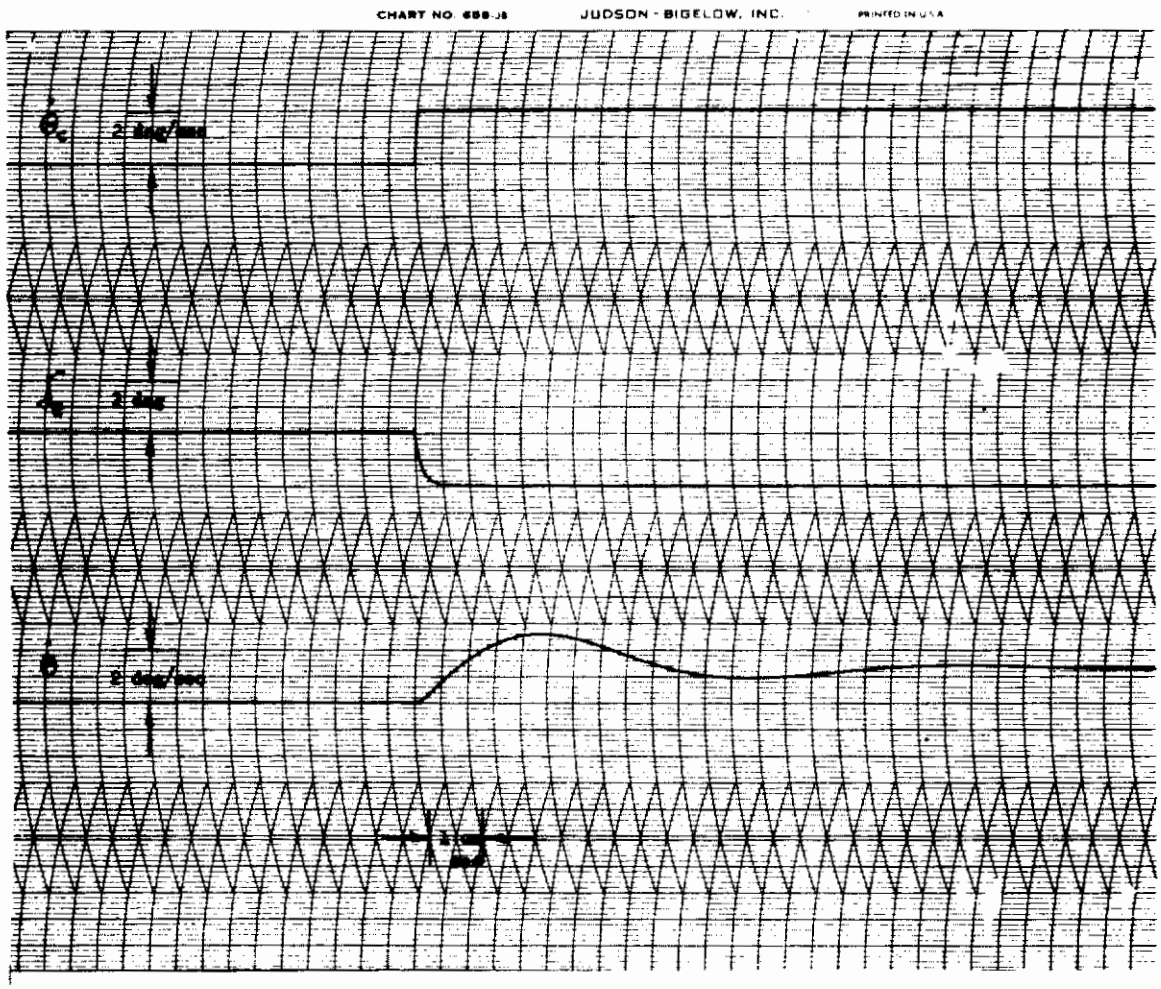

Figure 28. Flight Case 1, Airframe Response

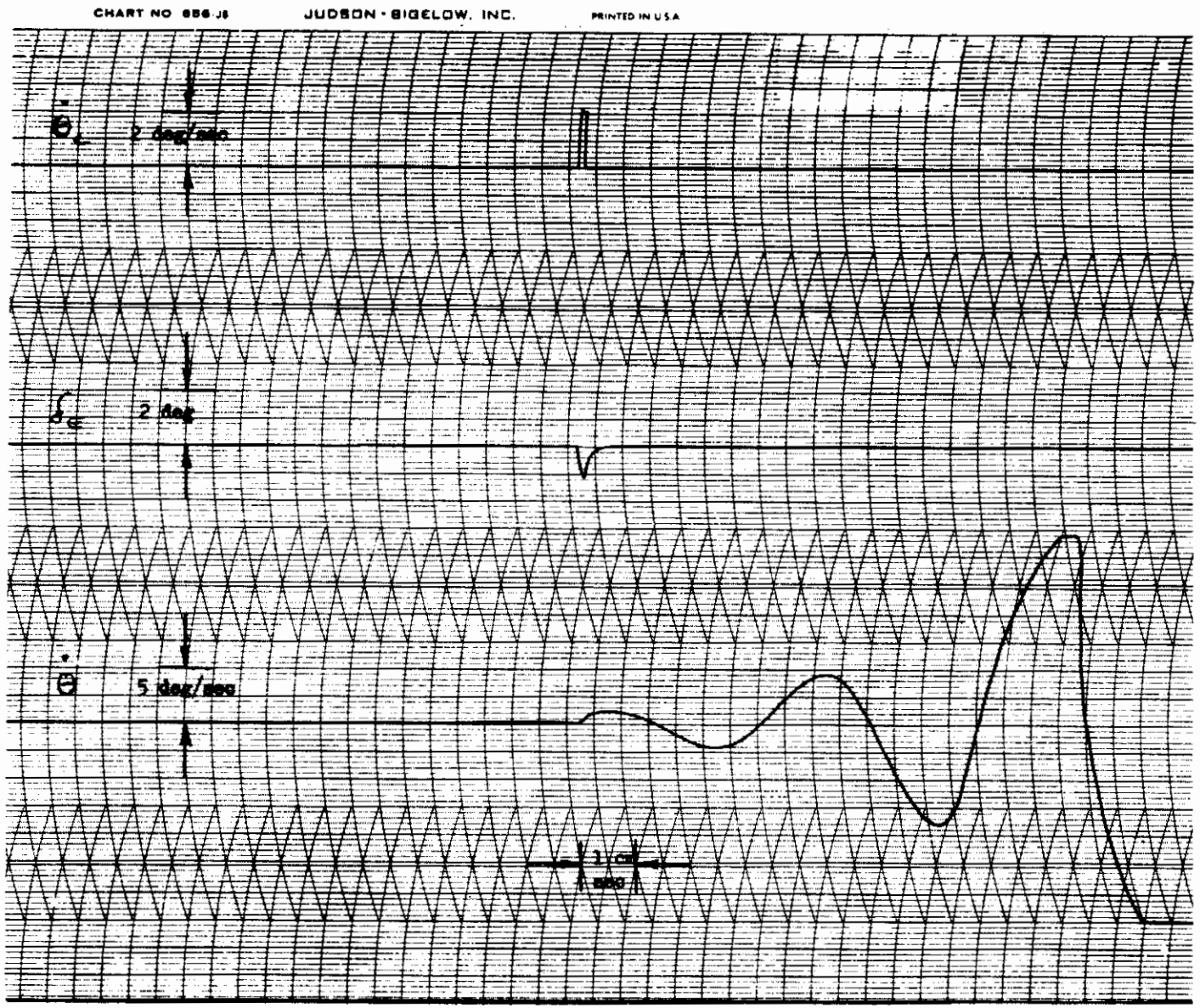

Figure 29. Flight Case 2, Airframe Response

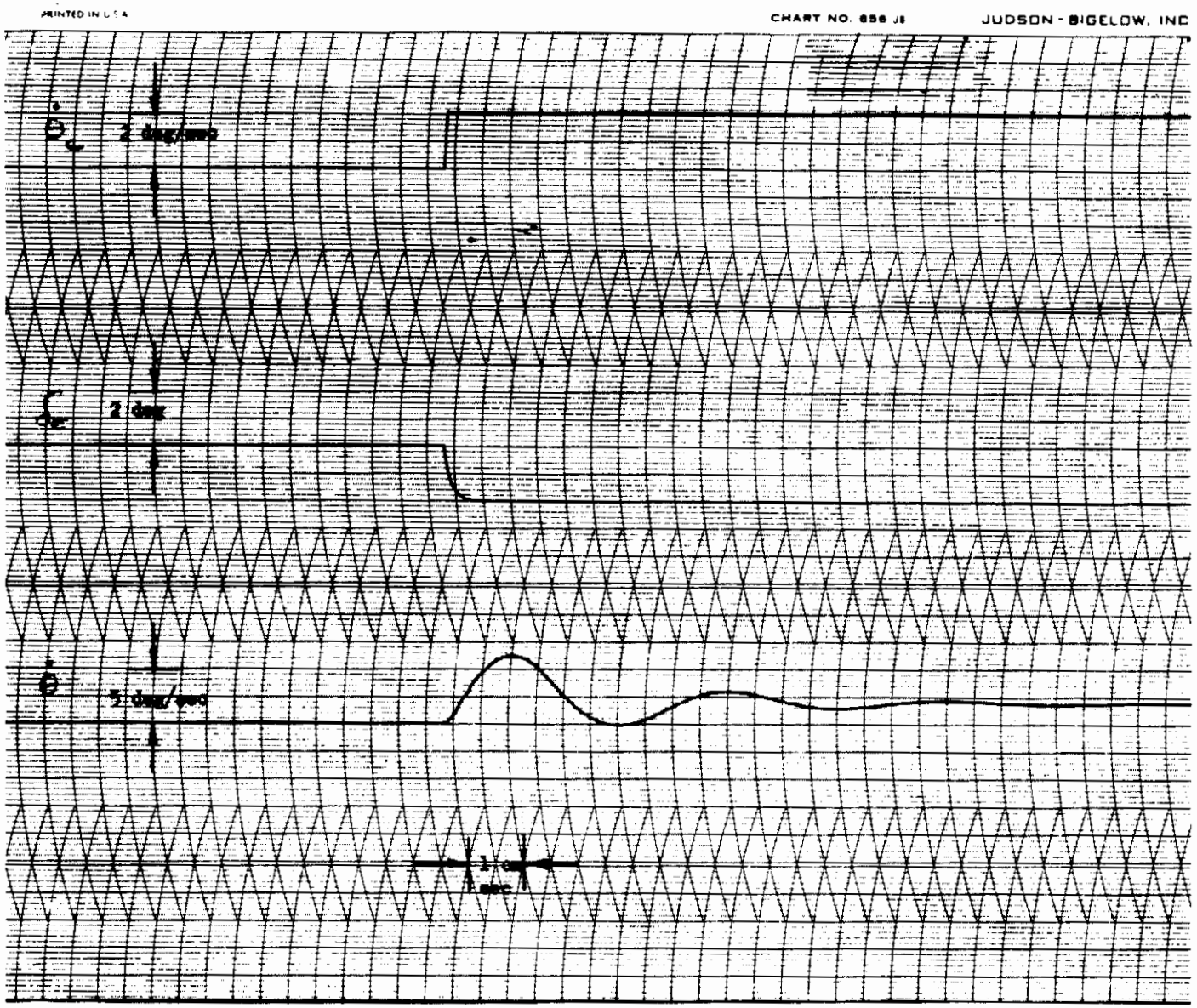

Figure 30. Flight Case 3, Airframe Response

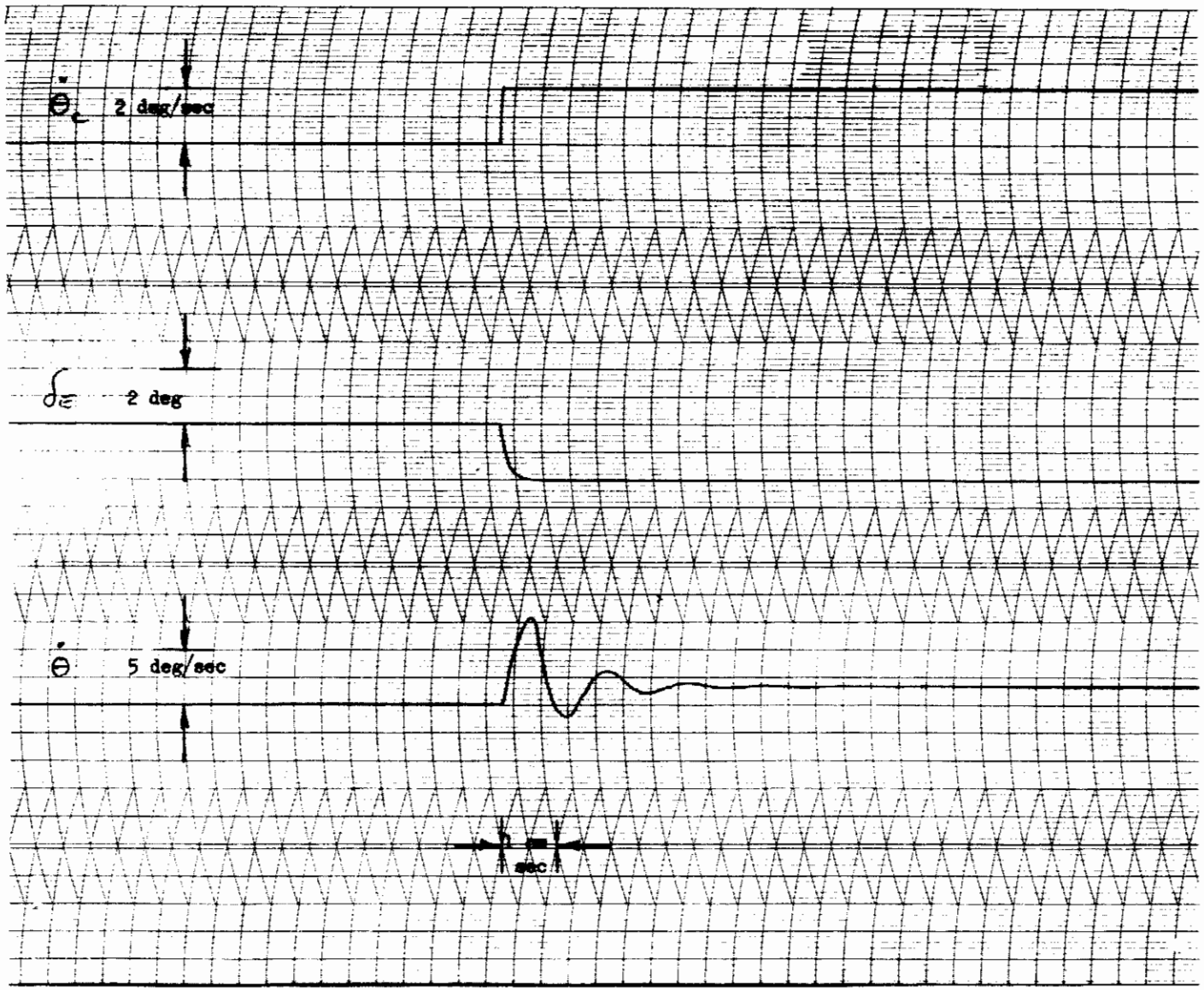

Figure 31. Flight Case 4, Airframe Response

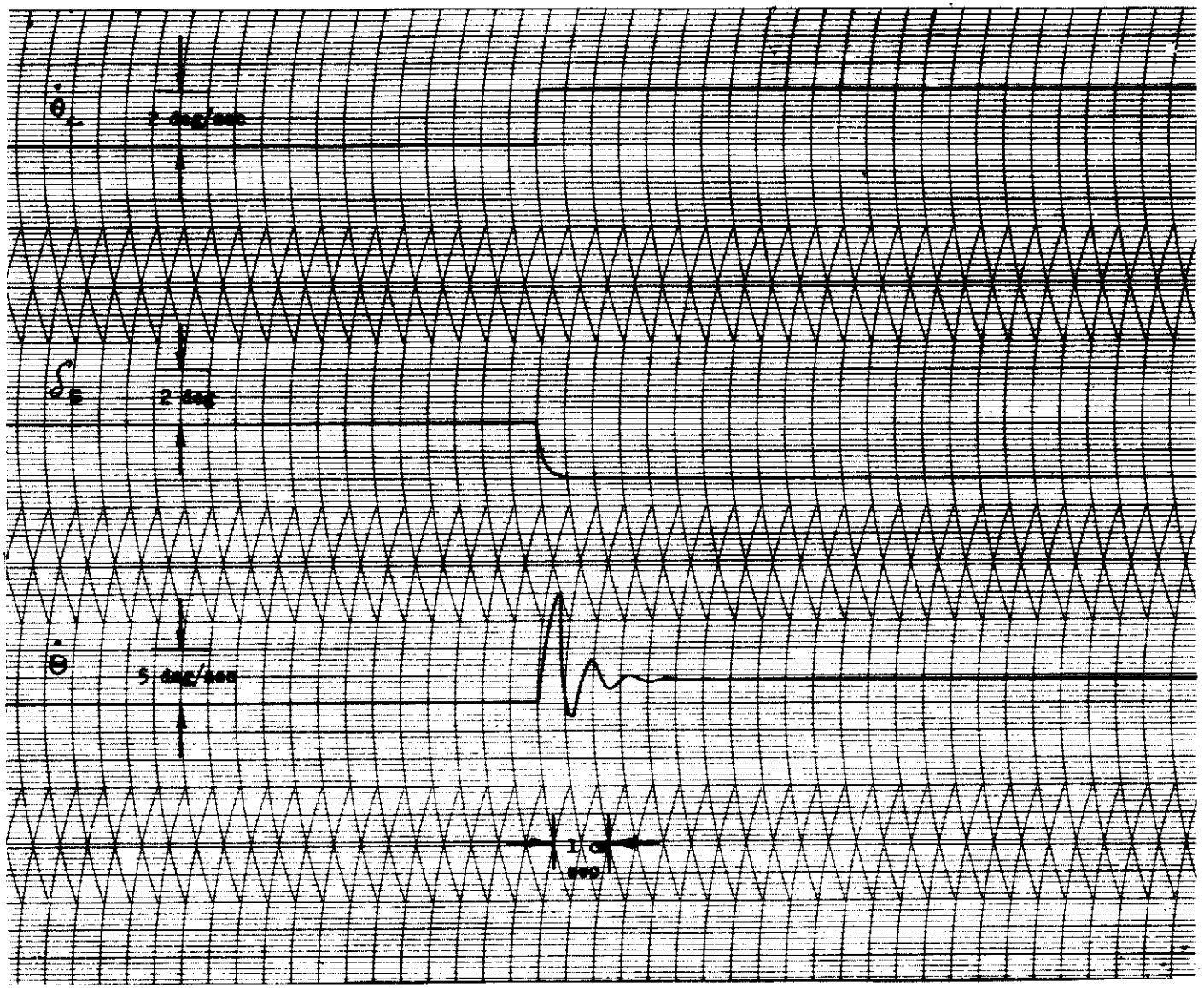

Figure 32. Flight Case 5, Airframe Response

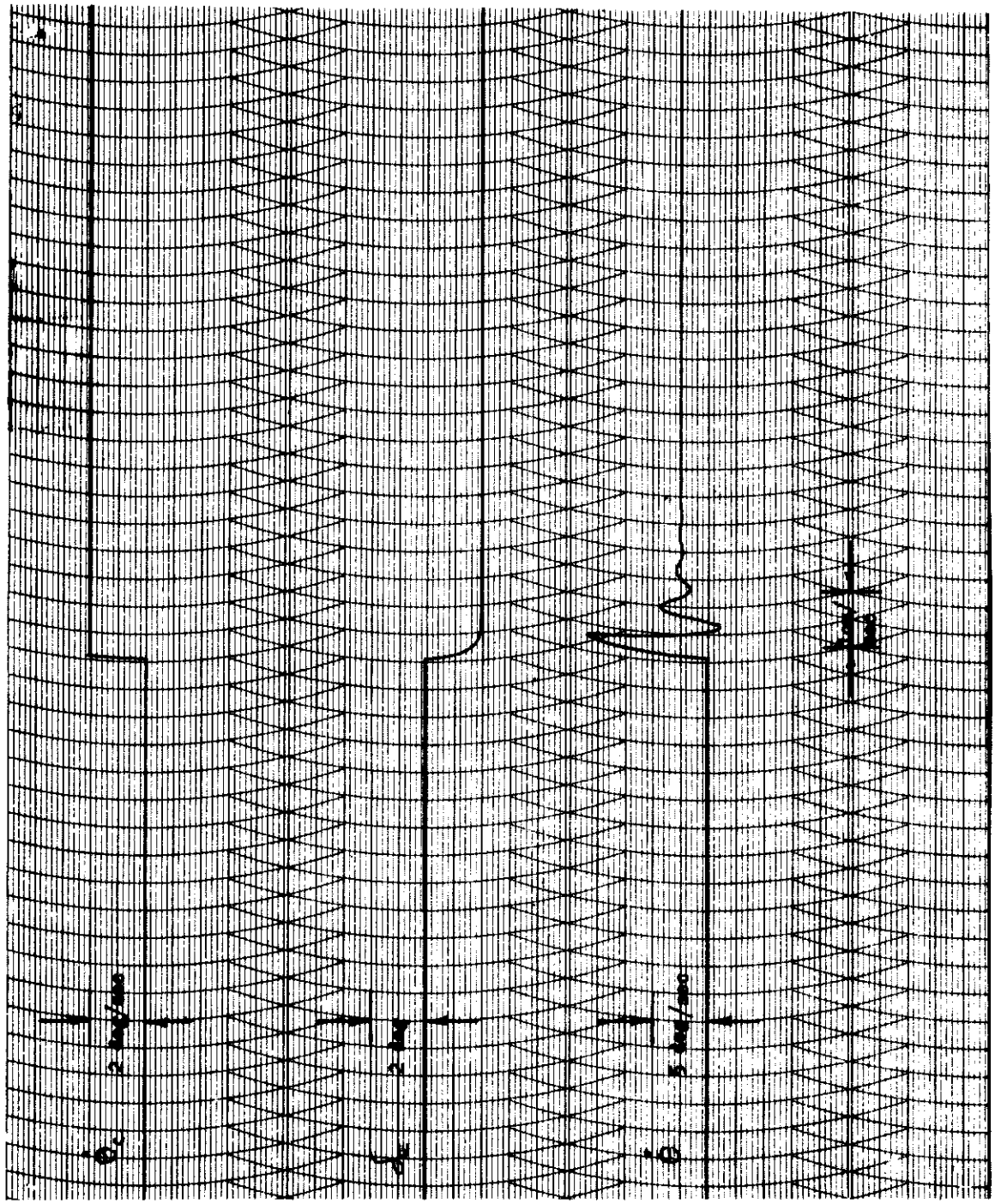

Figure 33. Flight Case 6, Airframe Response

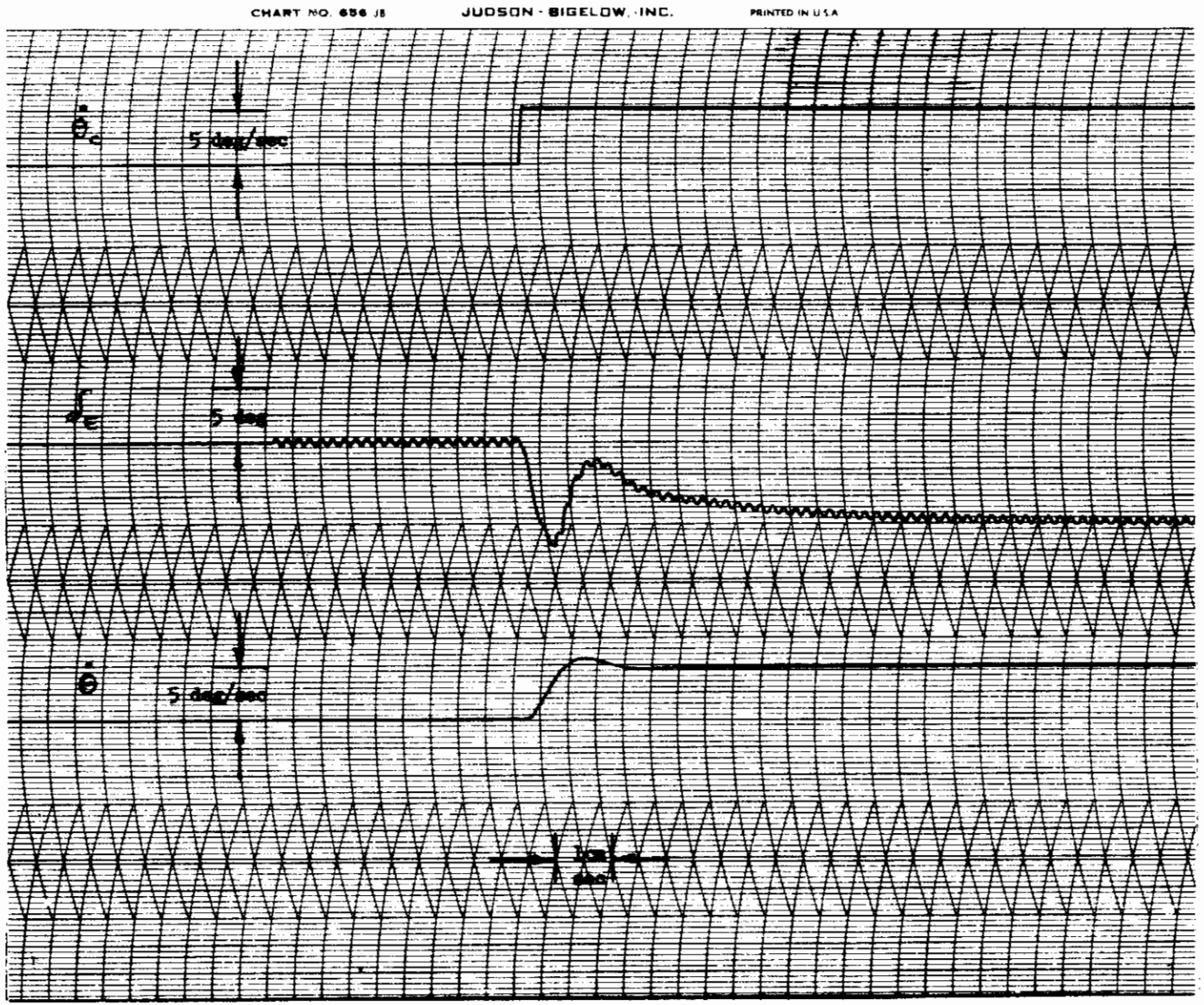

Figure 34. Flight Case 1, Augmented Transient Response

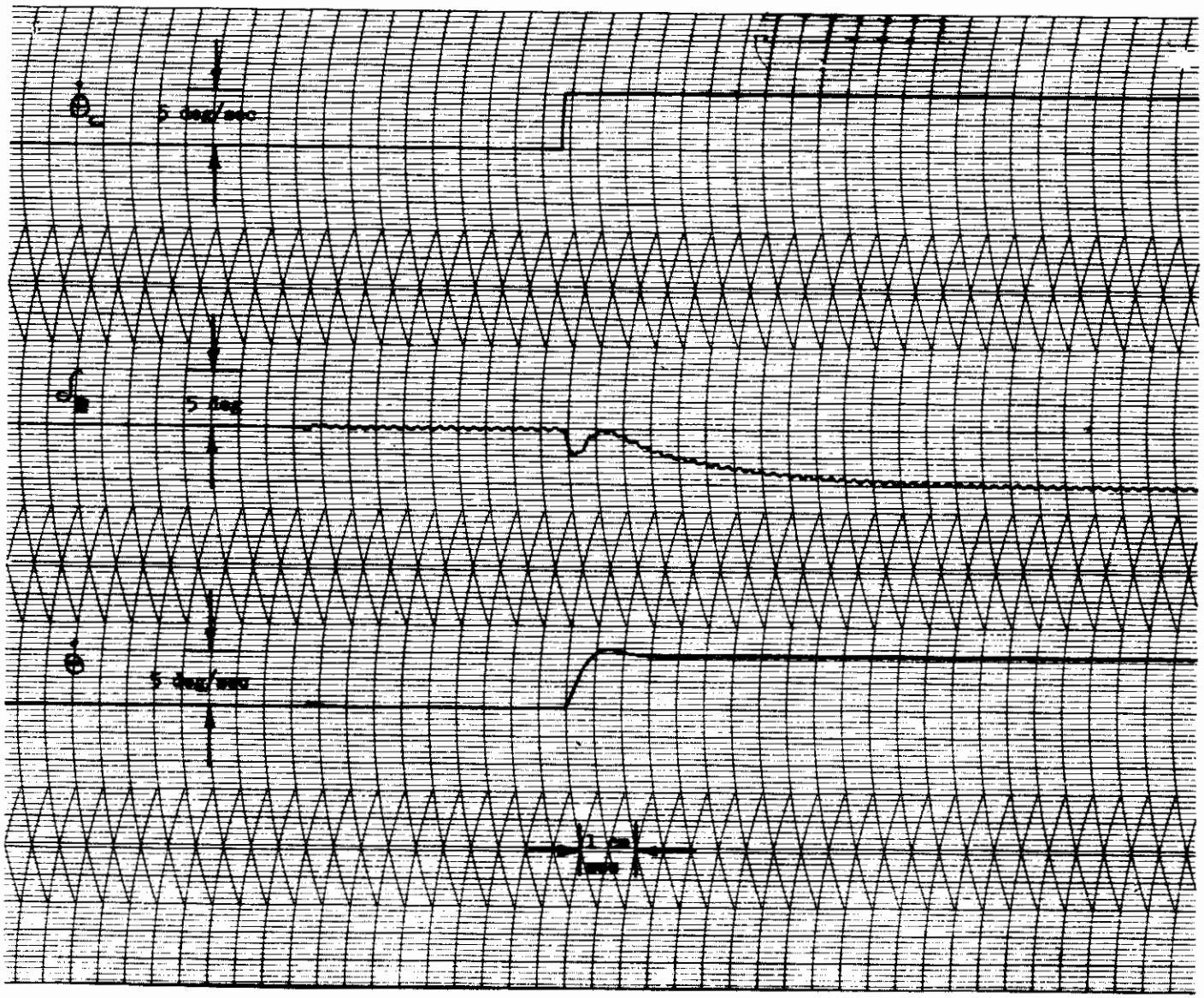

Figure 35. Flight Case 2, Augmented Transient Response

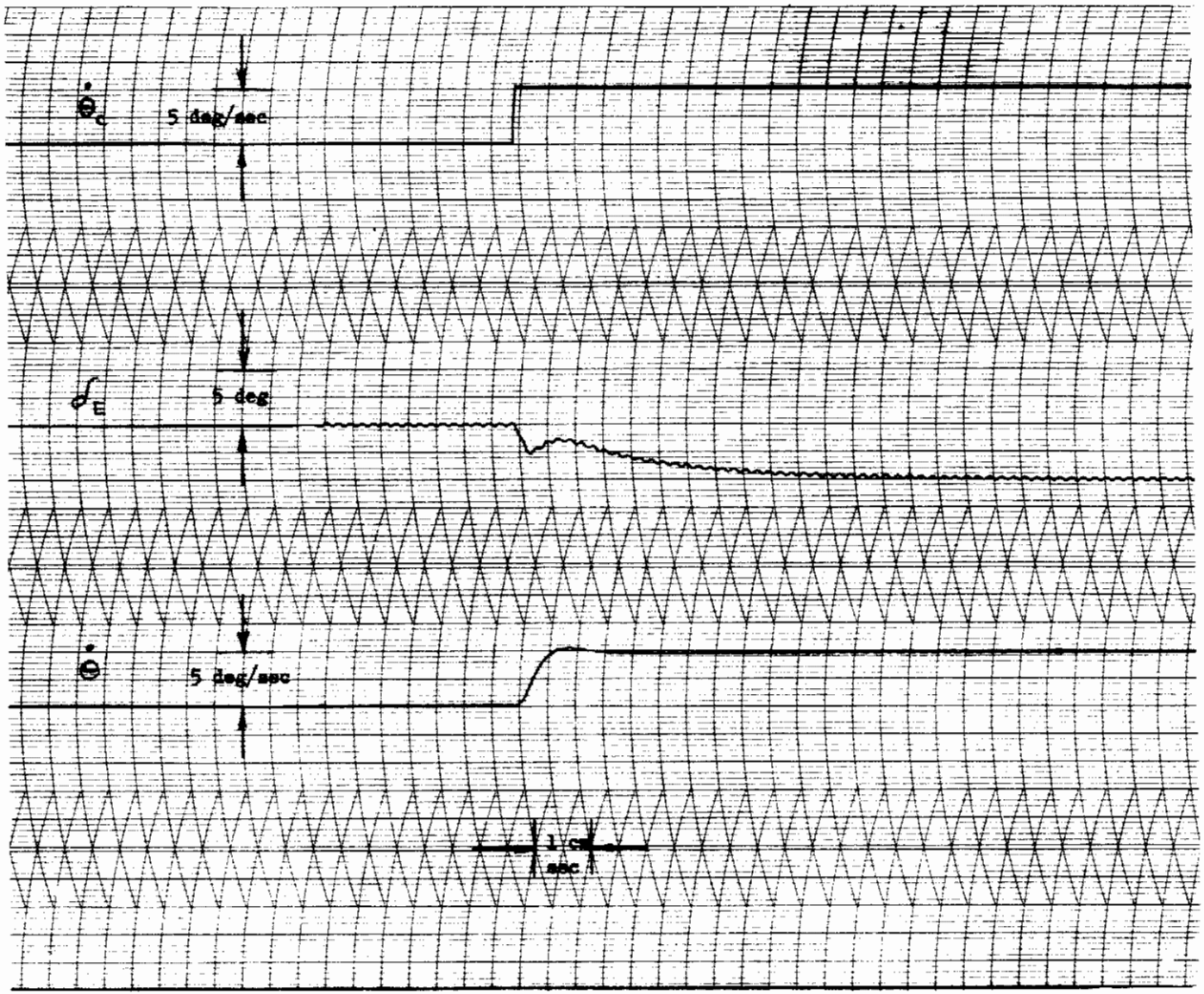

Figure 36. Flight Case 3, Augmented Transient Response

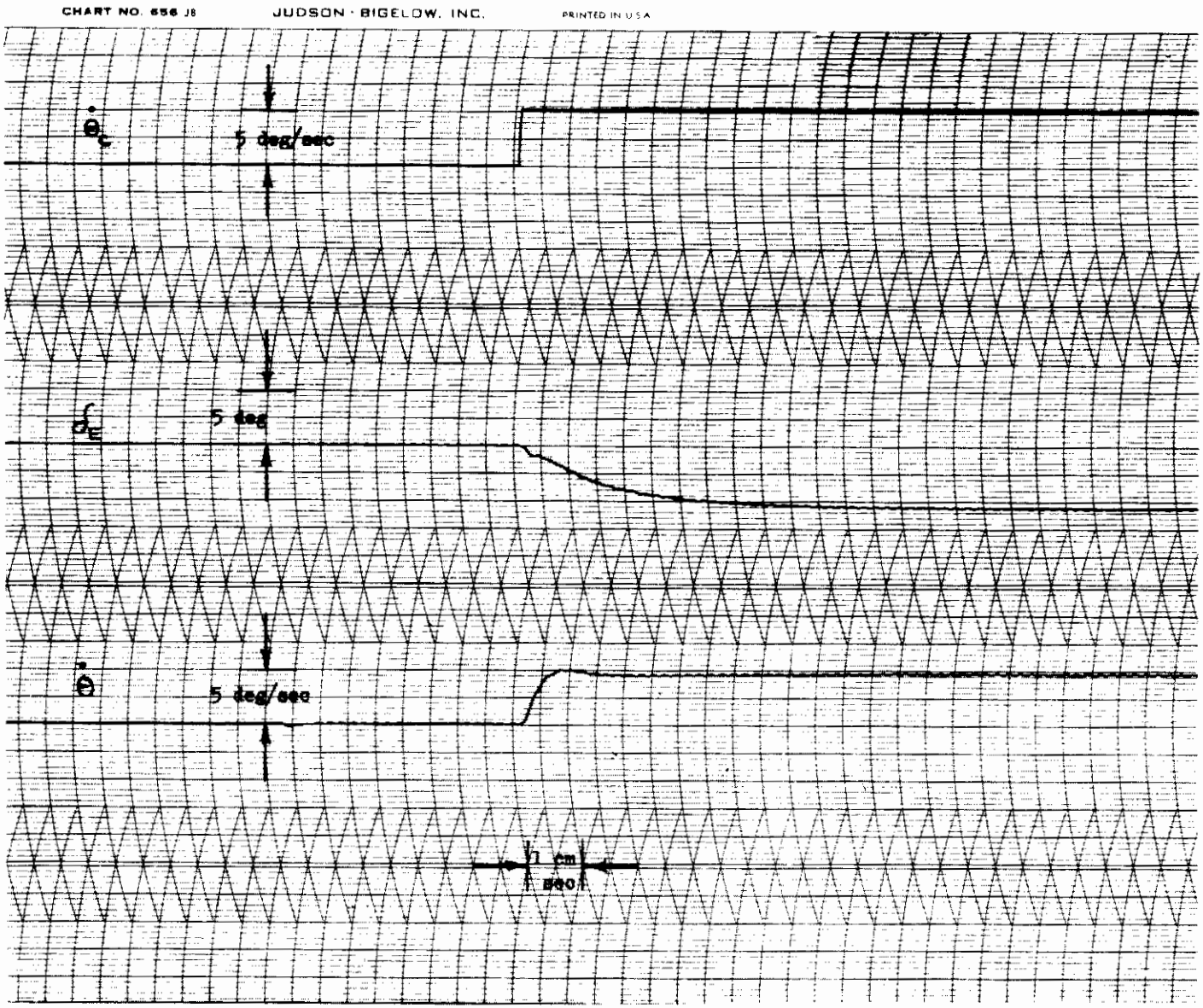

Figure 37. Flight Case 4, Augmented Transient Response

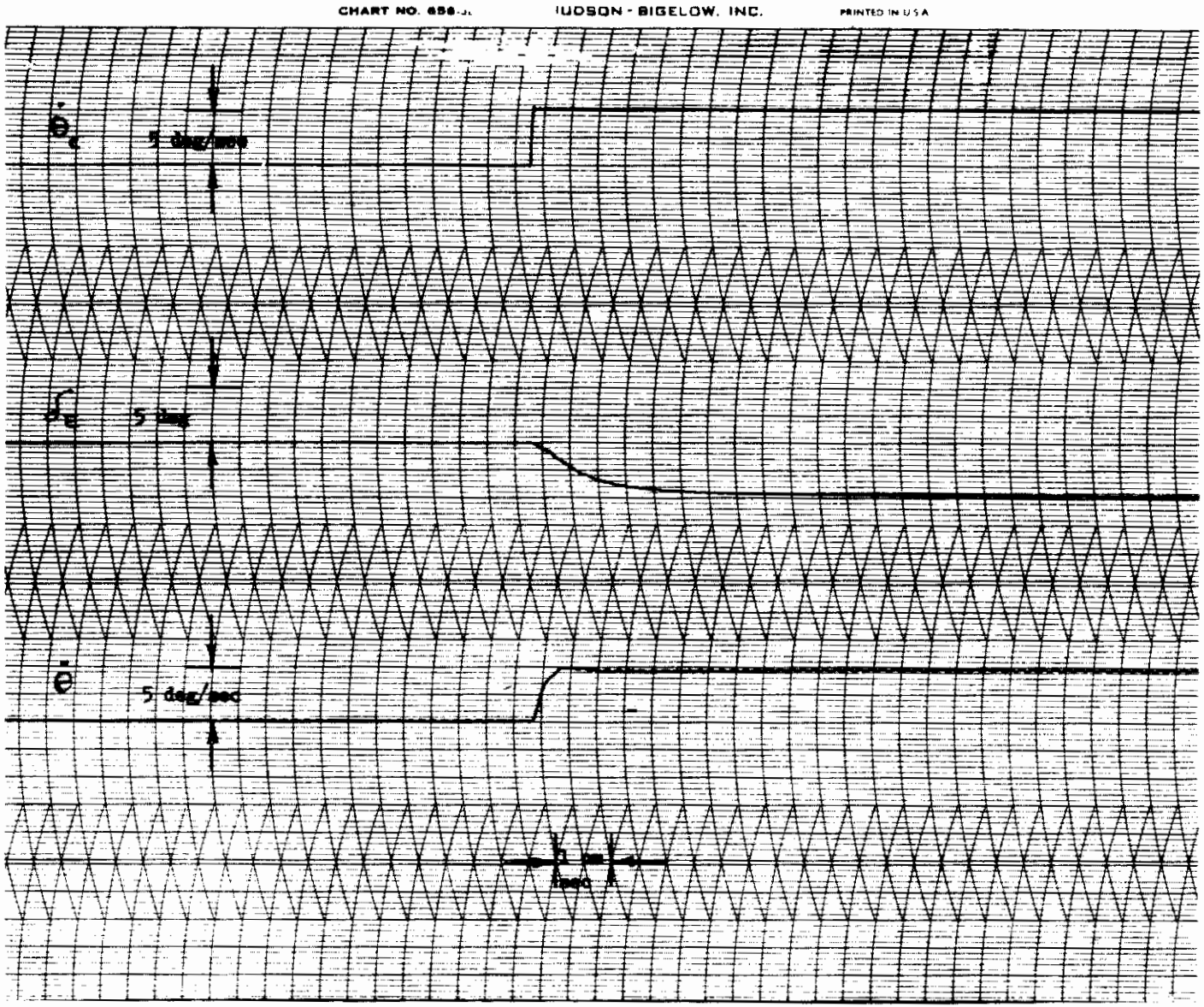

Figure 38. Flight Case 5, Augmented Transient Response

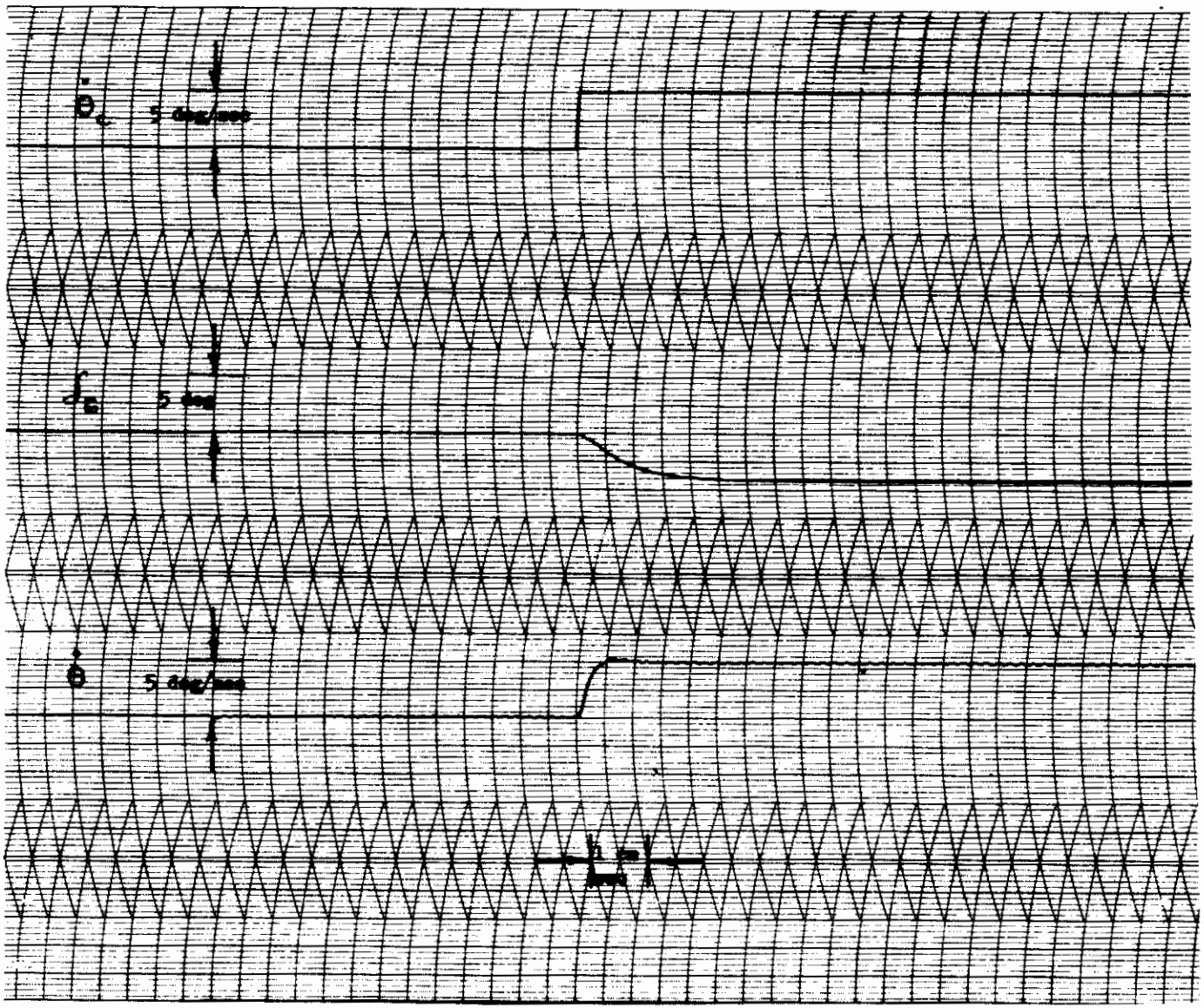

Figure 39. Flight Case 6, Augmented Transient Response

Table 5. Maximum Values for a 1 Deg/Sec Pitch Rate Command ($\dot{\theta}_c$)

	Magnitude	Units
$\dot{\theta}_s$	.08	deg/sec
$\dot{\theta}_e$	.04	deg/sec
δ_c	2.0	deg
δ_a	2.0	deg
$\dot{\theta}$	1.14	deg/sec
$\dot{\theta}_{BP}$	.061	deg/sec
$\lvert\dot{\theta}_{BP}\rvert$	.8	--
K_ϵ	.16	--
K_{δ_E}	5.0_{limit}	--
δ_E	1.8	deg

APPENDIX I. INSTRUCTION MANUAL FOR THE TRISAFE SINGLE AXIS STABILITY AUGMENTATION SYSTEM CONTRACT AF33(615)-1479

1.0 Introduction

The P101A SAS system consists of the following items:

(1) TRISAFE Controller Part No. 57200-507-1

(2) Flight Simulator Part No. 55080-399-1

(3) Recorder Part No. P2CBH

The TRISAFE controller assembly houses the electronic components and associated circuitry which enables the system to process simulated sensory data and generate the command terms to the flight simulator. There are three principal features in the system. First, all processing functions are triple redundant. By a unique approach, redundancy is achieved without the need for a monitoring function. The simplicity of this technique permits the application of redundancy at the unit level; e.g., an amplifier, with a resulting substantial increase in reliability. Second, the system is adaptive. With this capability the system automatically adjusts its gain to maintain a constant response to inputs despite large variations in the characteristics of the vehicle being controlled. Third, the electronic devices in the system are predominantly integrated circuits.

The Flight Simulator is a desk top analog computer that simulates the integration portion of the series servo, the closed loop power servo, and the open loop airframe. The gain as well as the pole-zero locations of the simulated aircraft may be changed to demonstrate the adaptive performance of the controller.

2.0 Operating Instructions

2.1 Material and Equipment

The following list of material and or equipment is necessary prior to testing or operating the system:

(1) TRISAFE Controller, Part No. 57200-507-1

(2) Flight Simulator, Part No. 55080-399-1

(3) Recorder, Part No. P2CBH

(4) Controller Interconnect Cable, Part No. 57214-507-1

(5) Recorder Interconnect Cable.

(6) Simulator Power Cable.

3.0 Environmental Conditions

Testing operations shall be performed at an ambient temperature of 25°C ± 5°C.

4.0 Detail Requirements

Connect the Single Axis Stability Augmentation System as shown in Figure 40.

5.0 Self Test of the Simulator

5.1 Periodically (approximately once a week) prior to operating the Controller, the Flight Simulator should be balanced and checked. The balancing procedure is described in the Operation Manual for the Flight Simulator.

6.0 Open Loop Testing of the Electronic Controller

6.1 Place Master Power switch on the Simulator to the ON position.

6.2 Calibrate channel No. 2 of the Recorder for 5 volts/cm and channel No. 1 for .05 volts/cm. (See Flight Simulator Operation Manual for calibration procedure.)

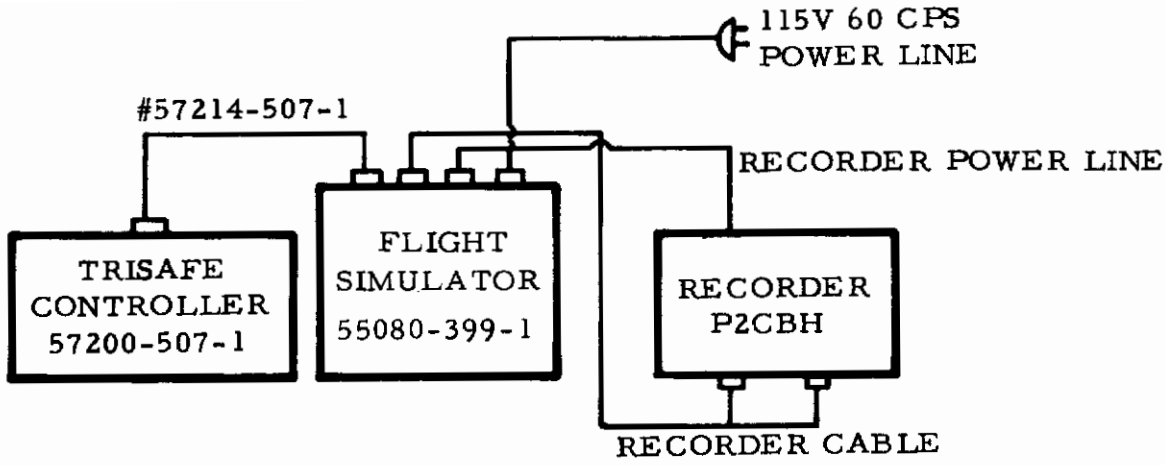

Figure 40. Single Axis Stability Augmentation System

6.3 Set Master Control switch on Simulator to RESET, Channel No. 1 Selection switch to $\dot{\theta}_c$ and Channel No. 2 Selection switch to δe.

6.4 Position the $\dot{\theta}_c$ Dial to .1 ^{o}/sec and start the Recorder at a speed of 1 mm/sec. Place the $\dot{\theta}_c$ switch to $-\dot{\theta}_c$. The stylus of Channel No. 1 shall deflect 4 mm (.02 volts). If not reposition dial for a 4 mm deflection.

6.5 Set the Flight Case Select switch to flight case No. 1 and the Master Control switch to Operate.

6.6 Place System Test switch No. 1 to the ON position and allow the recorder to run for 60 seconds.

6.7 Place the $\dot{\theta}_c$ switch to the $+\dot{\theta}_c$ position and allow the Recorder to run for 60 seconds.

6.8 Return the System Test switch No. 1 to the OFF position, the Master Control switch to the Reset position, and stop the Recorder.

6.9 The record on channel No. 2 shall fall within the tolerance band shown in Figure No. 41 from the 60-second to the 120-second points. Return the System Test switch No. 1 to the OFF position*.

7.0 Closed Loop System Operation

7.1 Place the System Test switch No. 1 and all Failure Mode switches, numbers 2 through 16, to the OFF position. Place the Master Control switch to RESET and the Flight Case Select switch to No. 1. Position the Channel No. 1 Recorder switch to $\dot{\theta}$ and Channel No. 2 to δ_e.

7.2 Position the $\dot{\theta}_c$ Dial to 5 ^{o}/sec.

7.3 At this point a step command of 5 ^{o}/sec can be applied to the system by positioning the $\dot{\theta}_c$ switch to $+\dot{\theta}_c$ or $-\dot{\theta}_c$.

7.4 Return the $\dot{\theta}_c$ switch to OFF (ext) and proceed to change the Flight Case Select switch to flight case No. 2. Once again a step input can be applied to the system. In this manner, first returning the $\dot{\theta}_c$ switch to the EXT $\dot{\theta}_c$ position and then changing flight cases, a demonstration of all flight cases 1 through 6 can be made. As the Flight Case switch is indexed from 1 through 6, ample time should be allowed for the system to adapt. It should be noted that a change in flight case by positioning the Flight Case switch is an unrealistic situation since an aircraft cannot change its flight environment as step functions. Therefore, as a flight case is introduced that requires less gain than the previous one, the system can go unstable until it adapts to the new flight case chosen. This can be demonstrated by positioning the Flight Case Select switch from No. 3 to No. 4 and noting the $\dot{\theta}$ trace. Figure 42 shows a trace of $\dot{\theta}$ as the Flight Case Select switch is positioned from 3 to 4 and from 4 to 5. Table 6 lists the various flight cases and Figure 43 shows the open loop airframe response for a 2 ^{o}/sec input. Figures 44 through 49 show the system response for a 5 ^{o}/sec step input with the SAS loop closed.

*Caution: This switch must remain in the OFF position for all remaining tests.

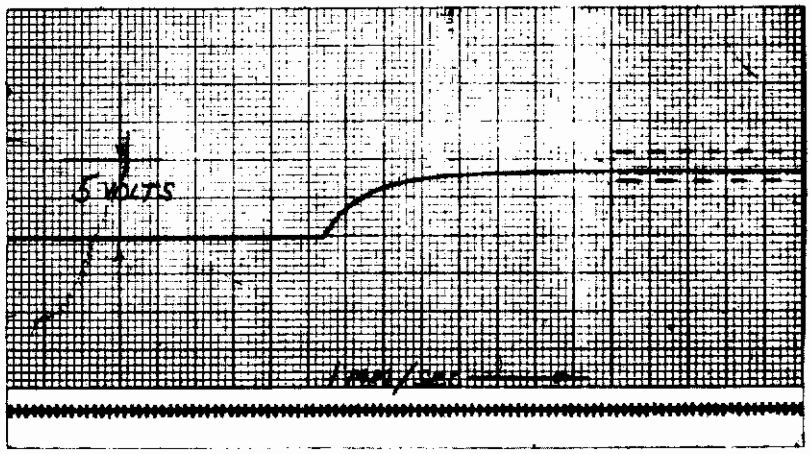

Figure 41. Open Loop Response $\delta e/\theta_c$

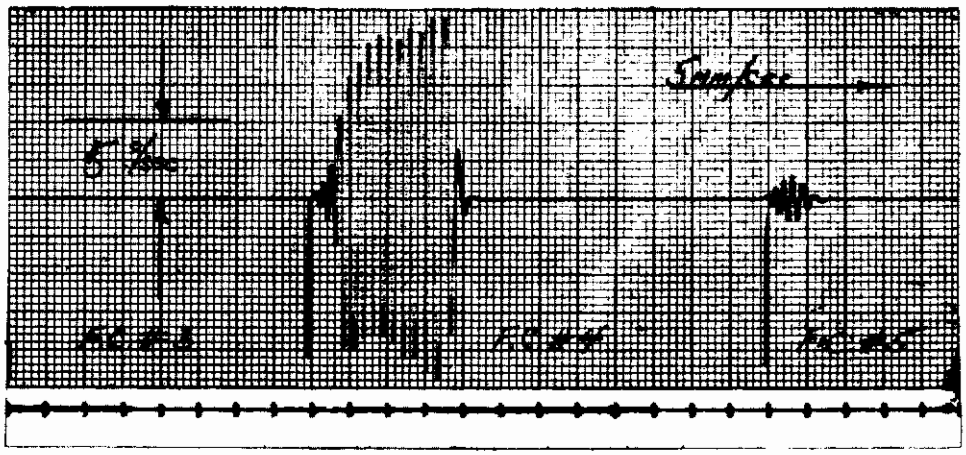

Figure 42. Closed Loop Response

Table 6. Flight Cases

Flight Case	Altitude (ft.)	Mach	$\dot{\theta}/\delta_e$	
1	0	.161	$\frac{-1.14\ (s + .415)}{s^2 + .604s + .7074}$	(27)
2	30,000	.6	$\frac{-5.31\ (s + .478)}{s^2 - .692s + 2.585}$	(28)
3	30,000	.6	$\frac{-5.31\ (s + .478)}{s^2 + .692s + 2.585}$	(29)
4	0	.7	$\frac{-22.97\ (s + .761)}{s^2 + 2.088s + 20.27}$	(30)
5	0	1.2	$\frac{-70\ (s + 1.27)}{s^2 + 4s + 85}$	(31)
6	0	1.4	$\frac{-84\ (s + 1.408)}{s^2 + 4.32s + 96.64}$	(32)

8.0 Demonstration of System Performance in the Presence of Circuit Failures

As was pointed out in the introduction, the TRISAFE feature of the system allows for multiple failures of various types throughout the electronics without degradation in performance. Failure compensation is inherent in the unit redundant concept and does not require monitors, voters, or switching out of the failed components.

To demonstrate TRISAFE, 15 various failures can be introduced and system performance can be observed. Figures 50 through 59 show the various portions of the system that the failures are being introduced.

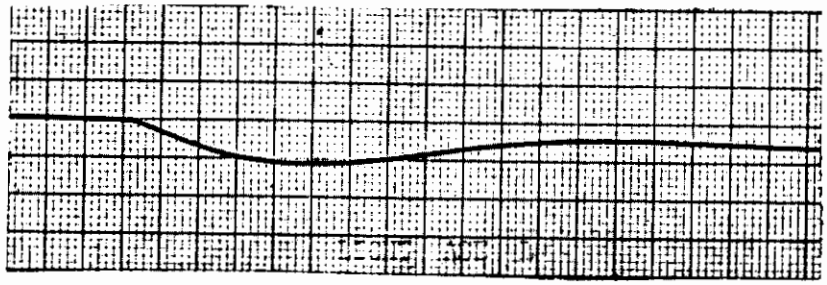

FLIGHT CASE #1

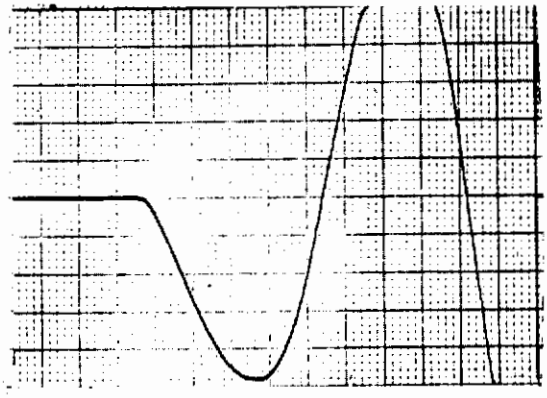

FLIGHT CASE #2

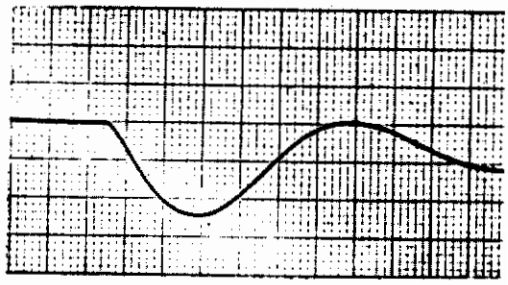

FLIGHT CASE #3

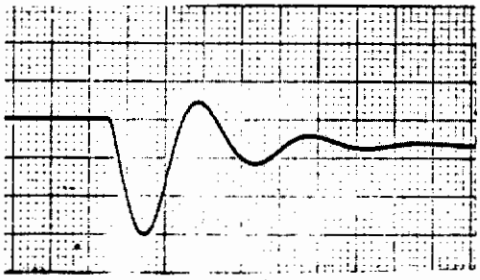

FLIGHT CASE #4

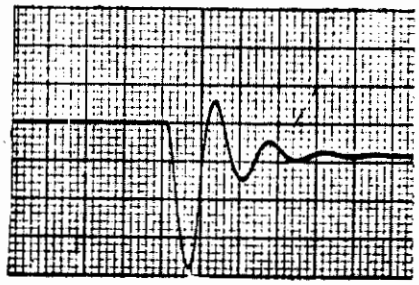

FLIGHT CASE #5

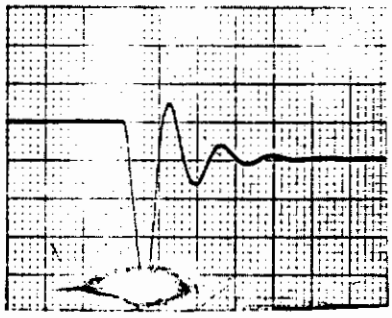

FLIGHT CASE #5

SCALE FACTOR = 5°/SEC PER CM

Figure 43. Open Loop Airframe Response (Pitch Rate) for a 2 °/sec Input Command

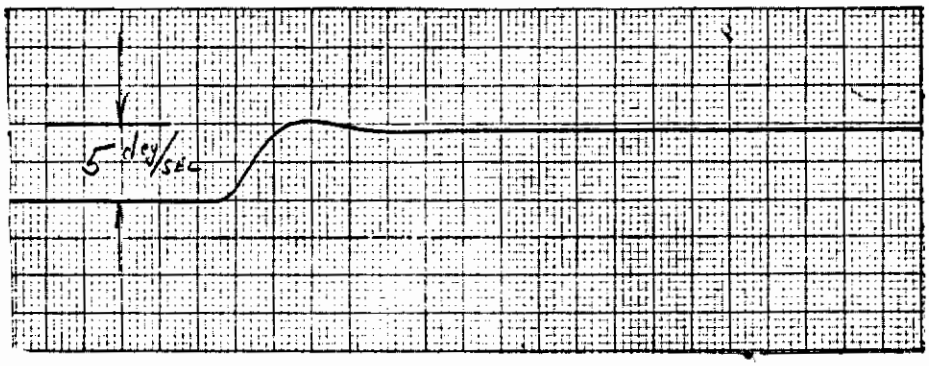

$\dot{\theta}$ RESPONSE

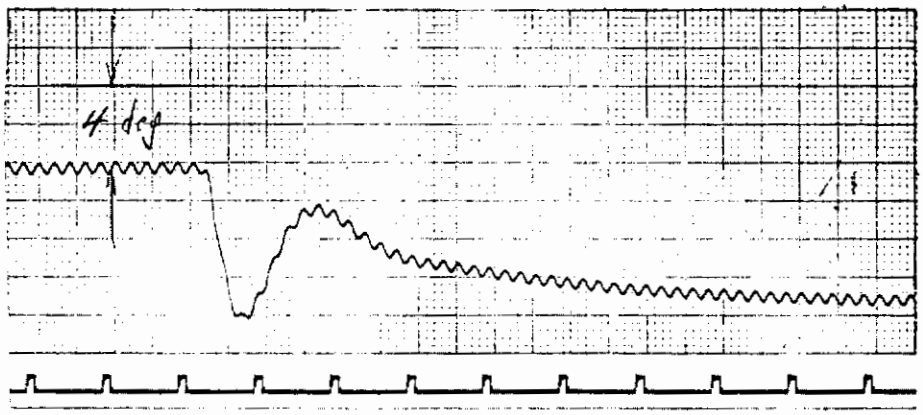

δE RESPONSE

CLOSED LOOP RESPONSE FOR 5 °/SEC INPUT COMMAND

Figure 44. Flight Case No. 1

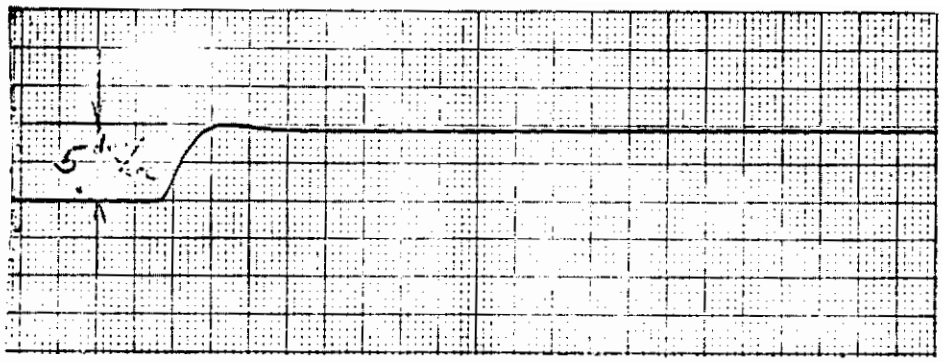

$\dot{\theta}$ RESPONSE

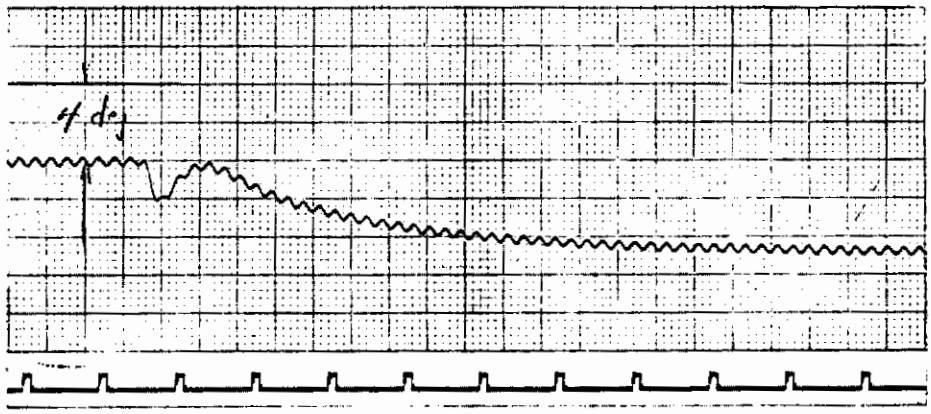

δE RESPONSE

CLOSED LOOP RESPONSE FOR 5 °/SEC INPUT COMMAND

Figure 45. Flight Case No. 2

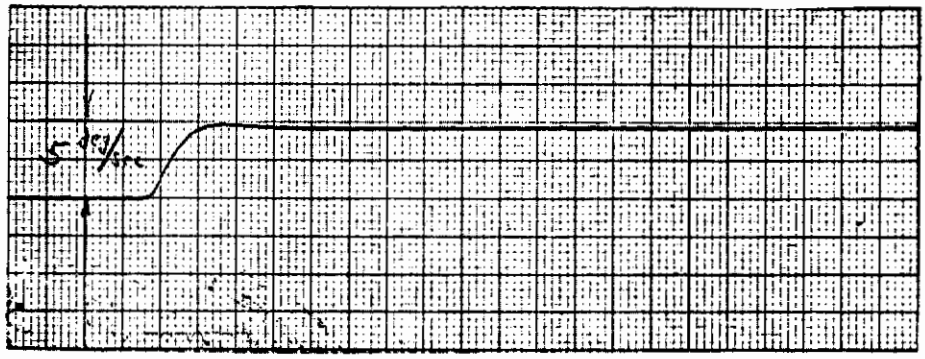

θ RESPONSE

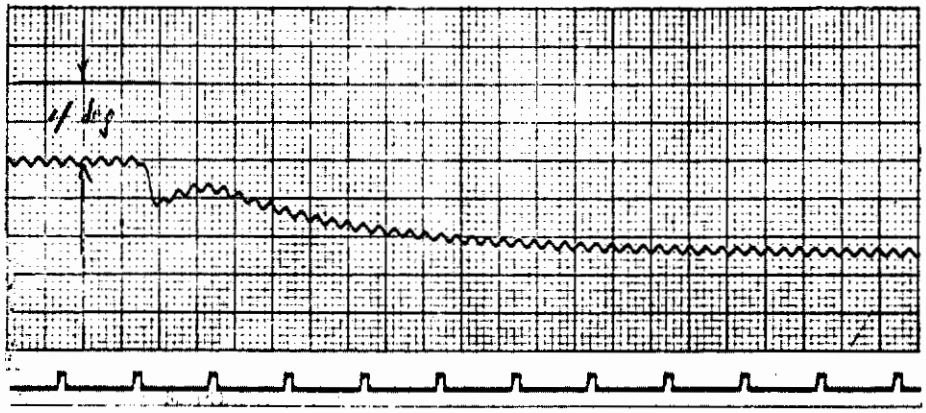

δE RESPONSE

CLOSED LOOP RESPONSE FOR 5 °/SEC INPUT COMMAND

Figure 46. Flight Case No. 3

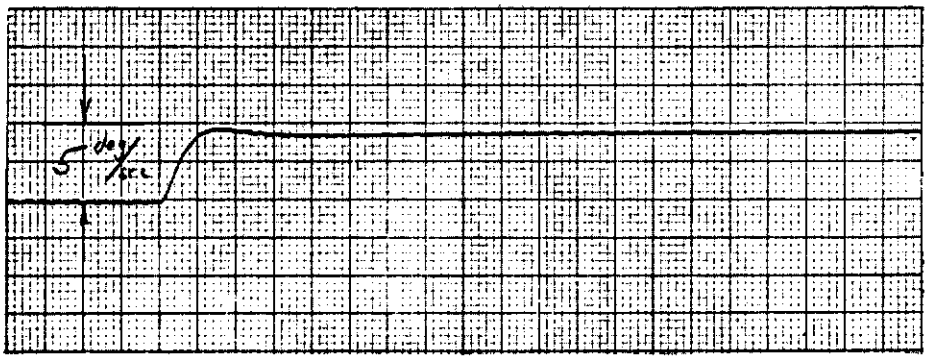

$\dot{\theta}$ RESPONSE

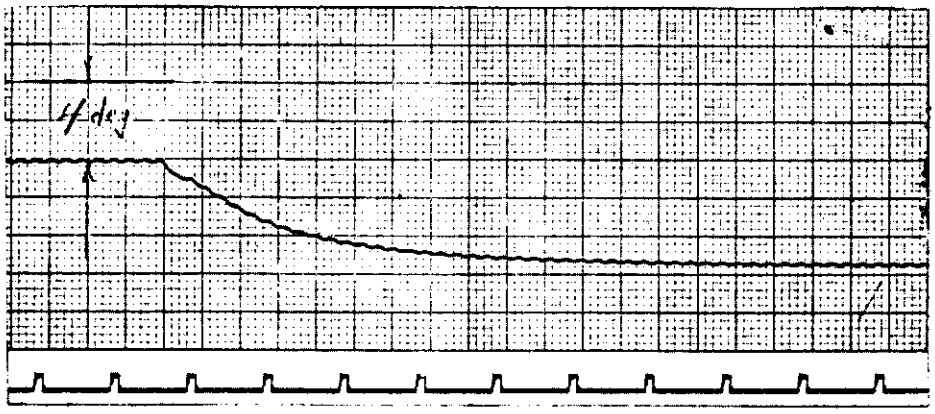

δE RESPONSE

CLOSED LOOP RESPONSE FOR 5 °/SEC INPUT COMMAND

Figure 47. Flight Case No. 4

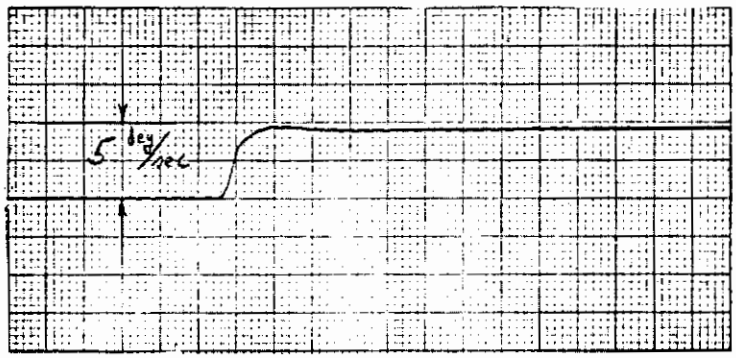

$\dot{\theta}$ RESPONSE

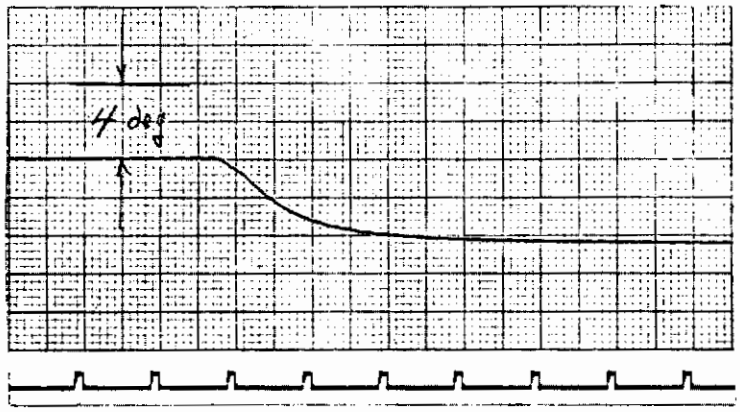

δ_E RESPONSE

CLOSED LOOP RESPONSE FOR 5 °/SEC INPUT COMMAND

Figure 48. Flight Case No. 5

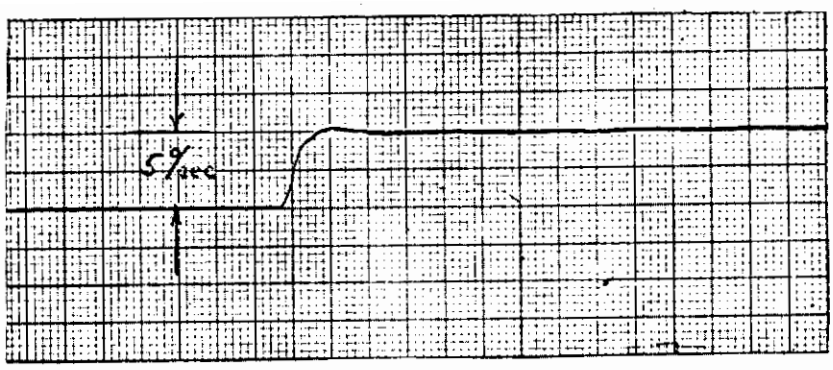

$\dot{\theta}$ RESPONSE

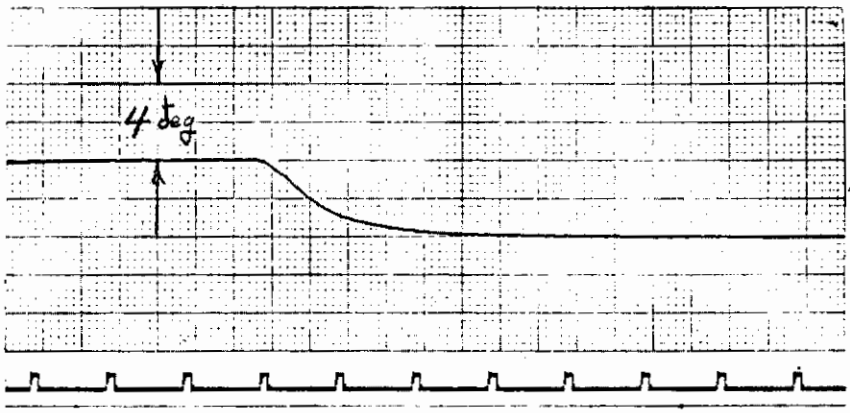

δ_E RESPONSE

CLOSED LOOP RESPONSE FOR 5 °/SEC INPUT COMMAND

Figure 49. Flight Case No. 6

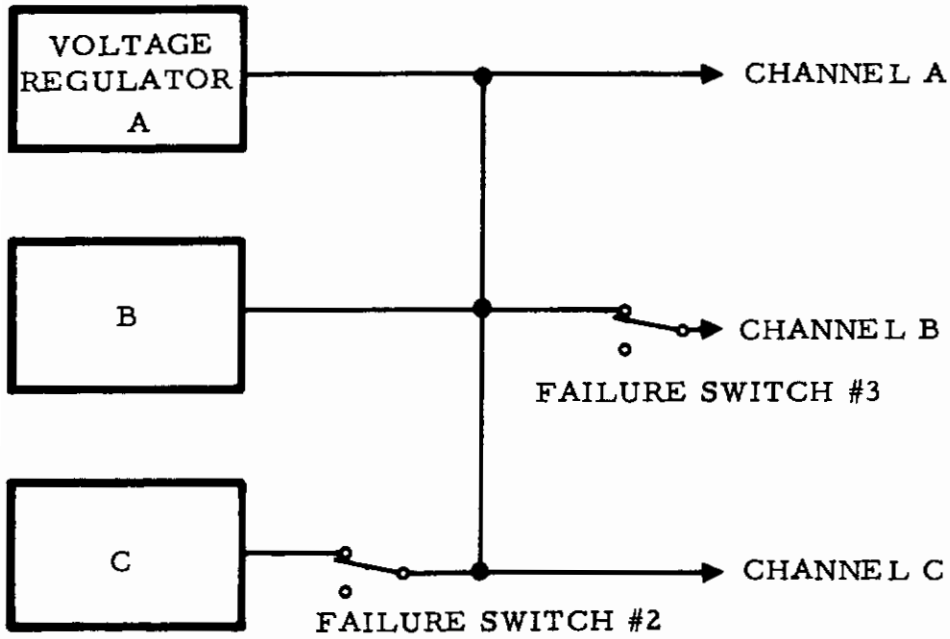

Figure 50. Failure Switches No. 2 and No. 3

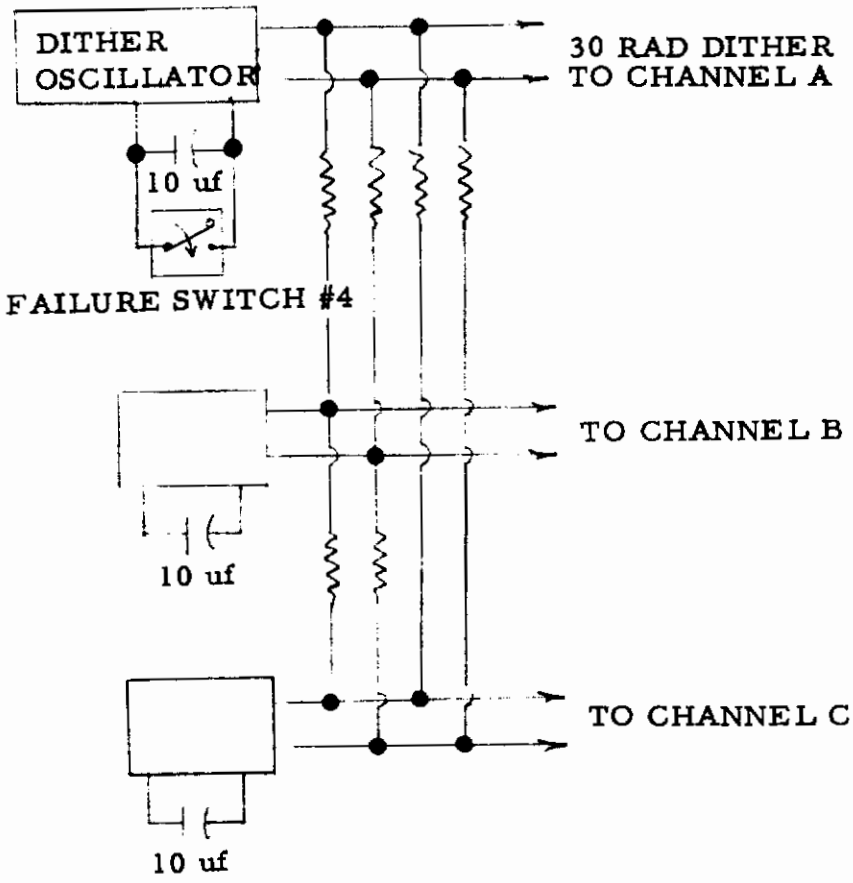

FAILURE SWITCH #4 - SHORTED CAPACITOR IN DITHER GENERATOR OF CHANNEL A.

THIS TYPE OF MALFUNCTION INTRODUCES A HARDOVER TYPE FAILURE IN THE NEXT UPSTREAM UNIT.

Figure 51. Failure Switch No. 4

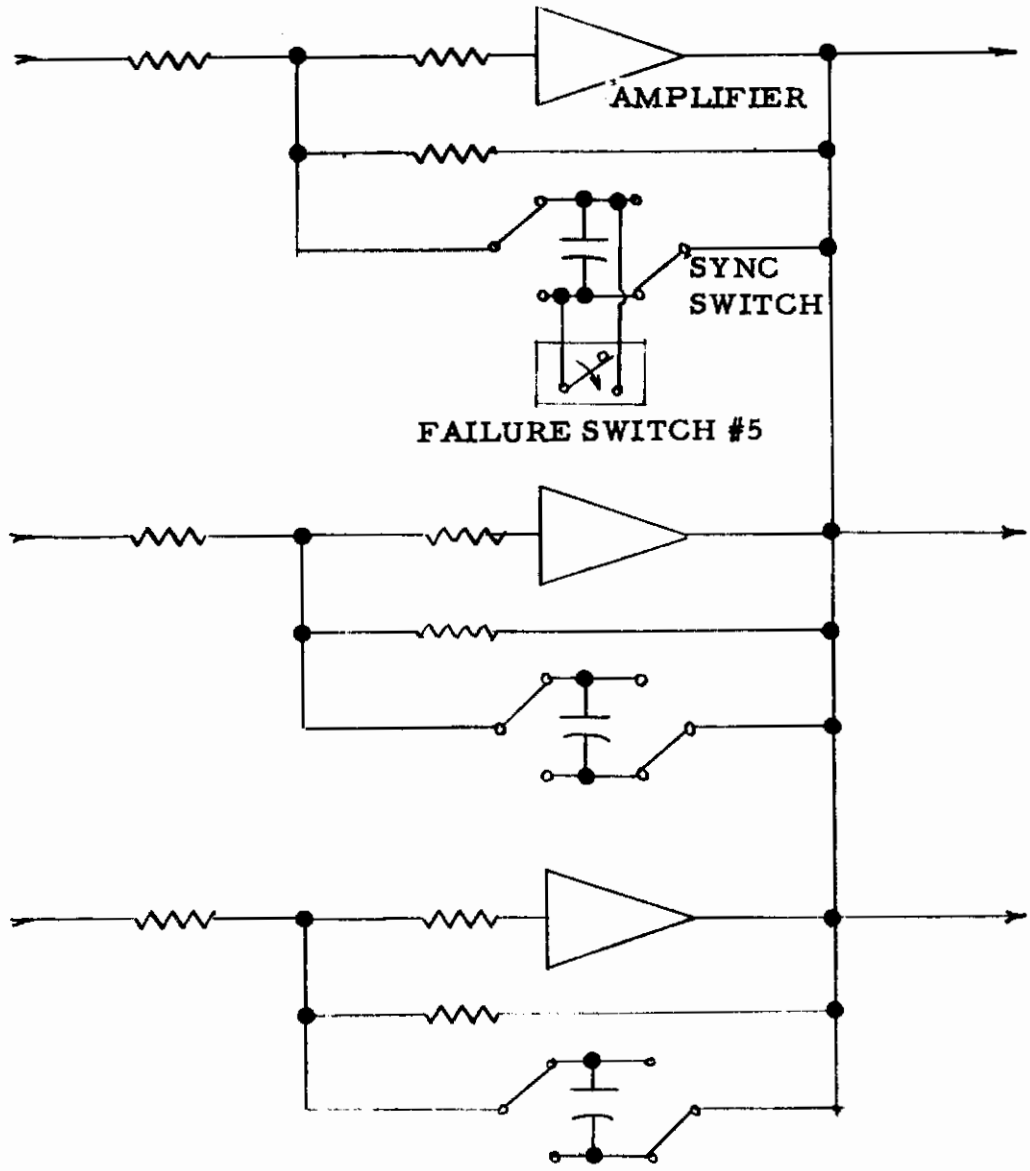

FAILURE SWITCH #5: SHORTED CAPACITOR IN ACTIVE LAG UNIT.

THIS TYPE OF FAILURE CAUSES ZERO OUTPUT OF THE AMPLIFIER IN CHANNEL A BUT DOES NOT EFFECT THE UNITS OUTPUT EXCEPT FOR A .13% CHANGE IN STEADY STATE GAIN.

Figure 52. Failure Switch No. 5

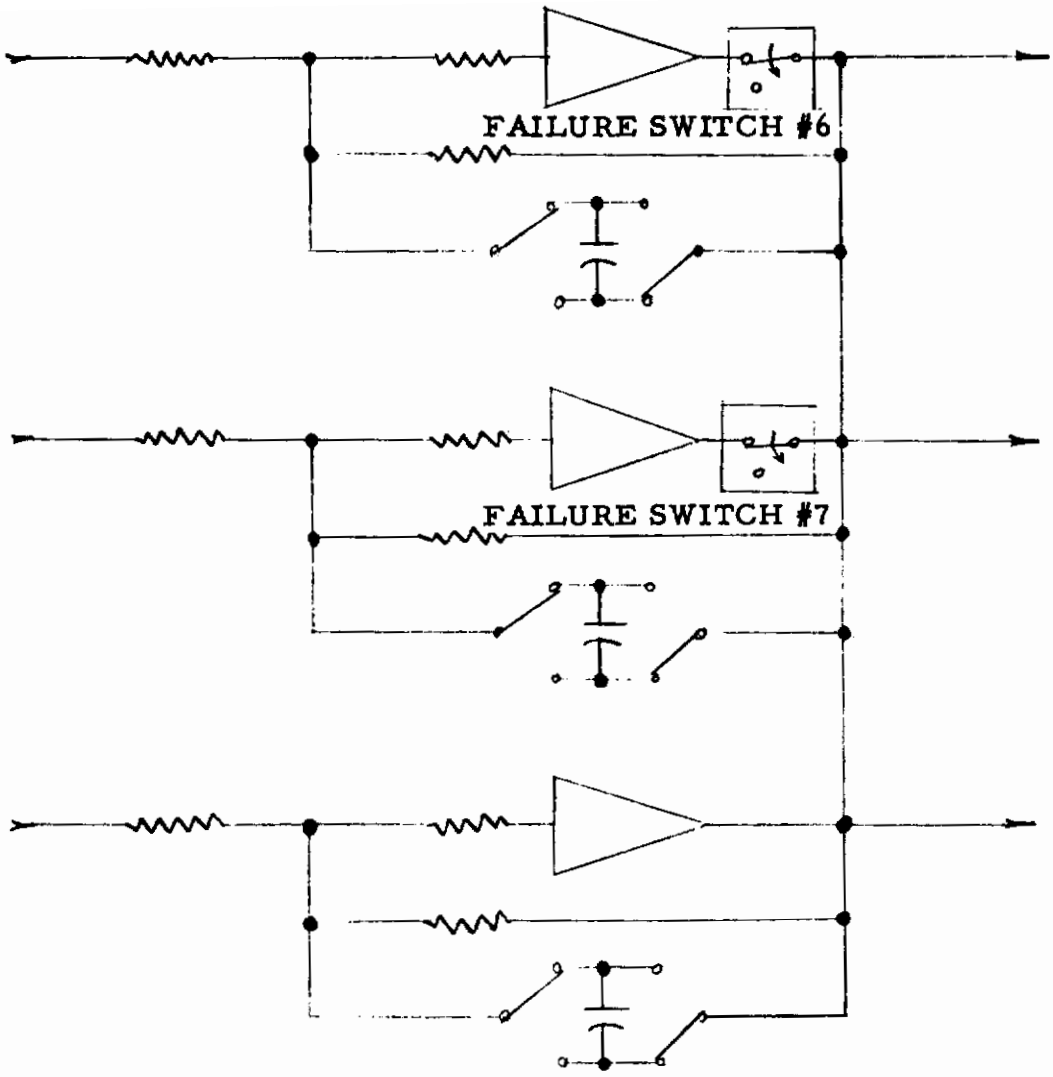

FAILURE SWITCHES #6 AND #7: OPEN AMPLIFIER IN CHANNEL A AND CHANNEL B OF THE SAME UNIT. THIS UNIT FORMS PART OF THE INVERSE MODEL COMPENSATION.

THIS TYPE OF FAILURE CAUSES A ZERO TYPE OUTPUT IN TWO AMPLIFIERS OF A TRIPLE REDUNDANT UNIT. THE OVERALL PERFORMANCE OF THIS UNIT IS NOT EFFECTED.

Figure 53. Failure Switches No. 6 and No. 7

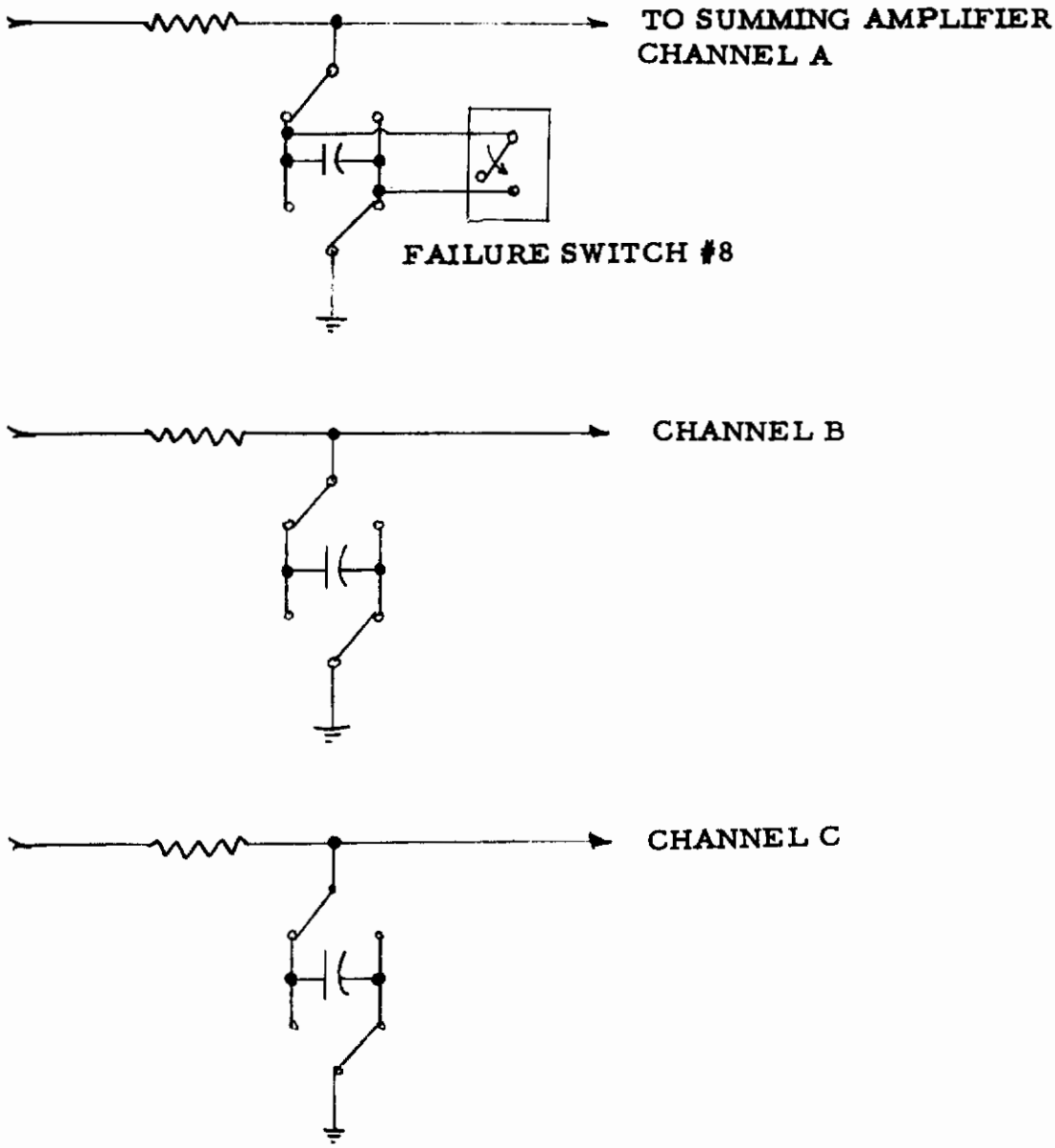

FAILURE SWITCH #8 - SHORTED CAPACITOR IN PASSIVE LAG NETWORK.

THIS MALFUNCTION CAUSES A HARDOVER TYPE FAILURE IN THE FOLLOWING UNIT CAUSING A .13% CHANGE IN ITS GAIN.

Figure 54. Failure Switch No. 8

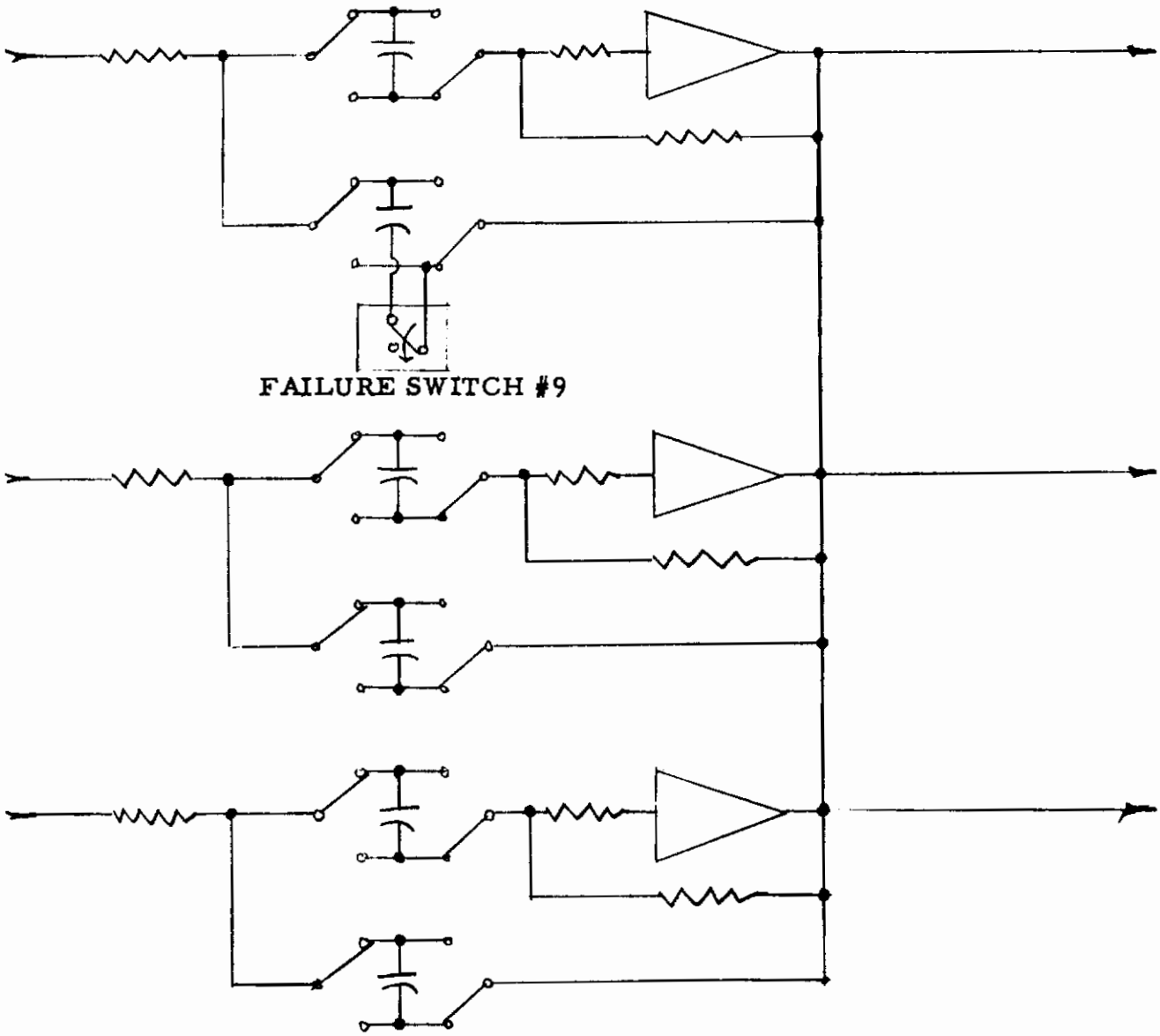

FAILURE SWITCH #9 - OPEN CAPACITOR IN THE FEEDBACK OF THE ACTIVE BANDPASS FILTER.

THIS TYPE OF MALFUNCTION CAUSES A HARDOVER TYPE FAILURE IN THE AMPLIFIER OF CHANNEL A. HOWEVER, THE TOTAL UNIT PERFORMANCE IS NOT NOTICEABLY EFFECTED.

Figure 55. Failure Switch No. 9

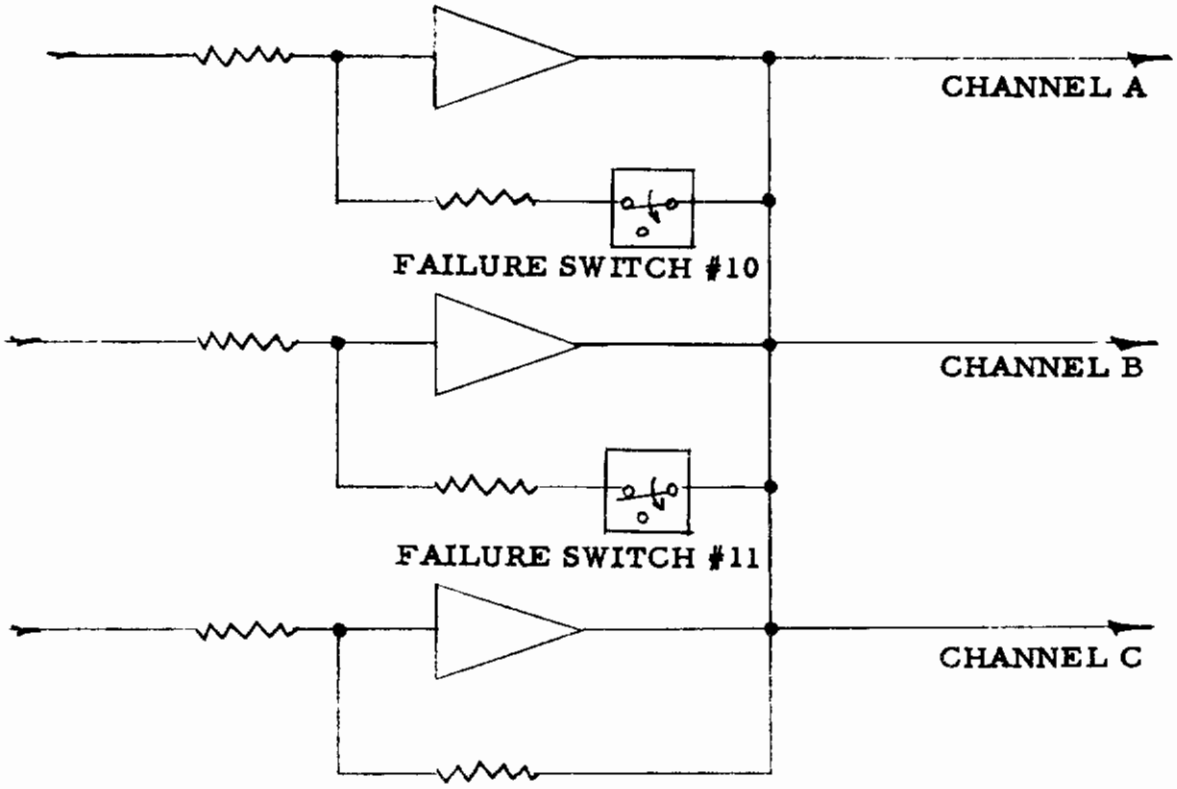

FAILURE SWITCHES #10 AND #11: OPEN FEEDBACK RESISTORS IN CHANNEL A AND CHANNEL B.

THIS TYPE OF FAILURE IN CHANNEL A ALONE OR CHANNEL B ALONE WILL NOT CAUSE A UNIT FAILURE. HOWEVER, IF BOTH OF THESE TYPE OF FAILURES OCCUR AT THE SAME TIME IN THE SAME UNIT, THE UNIT WILL FAIL. THESE FAILURES WERE INCLUDED TO SHOW THE EFFECT OF A UNIT FAILURE ON THE SYSTEM OPERATION.

Figure 56. Failure Switches No. 10 and No. 11

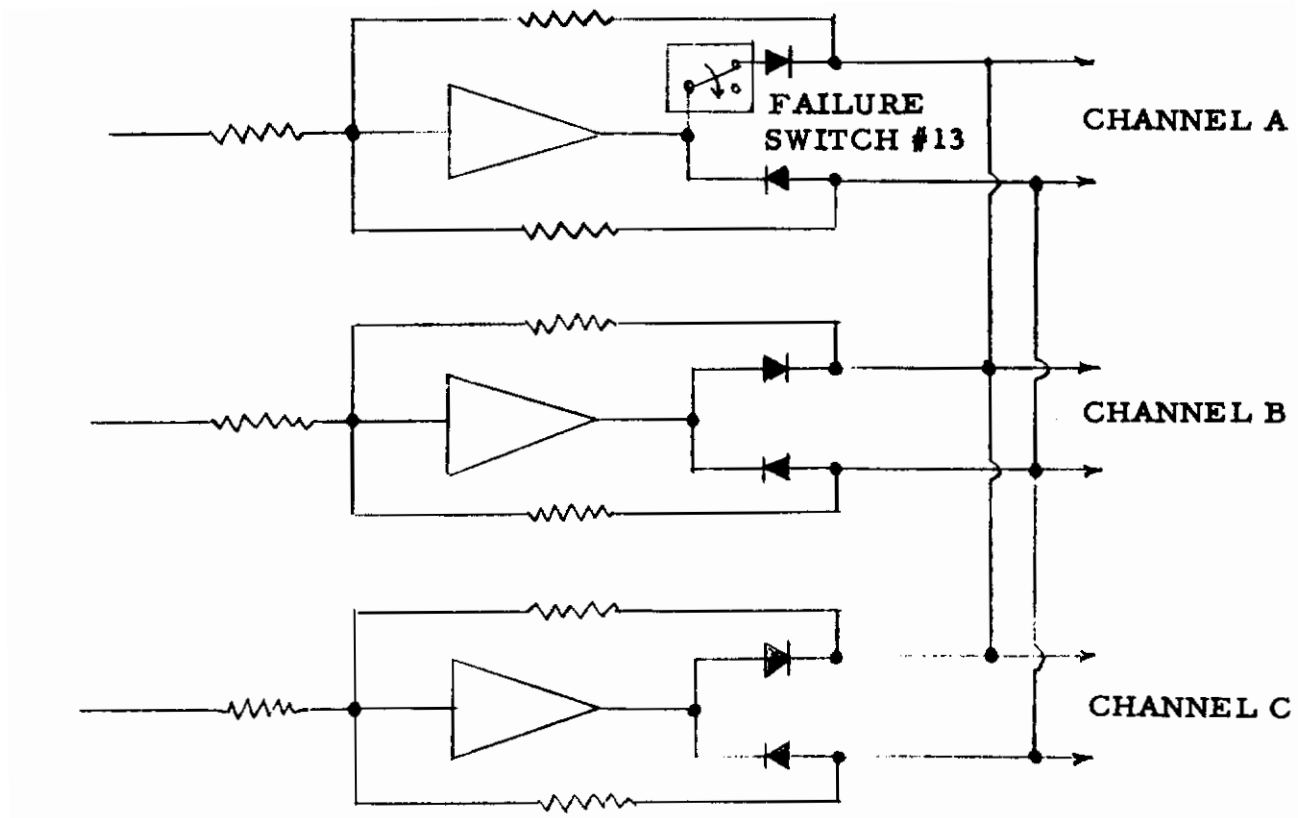

FAILURE SWITCH #13 - OPEN DIODE IN DETECTOR UNIT.

THIS FAILURE CAUSES THE A AMPLIFIER TO HAVE A ZERO TYPE FAILURE FOR EVERY HALF CYCLE.

Figure 57. Failure Switch No. 13

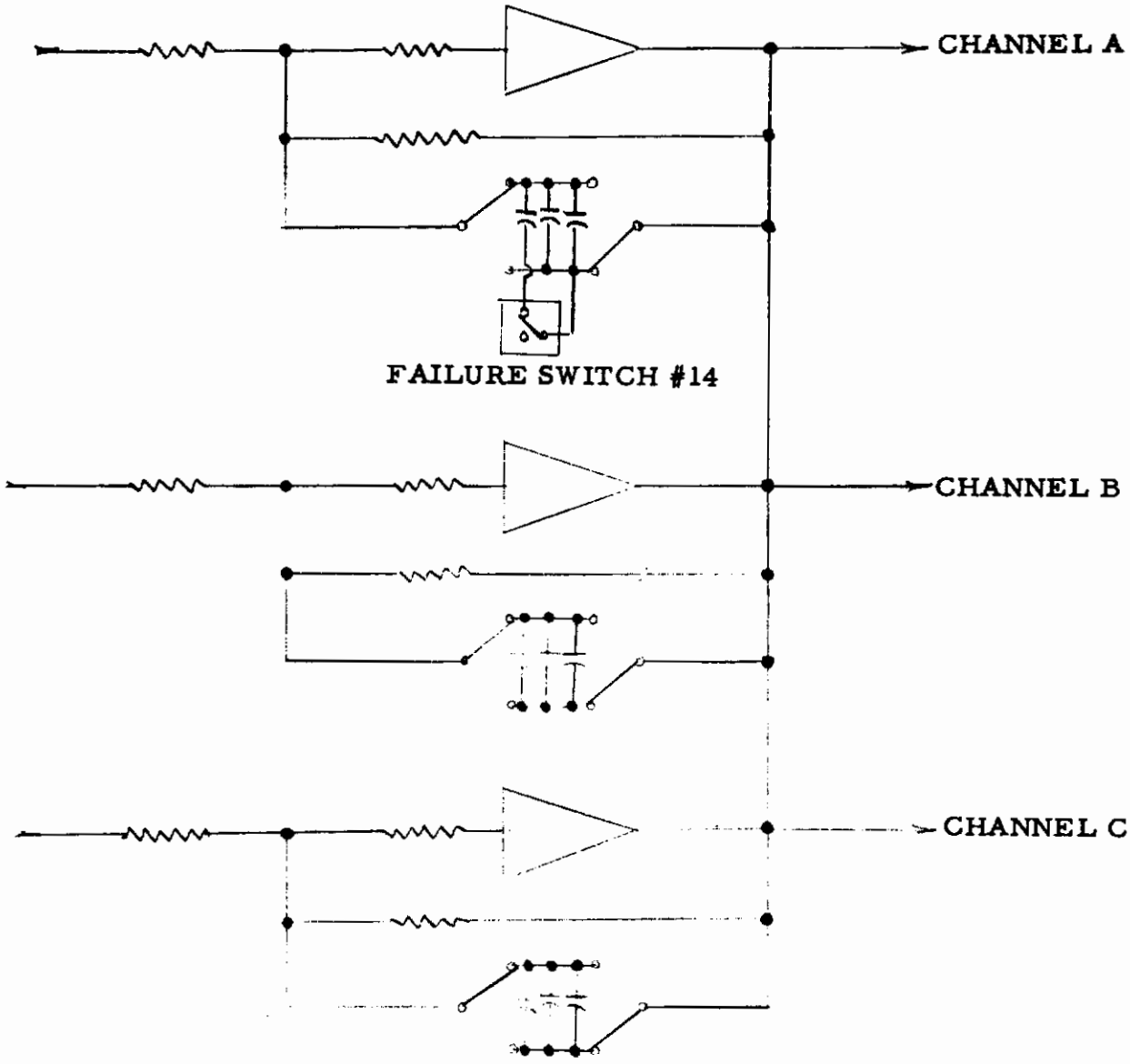

FAILURE SWITCH #14: CHANGE IN CAPACITANCE IN PSEUDO INTEGRATOR UNIT.

Figure 58. Failure Switch No. 14

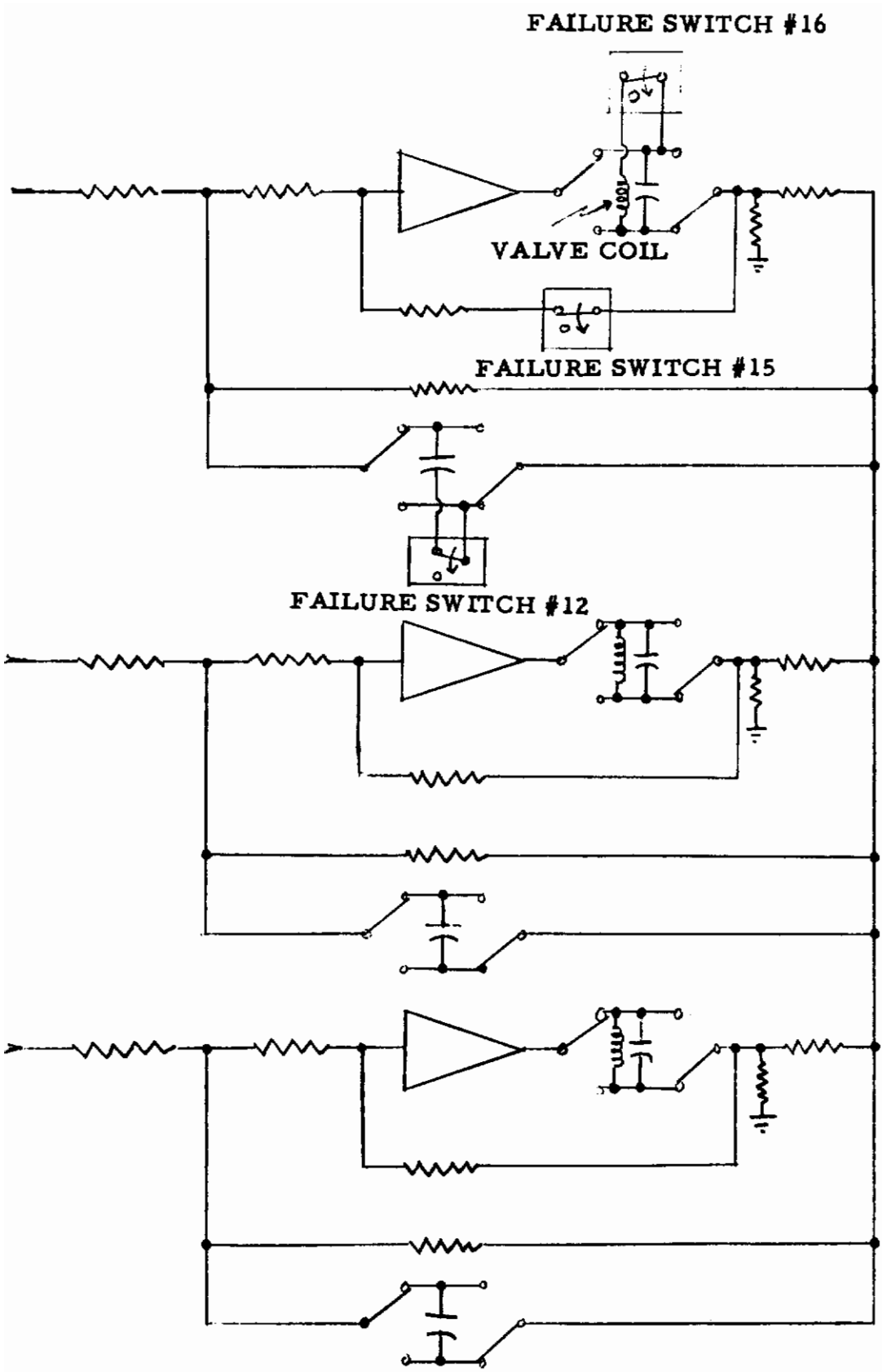

Figure 59. Failure Switches No.'s 12, 15, and 16

8.1 Failure performance can be demonstrated as follows:

8.2 Place the Master Control switch to RESET and the Flight Case Select switch to Number 2. Position the Channel No. 1 Recorder switch to $\dot{\theta}$ and Channel No. 2 to δe.

8.3 Position the $\dot{\theta}_c$ Dial to 5 ^{o}/sec.

8.4 Start the Recorder at a speed of 10 mm/sec and position the $\dot{\theta}_c$ switch to $+\dot{\theta}_c$. Allow the Recorder to run for 5 sec and then return the $\dot{\theta}_c$ switch to the EXT position.

8.5 Excite Failure switch No. 2 and repeat paragraph 8.4. This trace can now be compared with the original that has no failures.

8.6 In this manner, switches No. 3 through No. 16 may be engaged as long as no incompatible failure switches are chosen. Table 7 lists the non-compatible Failure switch combinations. A non-compatible failure is one in which there is a hardover type failure and a soft failure introduced in the same redundant unit or two hardover failures in the same direction in the same unit.

To correlate the failure switches with the actual circuit being failed, refer to Figures 54 through 63.

9.0 Securing Equipment.

9.1 Place Flight Case Select switch to No. 1, Master Control switch to RESET, Failure switches to OFF, and Master Power switch to OFF.

9.2 Place Recorder Power switch to the OFF position.

Table 7. Failure Compatibility Chart

Switch Number	2	3	4	5	6	7	8	9	10	11	12	13	14	15	16
2															
3			X	X			X	X	X		X			X	
4		X				X									
5		X													
6															
7			X												
8		X													
9		X													
10		X								X					
11									X						
12		X													X
13															
14															
15		X													
16											X				

X means not compatible

NOTE: A non-compatible failure is one in which there is a hardover type failure and a soft failure in the same unit or two hardover failures in the same direction in the same unit. In some cases depending on the signal level and flight case, a non-compatible mode will not result in a system failure. This is due to the adaptive loop compensating for a degraded unit.

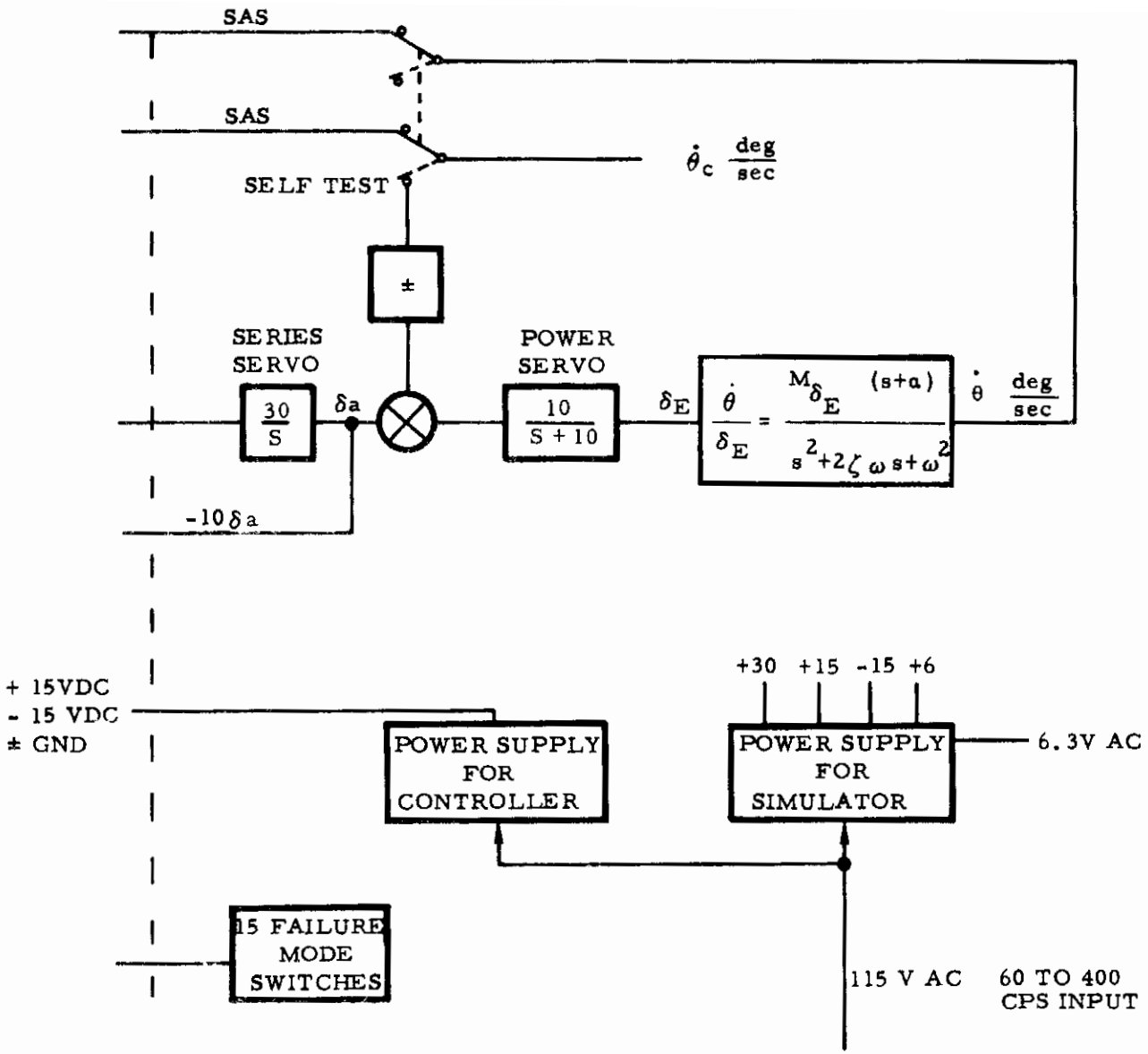

Figure 60. Simulator Block Diagram

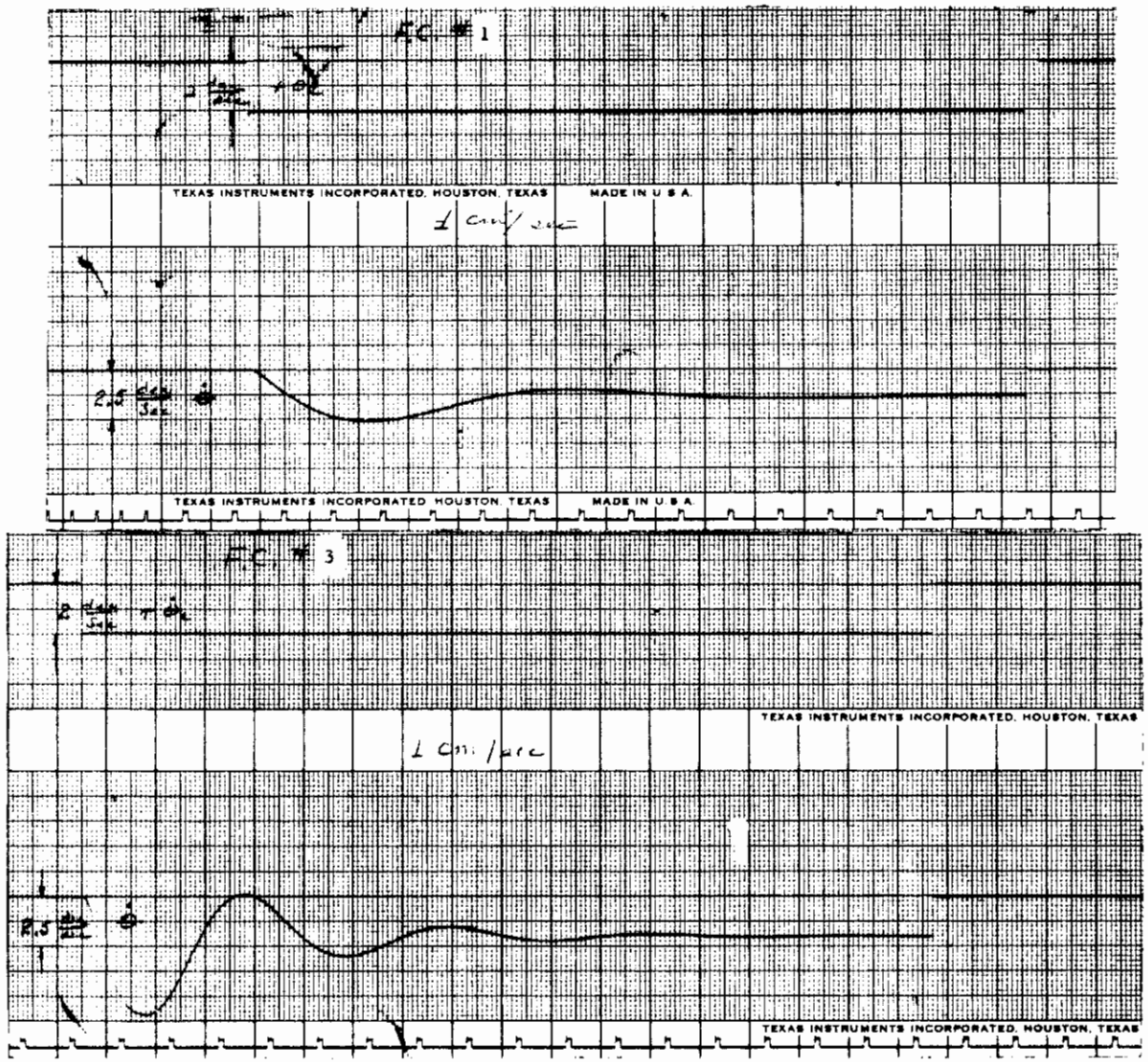

Figure 61. Flight Case No. 1 and No. 3

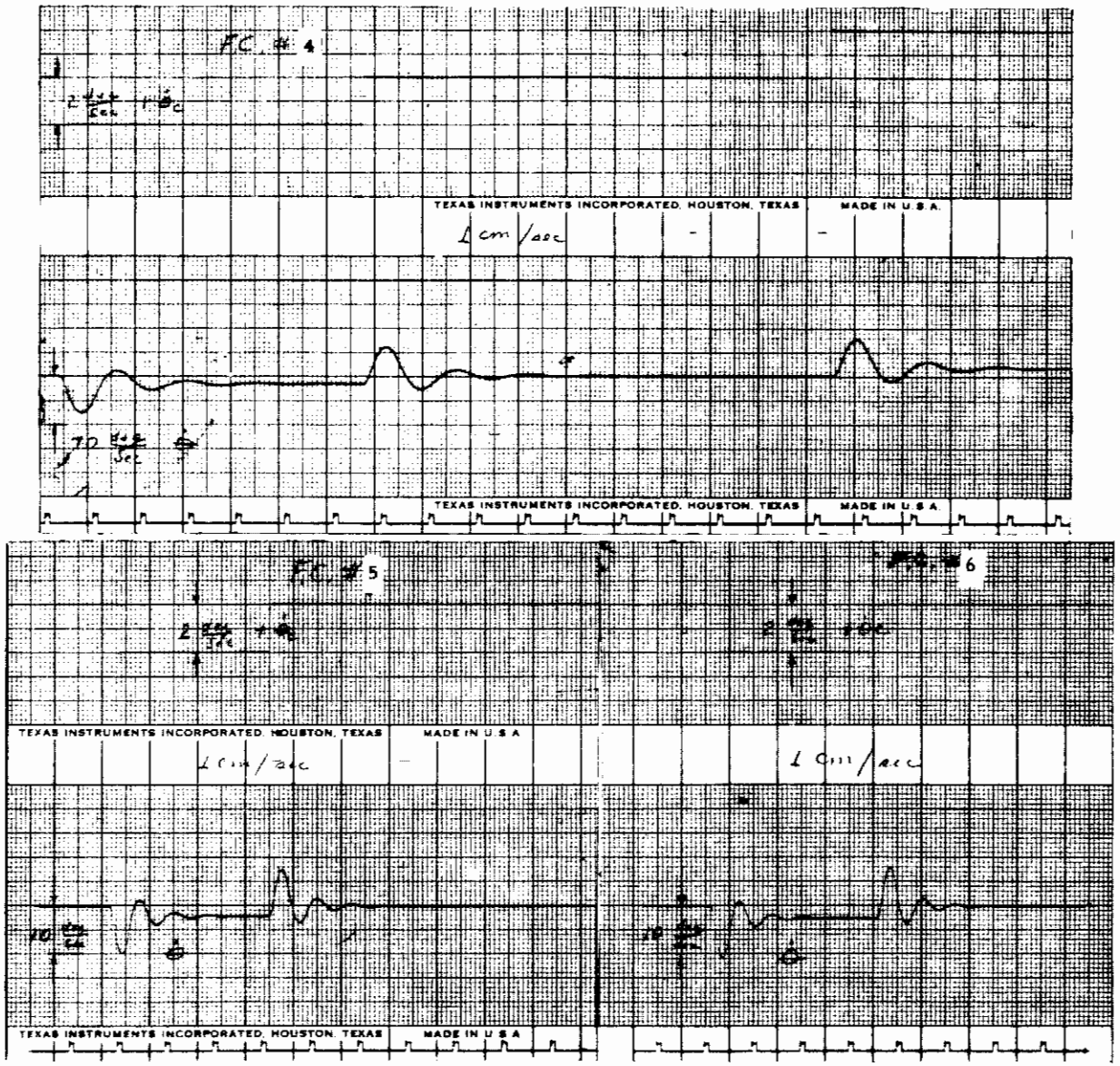

Figure 62. Flight Case No.'s 4, 5, and 6

APPENDIX II. FLIGHT SIMULATOR OPERATION MANUAL

A. GENERAL DESCRIPTION

The Simulator contains a series servo, power servo, airframe and power supplies. (See Figure 60.) The power supply for the Controller and failure mode control switches will be described later in detail. The Simulator provides $+10\,\delta a$, $-10\,\delta a$, $+\dot{\theta}$ and $-\dot{\theta}$ to the Controller for feedback to close the stability augmentation system loop. The Simulator also provides the $(\pm\dot{\theta}_c)$ input pitch rate command signal.

Self test features are incorporated as a means of testing the airframe and power servo for 5 of the 6 flight cases. The complete Simulator has 8 DC chopper stabilized amplifiers.

B. SELF TEST FEATURES

To perform a test of the airframe dynamics the following procedure is used: (After power is applied and amplifiers balanced)

1. Place Master Control switch to Bal Check
2. Place Flight Case switch on any position 1 thru 6 except 2
3. Put $\pm\dot{\theta}_c$ select switch in the vertical position
4. Place Master Control switch in Self Test mode
5. Put $\dot{\theta}_c$ select to left or right for + or $-\dot{\theta}_c$
6. $\dot{\theta}$ may be read on right hand meter
   $\dot{\theta}_c$ in this mode is a 2 deg/sec regardless what value is dialed and read on $\dot{\theta}_c$ meter
7. Data may be read on the recorder. The function desired may be choosen on each of the two Channel Select switches at the bottom of lower front panel. If slaving of the recorder paper drive is desired, then locate the Local Remote switch to Remote. This switch is located underneath the upper service cover of the Recorder, left front side. Local permits the

recorder paper drive switch to control the paper drive motor. Remote position will cause the paper drive motor to be actuated every time the Simulator is put in operate or self test mode. Figures 61 and 62 contain typical data from five of the six flight cases.

C. MANUAL FLIGHT CASE SETTINGS

Should it be desired to set up the flight cases with manual pots, do the following:

1. Put power ON and Master Control switch to Bal Check
2. Set Flight Case Select switch to Manual for the flight cases 4, 5, and 6. Set to $\left[M\delta_E{}^a \times 10,\ \omega^2 \times 10\right]$ for flight cases 1 and 3.
3. Set $\left[\frac{M\delta_E}{100}\right.$ to .8400, $\frac{M\delta_E{}^a}{200}$ to .5914, $\zeta\frac{\omega}{5}$ to .4320, $\frac{\omega^2}{100}$ to $\left..9664\right]$ for flight case 6 or as desired use complete table below.
4. Place Master Control switch to Self Test and $\dot{\theta}_c$ switch to (+) or (-), the transfer command $\dot{\theta}$ will be seen on the $\dot{\theta}$ meter and data can be recorded as previously described.

MANUAL SETTINGS FOR FLIGHT CASES

Flight case	$\frac{M\delta_E}{100}$	$\frac{M\delta_E{}^a}{200}$	$\frac{\zeta\omega}{5}$	$\frac{\omega^2}{100}$
1*	.0114	.0236**	.0604	.0707**
2				
3*	.0531	.1270**	.0692	.2585**
4	.2297	.0874	.2088	.2027
5	.7000	.4445	.4000	.8500
6	.8400	.5914	.4320	.9664

*Note For F. C. No. 1 and No. 3 the Flight Case Select switch must be set to $\left[\frac{M\delta_E{}^a}{200} \times 10,\ \frac{\omega^2}{100} \times 10\right]$ to give the gain shown with **

D. MAINTENANCE OF THE SIMULATOR

1. Power Requirements - 115VAC 60 to 400 cps.

AC Power Fuses - FS-1 and FS-2 should be 1 amp 3AG type, located on the rear middle panel. The AC power fuse for the P/N 10.179 power supply is located on the power supply and should be a 1 amp S. B.

2. Power Supply Adjustment

The power supply for the simulator (P/N 10.179) is available by releasing two cam-loc fasteners on the rear lower panel, which hinges down. This power supply may be removed from the Simulator by releasing the cam-loc hold down fastener at the top of the supply. A preliminary check of the power supply may be made prior to operation by doing the following:

1. Connect AC power to the rear of the Simulator, using the cable provided.

2. Set the Mode Control switch to Bal-Check.

3. Turn A.C. power switch to ON.

4. Check -15V, +15V and +30V DC power by a suitable instrument in the order given. All connections are banana jack terminations including ± gnd. These power voltages are all regulated. The 6.3VDC voltage is not regulated and not available to be read on the panel of the power supply.

3. Power Supply Adjustment (Alternate Method)

An alternate method for checking the adjustment of the -15VDC to the +15VDC supply is given. Both are used as reference sources in the Simulator. Release the top lid of the Simulator by depressing two finger release catches and lifting the lid. This exposes the amplifier balance meter and controls. Set the Amplifier Select switch to Ref-Balance. With the Master Control switch on Bal-Check position, this meter will then read the difference between the +15VDC to -15VDC supplies. Always adjust the -15 to the +15 since the +15VDC provides part of the +30VDC. All adjustments for D.C. power may be done on the front panel of the power supply.

4. Power Supply Trouble

Should trouble exist in the power supply (P/N 10.179), consult the Electronic Associates Inc. 10.179 Power Supply Manual.

5. Amplifier Balance

Set the Master Control switch to Bal-Check. Release the upper panel and set the Amplifier Select switch from 1 through 8 and balance each respective amplifier balance pot. It is recommended that the balance pot be turned in small increments, and to wait a few seconds for the meter to indicate the balance condition. When the balance meter is at midpoint, this indicates minimum offset. Always leave the Amplifier Select switch to OFF when not in use.

6. D. C. Amplifier Trouble

If trouble is experienced in any amplifier, consult the EAI P/N 6.368 D. C. Amplifier Manual. If the amplifier is to be removed and checked outside the Simulator, two connections must be made inside the amplifier to restore the internal balance pot of the amplifier. A tag inside the amplifier indicates this change. Also, to be used inside the Simulator again, these two connections must be removed.

7. Calibration

The $+\dot{\theta}_c$ is set to +2VDC by R94. The $-\dot{\theta}_c$ is set to -2VDC by R95. These two trim pots are adjustable from the bottom middle of the Simulator. Tolerance for the $\dot{\theta}_c$ is ±20 mv. The above adjustments should be made with the $\frac{\dot{\theta}_c}{10}$ potentiometer (R-29, R-30) at the maximum position. This affords correct loading when used normally. These voltages may be measured at the recorder cable (pin B is gnd, A is the voltage) by placing the Recorder Channel switch on $\dot{\theta}_c$.

8. Meter Calibration and Limits

1. To calibrate the $\dot{\theta}_c$ meter (M_1), do the following:

   a. Power switch to ON
   b. Master Control to Bal-Check
   c. Set $\dot{\theta}_c$ select switch (SW_3) to $+\dot{\theta}_c$
   d. Adjust $\frac{\dot{\theta}_c}{10}$ pot (R-29, R-30) to maximum clockwise
   e. Adjust R81-B until the $\dot{\theta}_c$ meter M_1 reads + 10 deg/sec. Lift top lid to reach adjustment. R81-B is located on CD9 resistor board.
   f. Check the calibration of the meter in the minus direction, by reversing the $\dot{\theta}_c$ select switch to $-\dot{\theta}_c$ position. The above check will be correct providing calibration, section 7, was done properly.

2. To calibrate $\dot{\theta}$ meter (M_2) do the following:

   a. Power switch to ON
   b. Master Control switch to Reset position
   c. Use a precision 1 meg resistor (.01% preferred), a precision voltage source adjusted to ±20 VDC within ±50 MV and a digital voltmeter or VTVM.
   d. Take the bottom cover of the Simulator off. Connect one end of the 1 meg resistor to pin S.J. of amp #7 (CD4-16) and the other end to the voltage source. The voltage source ± goes to gnd. This gives ±2 V out of amp #7. Check the value with an external meter. With ±2V out of amp #7, M_2 can be calibrated for + 10 deg/sec by adjusting R-82-B. Lift top lid to reach adjustment. R-82-B is located on CD9 resistor board. Refer to Figure 63.

   e. The limit of meter M_2 has been made by setting R-82-A so that zener diodes D-17 and D-18 are drawing current above ±2V input (amp #7 output). This adjustment has been preset and should require no further adjustment. Removing the lead from CD9-6 to the ground side of M_2 will indicate when zeners are drawing current. This limit is for meter protection only. CD9 resistor board is located directly behind meter panel.

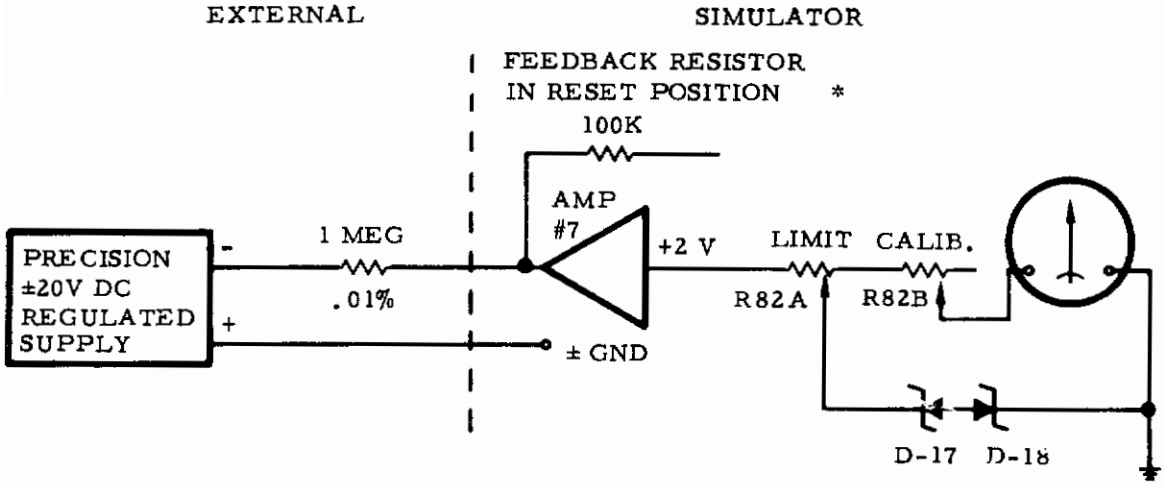

* SIMULATOR MASTER CONTROL MUST BE IN "RESET" POSITION

Figure 63. External Simulator

3. Calibration of M_3 amp balance meter. Calibration is not necessary as a relative condition of amplifier balance or offset only is shown. Limits are provided to protect the meter when unusual conditions exist, such as DC power fuse blown, a defective DC amplifier, bad reset resistor, etc. The limit has been set to clamp any excessive voltage appearing at the input to the meter (CD 10-1 resistor board). This limit pot R-79 (mounted on CD 10 resistor board) is located directly beneath M_3.

9. Calibration of Oscillo/Riter Recorder

1. Provision is made by the internal reference cell in the high gain DC amplifier to give a 2 cm deflection of the pen. This cell should be replaced annually per Recorder Instruction Manual.

2. An alternate method of calibration is available through a reference voltage supplied by R80 on the CD 10 resistor board. This pot has been set for +2V. By placing the Simulator Channel Select switches in the Cal position, the Oscillo/Riter Recorder may be set on the 2V scale and a pen deflection of one cm will be noted if the gain is set properly on the Recorder.

10. Recorder Trouble

For any malfunction regarding the Oscillo/Riter Recorder, refer to the Texas Instruments Recorder Manual No. 161684-4. Modifications of the recorder involve only slaving.

11. Power Supply for Controller

The power supply requires 115VAC 60 to 400 cps. The FS-2 (1 amp 3AG) fuse, on the rear of the panel, supplies the power from the Power ON-OFF switch. Two 15VDC voltages are connected to terminal strip TS-3, 4, 5, 6, and brought out to J6-N, P, R, S, respectively. TS-1 and TS-2 are the AC inputs for the supply. Should a malfunction exist, the supply is located behind the rear upper half of the Simulator. By removing the upper perforated metal panel, the terminal strip is exposed for check out. To remove the power supply do the following:

1. Turn power off and remove power cable.

2. Remove upper and middle rear panels.

3. Remove (6) six lugged wires from terminal strip TS-1 through TS-6.

4. Remove two socket head bolts, holding brackets for the power supply and pull straight out.

This power supply is not regulated. The regulator section is contained in the Controller.

E. FREQUENCY RESPONSE CHECK OF THE SIMULATOR

A complete frequency response check was made of the Simulator including the series servo, power servo, and airframe. An S plane frequency response program was run on the Recomp digital computer for five of the flight cases. The frequency was checked from O radian/sec to 45 rad/sec. Data from the digital program included values of gain and phase shift (ϕ).

The following equipment was used to perform the frequency response check, connected as shown in Figure 64.

1 - External D. C. Amplifier
(Chopper stabilized)

1 - Servoscope MOD 1100

1 - Counter HP-522B

1 - Oscilloscope HP-130 BR

2 - Scale factor potentiometers

The counter was used to measure the period of oscillation, in order to get accuracy at very low frequencies. The scope was used as a standard for the 1 VP. P. input signal and measurement of phase shift at the servoscope. The servoscope was used to directly read phase lead or lag (ϕ) of the system. The external D. C. amplifier was used to simulate the summing point in the controller. The scale factor pots were necessary to close the loop with the correct gain factor.

Table 8 gives data calculated by the S plane frequency response check and actual values tabulated for five of the flight cases, involving gain and phase.

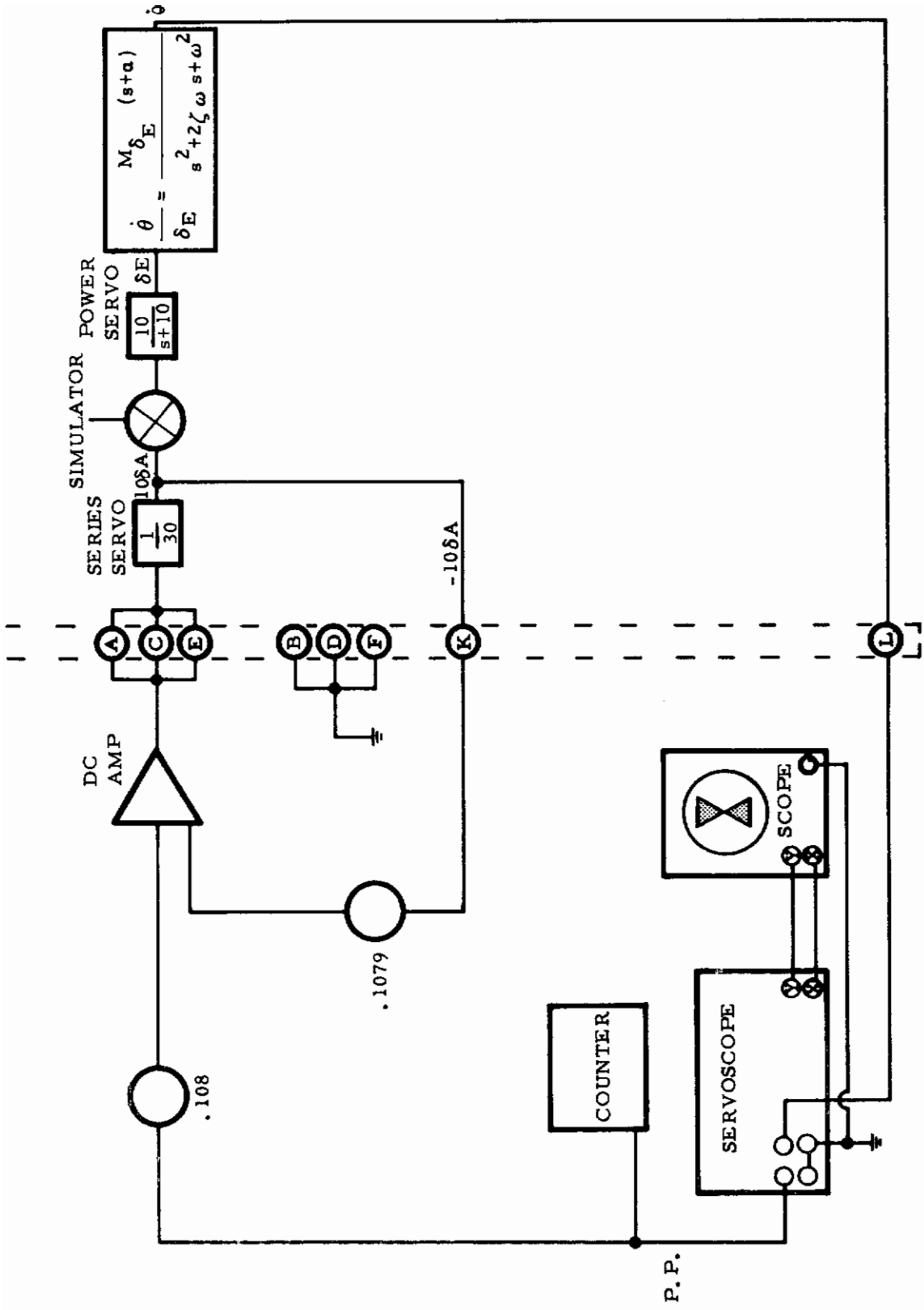

Figure 64. Frequency Response Check Block Diagram

Table 8. Frequency Response of System

	Frequency			Gain		Phase	
	CPS	$\frac{1}{c}$	Radians/sec	Actual	Calculated	Actual ϕ	Calculated ϕ
FC #1	.479	2.087	3.0	.375	.387	+71.7°	+72.03°
	.795	1.26	5.0	.2	.206	+55.5°	+56.3°
	1.43	.6993	7.0	.09	.09	+30.5°	+32.5°
	1.75	.57142	11.0	.06	.065	+24°	+23.13°
	2.23	.4484	14.0	.0405	.043	+10.°	+11.3°
	2.71	.369	17.0	.0285	.0296	+2°	+1.56°
FC #3	.479	2.087	3.0	2.15	2.28	+77.°	+76.46°
	.795	1.26	5.0	.99	1.03	+56.5°	+57.2°
	1.43	.6993	9.0	.42	.43	+31.0°	+32.8°
	1.75	.57142	11.0	.30	.311	+21°	+23.3°
	2.23	.4484	14.0	.196	.20	+9.2°	+11.4°
	2.71	.369	17.0	.138	.138	+1.°	+1.66°
FC#4	.479	2.087	3.0	5.3	5.253	-155.7°	-155.7°
	.795	1.26	5.0	8.4	8.94	+105.°	+110.9°
	1.43	.6993	9.0	2.2	2.32	+41.5°	+43.6°
	1.75	.57142	11.0	1.52	1.54	+29.5°	+31.0°

Table 8. (Cont)

	Frequency			Gain		Phase	
	CPS	$\frac{1}{c}$	Radians/sec	Actual	Calculated	Actual ϕ	Calculated ϕ
FC#4 (Cont)	2.23	.4484	14.0	.9	.95	+14.°	+16.8°
	2.71	.369	17.0	.63	.63	+3.5°	+5.8°
FC#5	.479	2.087	3.0	2.97	2.82	-144.8°	-144.3°
	.795	1.26	5.0	5.2	5.037	-160.°	-158.7°
	1.43	.6993	9.0	12.4	12.5	-112.2°	-119.6°
	1.75	.57142	11.0	8.4	8.61	+63.0°	+66.2°
	2.23	.4418	14.0	4.0	4.16	+29.2°	+32.1°
	2.71	.369	17.0	2.375	2.44	+12.3°	+15.08°
FC#6	.479	2.087	3.0	3.15	2.994	-146.7°	-145.9°
	.795	1.26	5.0	5.20	5.145	-159.5°	-158.5°
	1.43	.6993	9.0	13.00	13.00	+127.2°	+134.°
	1.75	.57142	11.0	10.8	11.01	+74.0°	+77.6°
	2.23	.4484	14.0	5.1	5.35	+33.°	+36.1°
	2.71	.369	17.0	2.95	3.06	+14.5°	+17.°

APPENDIX III. FUNCTIONAL TEST SPECIFICATIONS

A. VOLTAGE REGULATOR P/N 56650-401

1. The following equipment shall be used to perform the functional test.

   (1) Differential D C Voltmeter.

   (2) Oscilloscope, Tektronix 545 or equivalent.

   (3) Unregulated DC voltage source capable of delivery 15 - 22 vdc @ 200 ma.

   (4) Resistor, 100 ohms ± 1%, 1 watt.

   (5) Resistor, 75 ohms ± 1%, 3 watts.

   (6) Decade box, 0-100K.

   (7) Resistor, 50 ohms ± 1%, 1 watt.

2. Output Voltage

2.1 Connect the regulator module as shown in Figure 65.

2.1.1 Set switch S1 to position 2.

2.1.2 Set decade box to 100 ohms.

2.1.3 Turn on the unregulated d-c voltage source and set the unregulated voltage to 18 ± 0.1 v dc.

2.1.4 Adjust the decade box until the voltage at terminal E is 12 ± 0.01 v dc.

3. Regulation

3.1 Vary the unregulated d-c voltage from 16 to 18 v dc.

3.1.1 The output voltage at E should not change more than ± 15 mv.

3.2 Set the unregulated d-c voltage to 18 v dc.

3.2.1 Set switch S1 to position 2.

3.2.2 The voltage at E should not change by more than 25 mv.

3.2.3 Measure the ac ripple voltage at E. The ripple voltage shall be less than 15 mv peak-to-peak.

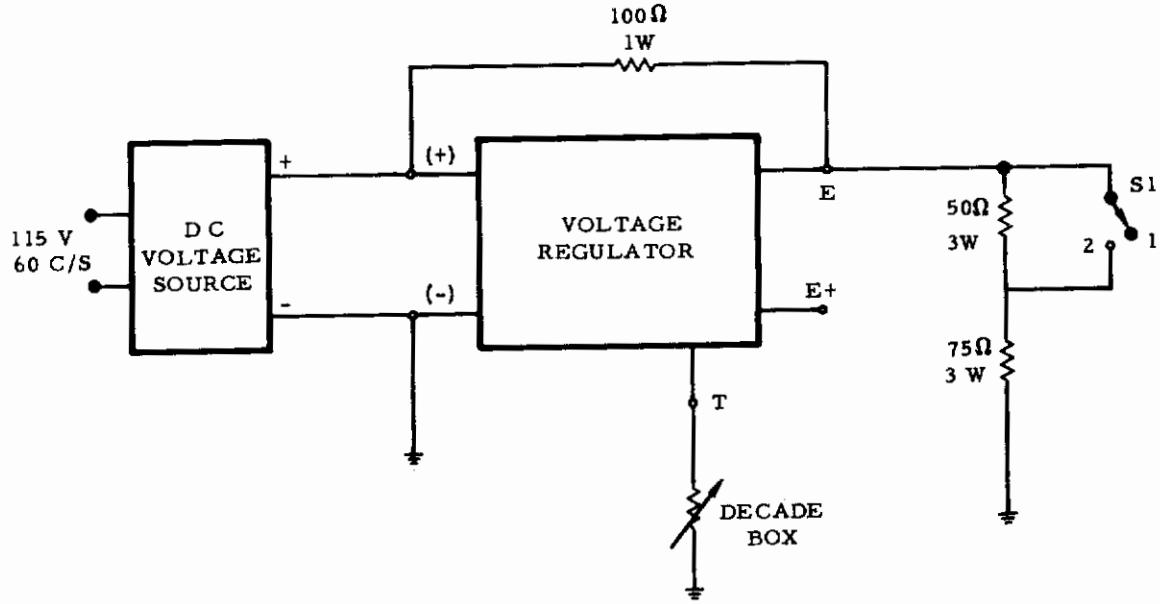

Figure 65. Regulator Test Circuit

B. A-C AMPLIFIER P/N 55150-502

1. The following equipment shall be used to perform the functional test.

   (1) Oscillator - H. P. Model 650A or equivalent.

   (2) A-C Amplifier Test Fixture.

   (3) Oscilloscope - Tektronix 545 or equivalent.

   (4) SAS Functional Test Box.

   (5) RMS Voltmeter, H. P. Model 400H or equivalent.

2. Performance Test

2.1 Connect the a-c amplifier module into the a-c amplifier test fixture as shown in Figure 66.

2.2 Open Loop Gain

Set switch S1 to position 1, switch S2 to position 1, and switch S3 to position 1.

2.2.1 Turn on ± 12 v dc power supplies.

2.2.2 Set the sinewave oscillator at 2.0 kc and adjust the oscillator output for an 8 volt peak-to-peak signal output at C.

2.2.3 Vary the frequency of the oscillator (2 to 10 kc) to determine the frequency at which the output will peak.

2.2.4 Record the frequency at which the amplifier peaks and measure S and C in volts rms.

2.2.5 The open loop gain of the amplifier will be:

$$K = \frac{C}{S} = 880 \text{ v/v}$$

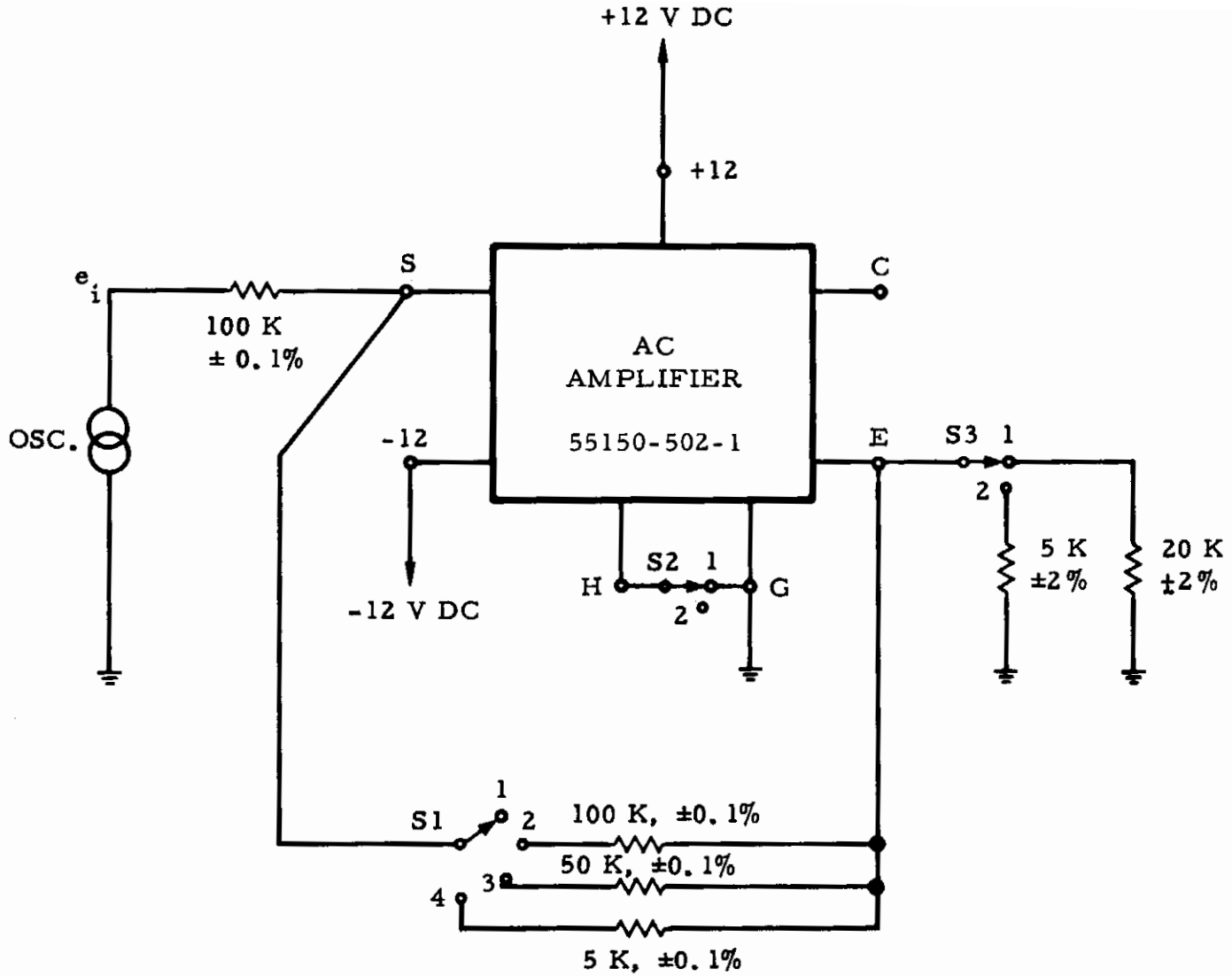

Figure 66. AC Amplifier Test Circuit

2.2.6 Set switch S2 to position 2. Adjust the output of the oscillator so that the output at C reads 8 volts peak-to-peak.

2.2.7 The new gain $K' = \frac{C}{S} = 74$ v/v

2.3 Closed Loop Gain Stability

2.3.1 With the conditions of 2.2.6, set S1 to position 2.

2.3.2 Adjust the oscillator for an 8v peak-to-peak output at e_o. The amplifier should exhibit no signs of instability and the forward gain $K = R_f/R_i = 1$

2.3.3 Adjust the oscillator output until the signal at C just starts to clip the top or bottom of the waveform. The maximum amplifier output swing should be 10 ± 0.5 v peak-to-peak.

2.3.4 Repeat 2.3.2 with switch S2 in position 3 and position 4. In each case the amplifier should exhibit no signs of instability and the forward gain is $K = R_f/R_i$

2.4 Current Limiter

Connect the amplifier as in 2.2.6 and set S3 to position 2. Adjust the oscillator output until the waveform at C just starts to clip at the top or bottom. The voltage at E should be 5.7v ± 0.12 volts peak-to-peak.

C. CARRIER GENERATOR P/N 55160-502

1. The following equipment shall be used to perform the functional test.

(1) SAS Functional Test Box

(2) Oscilloscope - Tektronix 545 or equivalent.

(3) Capacitor, 0.12 Mf, 100V, Electrocube type, 217A1B124F or equivalent.

2. Performance Test

Connect the carrier generator module as shown in Figure 67.

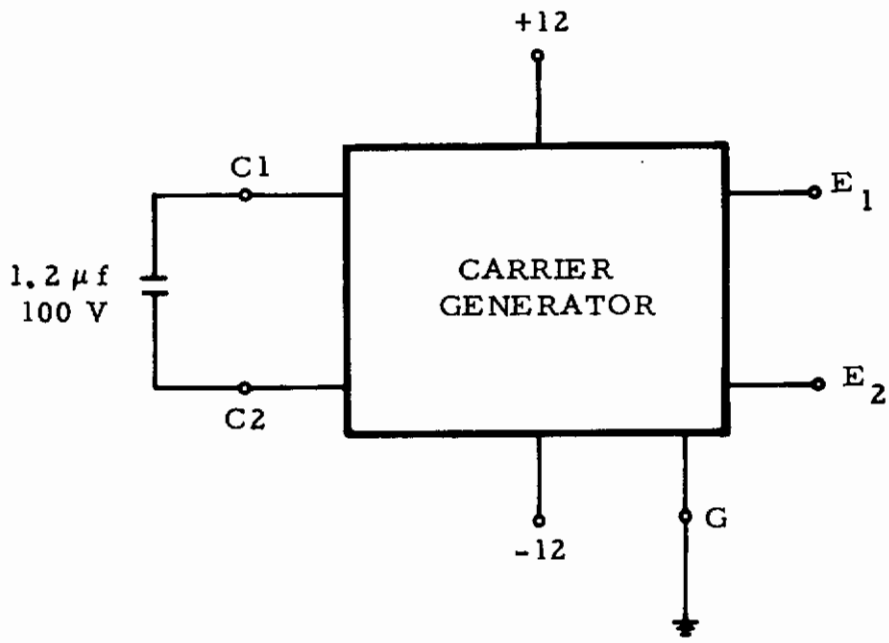

Figure 67. Carrier Generator Test Circuit

2.1 Frequency Check

2.1.1 Turn on the ± 12 v dc power supplies.

2.1.2 Connect the oscilloscope to terminal E1.

2.1.3 The square wave output at E1 should be ± 1 v peak.

2.1.4 Measure the period of the waveform. Each half cycle should be 1.25 milliseconds ± 5%.

2.2 Rise and Fall Time

2.2.1 Set the sweepspeed of the oscilloscope to 0.1 microseconds per centimeter.

2.2.2 The rise and fall time of the wave should be less than 30 nanoseconds.

2.3 Connect the oscilloscope to output E2.

2.3.1 Repeat sections 2.1.3 through 2.2.2.

D. SYNCHRONOUS SWITCH P/N 55100-504

1. The following equipment shall be used to perform the functional test.

   (1) SAS Functional Test Box.

   (2) Synchronous Switch Test Fixture.

   (3) Oscilloscope, Tektronix 545.

2. Synchronous Switch No. 1.

2.1 OFF Impedance

2.1.1 Plug in the synchronous switch module into the synchronous switch test fixture.

2.1.2 Set the switches to the following positions:

   (1) S-1 - position 1

   (2) S-2 - position 1

   (3) S-3 - position 1

   (4) S-4 - position 1

2.1.3 Connect the 10 meg probe of the scope to V_s on the SAS functional test box. Set the 400 cps square wave to ± 5v peak.

2.1.4 Connect the scope probe to D_{2-3}. The voltage should be greater than ± 4.5v peak.

2.1.5 Set switch S3 to position 2.

2.1.6 Connect the 10 meg probe to D_{1-4}. The voltage at this terminal should be greater than ± 4.5v peak.

2.2 ON Resistance

Set switch S3 to position 3.

2.2.1 Connect the 10 meg probe to D_{1-4}. The voltage at this terminal should be equal to or greater than ± 3.5v peak.

2.2.2 Set switch S-3 to position 4.

2.2.3 Connect the 10 meg probe to D_{2-3}. The voltage at this terminal should be equal to or greater than ± 3.5v peak.

2.3 Rise Time

With the conditions stated in 3.2.1, measure the rise and fall time of the square wave. The rise and fall time should be less than 50 nanosec.

2.4 Null

2.4.1 Set switch S-3 to position 5.

2.4.2 Connect a direct probe from the oscilloscope to terminal D_{1-4}. The signal voltage should not exceed 30 mv peak-to-peak.

2.4.3 Set switch S1 to position 2.

2.4.4 The signal voltage at terminal D_{1-4} should not exceed 30 mv peak-to-peak.

2.4.5 Set switch S3 to position 6.

2.4.6 Connect the direct probe to terminal D_{2-3}. The signal voltage should not exceed 30 mv peak-to-peak.

2.4.7 Set switch S1 to position 1.

2.4.8 The signal voltage at D_{2-3} should not exceed 30 mv peak-to-peak.

3. Synchronous Switch No. 2

3.1 Set the switches to the following positions:

(1) S1 - position 1

(2) S2 - position 2

(3) S3 - position 1

(4) S4 - position 2

3.1.1 Repeat steps 2.1.3 through 2.4.8.

E. SYNCHRONOUS SWITCH DRIVER P/N 55105-504

1. The following test equipment shall be used to perform the functional test:

(1) Square Wave Generator, H. P. model 211AR

(2) Oscilloscope - Tektronix 545 or equivalent

(3) SAS Functional Test Box

(4) Two fixed resistors, 100 Ω ± 2%, 2 watt.

2. Performance Test

Connect the Synchronous Switch Driver module as shown in Figure 68. Terminals S1 and S2 are connected to the output of the carrier generator in the SAS functional test box.

2.1 Connect the oscilloscope to terminal E1.

2.1.1 Turn on the power to the SAS controller functional test box.

2.1.2 The waveform at e_{o1} will be a 400 cps square wave with a peak amplitude equal to the value of 11 v ± 0.2v. The negative peak amplitude should have the same peak value ± 0.02 volts.

2.2 Rise and Fall Time

2.2.1 Set the sweep time of the oscilloscope to 0.1 microseconds per centimeter. · The rise and fall time of the waveform at E1 should be less than 50 nanoseconds.

2.3 Connect the oscilloscope to terminal E2.

2.3.1 Repeat steps 2.1.2 through 2.2.1.

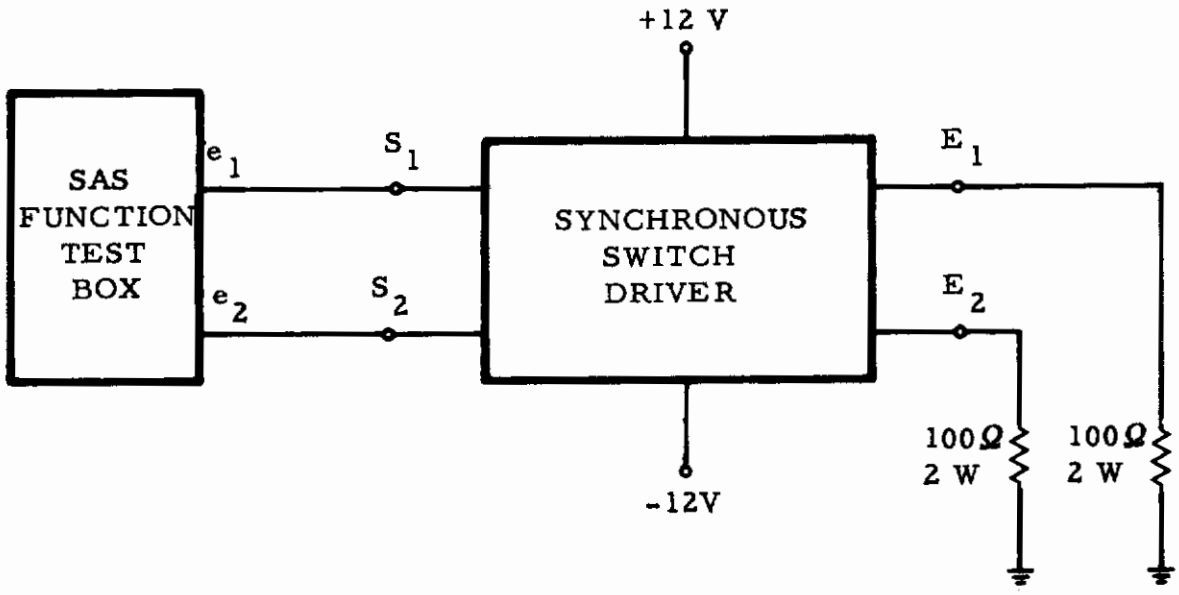

Figure 68. Synchronous Switch Driver Test Circuit

APPENDIX IV. TRISAFE SINGLE AXIS FLIGHT CONTROL SYSTEM

A. LIST OF DRAWINGS:

1. Controller

Drawing Number	Nomenclature
57200-507	Assembly, Controller
57201-507	Schematic, Controller
57202-507	Subassembly, Electronic
57213-507	Nameplate
56650-401	Assembly, Regulator
56651-401	Schematic, Regulator
56652-401	Circuit Board
56653-401	Circuit Board
56654-401	Header
55155-502	Terminal
55168-502-1	Label
55150-502	Assembly, AC Amplifier
55151-502	Schematic, AC Amplifier
55152-502	Circuit Board
55153-502	Circuit Board
55154-502	Header
55155-502	Terminal

Drawing Number	Nomenclature
55167-502-1	Label
55160-502	Assembly, Carrier Generator
55161-502	Schematic, Carrier Generator
55162-502	Circuit Board
55163-502	Circuit Board
55164-502	Header
55155-502	Terminal
55167-502-3	Label
55100-504	Assembly, Synchronous Switch
55101-504	Schematic, Synchronous Switch
55102-504	Circuit Board
55103-504	Circuit Board
55104-504	Header
55155-502	Terminal
55171-502-1	Label
55105-504	Assembly, Synchronous Switch Driver
55106-504	Schematic, Synchronous Switch Driver
55107-504	Circuit Board
55108-504	Circuit Board
55109-504	Header
55155-502	Terminal
55169-502-1	Label

2. Simulator

Drawing Number	Nomenclature
55080-399	Top Assy, Simulator
55081-399	Sub-Assy, Amplifiers And Power Supply
55082-399	Mounting Brackets, Bottom Plate
55083-399	Layout, Rear Panel
55084-399	Schematic, Simulator
55085-399	Assy, Resistor Boards CD1, 2, 3 and 4
55086-399	Assy, Resistor Boards CD5, 6, 7, 8, 9, 10
55087-399	Location Chart, Amplifiers

B. LIST OF VENDOR SUPPLIED INFORMATION

1. Controller

Part Number	Nomenclature	Vendor
30087 (Drawing)	Assembly, Dust Cover	Electronic Enclosures

2. Simulator

Part Number	Nomenclature	Vendor
30044 (Drawing)	Cabinet, Simulator	Electronic Enclosures
6.368 (Manual)	Dual DC Amplifier	Electronic Associates
10.179 (Manual)	Power Supply	Electronic Associates

3. Recorder

Part Number	Nomenclature	Vendor
161684-4 (Manual)	Oscillo/Riter Recorder	Texas Instruments

Unclassified

Security Classification

DOCUMENT CONTROL DATA - R&D

(Security classification of title, body of abstract and indexing annotation must be entered when the overall report is classified)

1. ORIGINATING ACTIVITY (Corporate author)	2a. REPORT SECURITY CLASSIFICATION
North American Aviation, Inc. Autonetics Division 3370 Miraloma Ave., Anaheim, California	Unclassified
	2b. GROUP N/A

3. REPORT TITLE

TRISAFE SINGLE AXIS FLIGHT CONTROL SYSTEM

4. DESCRIPTIVE NOTES (Type of report and inclusive dates)

Final

5. AUTHOR(S) (Last name, first name, initial)

Williams, H. O. Ehlers H. L.
Blosser, R. D.

6. REPORT DATE	7a. TOTAL NO. OF PAGES	7b. NO. OF REFS
March 1965	121	0

8a. CONTRACT OR GRANT NO.	9a. ORIGINATOR'S REPORT NUMBER(S)
AF33(615)-1479 b. PROJECT NO. 8225 cTask No. 822504 d.	AFFDL-TR-65-89
	9b. OTHER REPORT NO(S) (Any other numbers that may be assigned this report) N/A

10. AVAILABILITY/LIMITATION NOTICES

Qualified requestors may obtain copies from DDC or the sponsor, FDCL, Wright-Patterson AFB, Ohio. CFSTI and foreign distribution is limited because of report contents identifiable with DOD strategic embargo list.

11. SUPPLEMENTARY NOTES	12. SPONSORING MILITARY ACTIVITY
N/A	AF Flight Dynamics Laboratory FDCL Wright-Patterson AFB, Ohio 45433

13. ABSTRACT

The TRISAFE Single Axis Flight Control System developed for the Research and Technology Division of the Air Force consists of a deliverable controller and simulator with associated recorder. This equipment is to be used primarily as a laboratory demonstration model of a triple redundant, self-adaptive flight control system.

The controller incorporates the Autonetics developed triple redundant, analog circuit technique called TRISAFE that represents nearly optimum in redundancy, efficiency and reliability. To compensate for the normal increase in size and weight due to the triple redundancy, the use of a square wave 400 cps carrier has been employed to reduce the number of components, and molecular integrated circuits are used to reduce the size of the components. A multi-layer circuit board is used to further reduce the weight and volume of the controller. The controller measures 3 x 9.7 x 12 inches and weighs approximately 6 pounds. Plug-in modular packaging is used for maintainability.

The controller is based on the dynamics of a high performance tactical aircraft and provides stability augmentation for the pitch axis. To provide for optimum gain throughout the performance range of the aircraft, a self-adaptive system is used. Known as the dither-adaptive technique, it employs a low level test signal to measure the response of the airframe and adjusts the gain accordingly.

DD FORM 1 JAN 64 1473

Unclassified

Security Classification

14. KEY WORDS	LINK A		LINK B		LINK C	
	ROLE	WT	ROLE	WT	ROLE	WT
TRISAFE fail-safe concept Flight Control Demonstration Model Triple Redundant Self-Adaptive Reliability Molecular Integrated Circuits Dither-Adaptive Automatic Gain						

INSTRUCTIONS

1. ORIGINATING ACTIVITY: Enter the name and address of the contractor, subcontractor, grantee, Department of Defense activity or other organization *(corporate author)* issuing the report.

2a. REPORT SECURITY CLASSIFICATION: Enter the overall security classification of the report. Indicate whether "Restricted Data" is included. Marking is to be in accordance with appropriate security regulations.

2b. GROUP: Automatic downgrading is specified in DoD Directive 5200.10 and Armed Forces Industrial Manual. Enter the group number. Also, when applicable, show that optional markings have been used for Group 3 and Group 4 as authorized.

3. REPORT TITLE: Enter the complete report title in all capital letters. Titles in all cases should be unclassified. If a meaningful title cannot be selected without classification, show title classification in all capitals in parenthesis immediately following the title.

4. DESCRIPTIVE NOTES: If appropriate, enter the type of report, e.g., interim, progress, summary, annual, or final. Give the inclusive dates when a specific reporting period is covered.

5. AUTHOR(S): Enter the name(s) of author(s) as shown on or in the report. Enter last name, first name, middle initial. If military, show rank and branch of service. The name of the principal author is an absolute minimum requirement.

6. REPORT DATE: Enter the date of the report as day, month, year; or month, year. If more than one date appears on the report, use date of publication.

7a. TOTAL NUMBER OF PAGES: The total page count should follow normal pagination procedures, i.e., enter the number of pages containing information.

7b. NUMBER OF REFERENCES: Enter the total number of references cited in the report.

8a. CONTRACT OR GRANT NUMBER: If appropriate, enter the applicable number of the contract or grant under which the report was written.

8b, 8c, & 8d. PROJECT NUMBER: Enter the appropriate military department identification, such as project number, subproject number, system numbers, task number, etc.

9a. ORIGINATOR'S REPORT NUMBER(S): Enter the official report number by which the document will be identified and controlled by the originating activity. This number must be unique to this report.

9b. OTHER REPORT NUMBER(S): If the report has been assigned any other report numbers *(either by the originator or by the sponsor)*, also enter this number(s).

10. AVAILABILITY/LIMITATION NOTICES: Enter any limitations on further dissemination of the report, other than those imposed by security classification, using standard statements such as:

(1) "Qualified requesters may obtain copies of this report from DDC."

(2) "Foreign announcement and dissemination of this report by DDC is not authorized."

(3) "U. S. Government agencies may obtain copies of this report directly from DDC. Other qualified DDC users shall request through _____."

(4) "U. S. military agencies may obtain copies of this report directly from DDC. Other qualified users shall request through _____."

(5) "All distribution of this report is controlled. Qualified DDC users shall request through _____."

If the report has been furnished to the Office of Technical Services, Department of Commerce, for sale to the public, indicate this fact and enter the price, if known.

11. SUPPLEMENTARY NOTES: Use for additional explanatory notes.

12. SPONSORING MILITARY ACTIVITY: Enter the name of the departmental project office or laboratory sponsoring *(paying for)* the research and development. Include address.

13. ABSTRACT: Enter an abstract giving a brief and factual summary of the document indicative of the report, even though it may also appear elsewhere in the body of the technical report. If additional space is required, a continuation sheet shall be attached.

It is highly desirable that the abstract of classified reports be unclassified. Each paragraph of the abstract shall end with an indication of the military security classification of the information in the paragraph, represented as *(TS), (S), (C), or (U)*.

There is no limitation on the length of the abstract. However, the suggested length is from 150 to 225 words.

14. KEY WORDS: Key words are technically meaningful terms or short phrases that characterize a report and may be used as index entries for cataloging the report. Key words must be selected so that no security classification is required. Identifiers, such as equipment model designation, trade name, military project code name, geographic location, may be used as key words but will be followed by an indication of technical context. The assignment of links, rules, and weights is optional.